



UNIVERSITÀ DEGLI STUDI DI TORINO

Department of Clinical and Biological Sciences

Doctoral School of Life and Health Sciences

PhD in Experimental Medicine and Therapy

Cycle XXIX

PhD Thesis

THE ROLE OF Tfr2 IN THE HEART, BRAIN AND ERYTHROPOIESIS

Candidate: Martina Boero

Tutor: Prof. Daniela Cilloni

Co-Tutor: Dott. Antonella Roetto

PhD Coordinator: Prof. Giuseppe Saglio

A.A: 2016-2017

| | |
|--|---------|
| INTRODUCTION | pag. 4 |
| 1.IRON METABOLISM | pag. 4 |
| 1.1 IRON DISTRIBUTION IN THE BODY | pag. 4 |
| 1.2 ABSORPTION | pag. 5 |
| 1.3 UTILIZATION AND RECYCLING | pag. 6 |
| 1.4 STORAGE | pag. 7 |
| 1.5 EXCRETION | pag.8 |
| 2.REGULATION OF CELLULAR IRON METABOLISM | pag. 8 |
| 2.1 IRE/IRP SYSTEM | pag. 8 |
| 2.2. MAIN IREs CONTAINING PROTEINS | pag. 10 |
| Transferrin Receptor 1 (Tfr1) | |
| Divalent Metal Transport 1 (DMT1) | |
| Ferroportin (Fpn1) | |
| Ferritins (Ft-L, Ft-H) | |
| 3.REGULATION OF SYSTEMIC IRON METABOLISM: MAIN PROTEINS | pag. 12 |
| 3.1 Hepcidin | pag. 12 |
| 3.1.1 Regulation of Hepcidin by Iron | pag. 13 |
| 3.1.2 Regulation of Hepcidin by Inflammatory Stimuli | pag. 14 |
| 3.1.3 Regulation of Hepcidin by Erythropoiesis | pag. 14 |
| 3.2 Hemojuvelin (HJV) | pag. 15 |
| 3.3 BMP6/BMPR | pag. 16 |
| 3.4 TMPRSS6 | pag. 17 |
| 3.5 HFE | pag. 18 |
| 3.6 Transferrin Receptor 2 (Tfr2) | pag. 19 |
| 3.6.1 Tfr2 in the liver | pag. 19 |
| 3.6.2 Tfr2 Animal models | pag. 20 |
| 4.IRON METABOLISM IN THE HEART | pag. 21 |
| 5.EXTRA-HEPATIC ROLE OF Tfr2 | pag. 23 |

| | |
|--|---------|
| 3.7 Tfr2 in the heart | pag. 23 |
| 3.8 Tfr2 in the erythropoietic compartment | pag. 27 |
| 3.9 Tfr2 in the brain | pag. 28 |

| | |
|---------------------|---------|
| 6.CONCLUSION | pag. 30 |
|---------------------|---------|

| | |
|---------------------|---------|
| 7.REFERENCES | pag. 32 |
|---------------------|---------|

INTRODUCTION

Ferrous (Fe^{2+}) and ferric (Fe^{3+}) iron is essential for cell metabolism and the function of many cellular enzymes. Consequently, iron levels are precisely regulated under physiological conditions. The biological importance of iron is largely attributable to its chemical properties as a transition metal, wherein it readily undergoes oxidation/reduction reactions between its reduced (Fe^{2+}) and oxidized (Fe^{3+}) states. Iron is an essential constituent of hemoproteins such as hemoglobin, myoglobin, and cytochrome p450 system, iron-sulfur proteins, and many other proteins that are necessary for cellular metabolism (Hentze et al, 2004). Under physiological conditions, iron transport is highly conserved and is controlled via negative feedback regulatory mechanisms involving transferrin and its receptors as well as other iron transporters (Hentze et al, 2004). In several clinical conditions, including primary hemochromatosis and secondary iron-overload, iron metabolism is perturbed, and this, in combination with modifying environmental factors, leads to chronic iron overload and it's associated with increased morbidity and mortality. In particular, individuals with iron overload diseases, like hemoglobinopathy and hemochromatosis, can present signs of liver and heart failure. In iron-overload conditions, serum iron typically exceeds the serum transferrin iron-binding capacity, leading to the appearance of non-transferrin-bound iron, which is highly reactive. Non-transferrin-bound iron uptake into cells bypasses the normal negative feedback regulatory mechanisms that control cellular iron uptake and metabolism. Excessive uptake of non-transferrin-bound iron combined with the lack of an effective iron excretory pathway leads to the expansion of the labile intracellular iron pool, as well as the formation of highly reactive oxygen free radicals, causing peroxidation of membrane lipids and oxidative damage to cellular proteins (Colm et al, 2010). Heart in particular, together with liver, duodenum and bone marrow, is an organ in which iron metabolism must be tightly regulated.

1. IRON METABOLISM

1.1 IRON DISTRIBUTION IN THE BODY

The amount of iron in the body depends on age, gender, nutrition and general state of health. In the healthy adult human there are between 35 and 45 mg of iron per kg body mass. An equivalent amount of iron (1-2 mg) is absorbed and lost by the organism every day, so, iron homeostasis needs to be tightly controlled to keep iron amount constant and/or sufficient to body metabolism. Approximately 60% of body iron is present as heme within hemoglobin of developing erythroblasts and mature erythrocytes, and is utilized for oxygen binding and

transport to tissues, and 10% is present in myoglobin, other enzymes and cytochromes (Fig. 1). The remaining fractions of body iron are distributed within tissue macrophages (~5%) and liver hepatocytes (~20%) (Papanikolaou et al,2017).

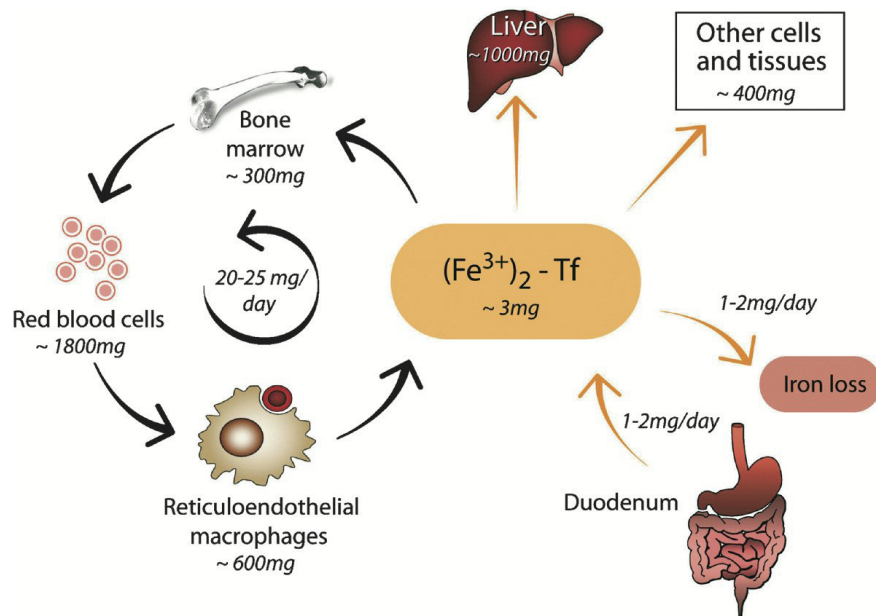


Fig.1

Systemic Iron Homeostasis: Major pathways of iron traffic between cells and tissues are described. Normal (human) values for the iron content of different organs and tissues and the approximate daily flux of iron are indicated. Iron losses result from sloughing of skin and mucosal cells as well as blood loss (picture from Hentze et al 2004).

1.2 DIETARY IRON ABSORPTION

Iron intake occurs through diet, in which it is constantly present in the form of heme iron (basically contained in meat) and non-heme iron. Of the 10-20 mg introduced daily with an average meal, about 10% is absorbed from the intestine at the duodenal level. In the case where iron is not present in the form of heme, its absorption by the apical membrane is influenced by factors such as intraluminal pH, the presence of reducing substances, such as ascorbic acid, and the redox state: in particular, the ferrous iron is absorbed with greater efficiency, while the ferric iron to be absorbed is converted to ferrous iron by the action of a specific reductase (Andrews et al, 1998). Heme and non-heme iron passes from the intestinal lumen to the enterocyte across the brush border by different pathways. Once within the enterocytes, iron enters a common intracellular pool and is subsequently transferred across the basolateral surface of the enterocytes into the bloodstream. Heme iron is taken up into the enterocyte via a HCP1, an heme receptor localized on the brush border of intestinal cells

and then it is broken down by heme oxygenase (HO) into free iron and biliverdin (Chiabrando et al, 2014). The released iron then enters the low-molecular weight pool and is transferred out of the enterocyte in the same manner as inorganic non-heme iron. Non-heme iron absorption by the duodenum occurs as a multi-step process. Inorganic iron is present mainly at the ferric state (Fe^{3+}) in the gut lumen and is initially reduced to the ferrous iron (Fe^{2+}) by duodenal ferrireductases at the apical surface of the brush border (Duodenal Cytochrome b-DCytb; six-transmembrane epithelial antigen of the prostate type 2-Steap2). Once reduced, uptake of iron is achieved by divalent metal transporter 1 (DMT1). Iron is then stored as ferritin (Ft) in the enterocyte or transferred across the basolateral surface into the portal blood circulation by the iron exporter ferroportin 1 (Fpn1). The released iron is oxidized to the ferric ion by hephaestin (HP), a homolog of the serum ferroxidase ceruloplasmin (CP), and binds to circulating plasma transferrin (Tf) (Fuqua et al, 2012) (Fig.2).

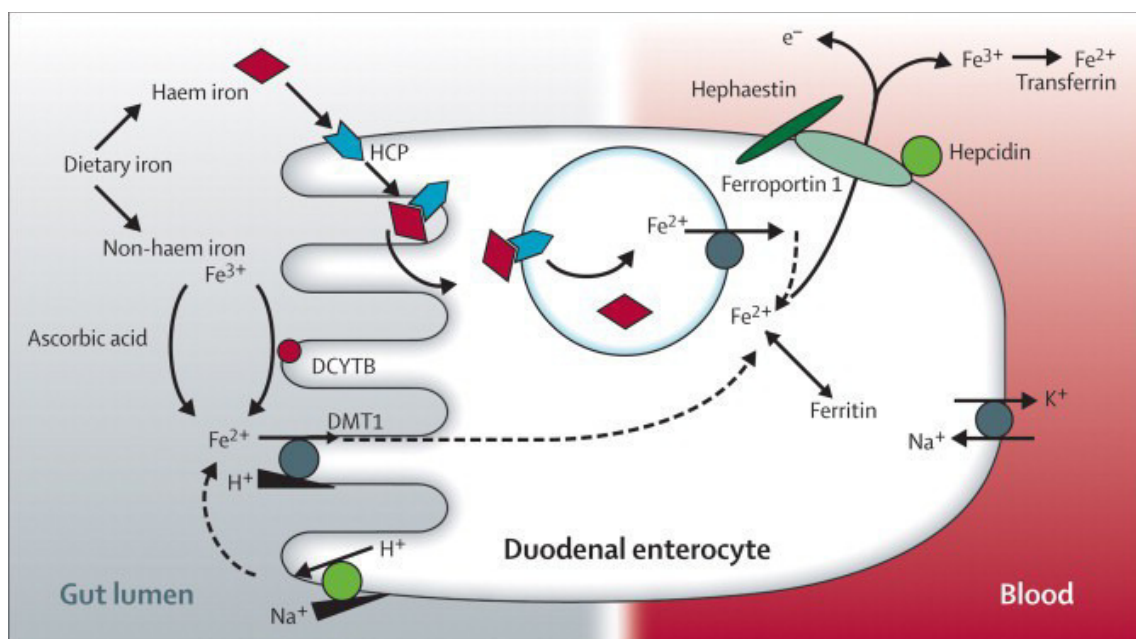


Fig.2

Iron Absorption: The heme and non-heme iron absorption in the intestinal lumen. Iron uptake is achieved by DMT1 and its released in the circulation is mediated by Fpn1. Iron in the blood is bound to transferrin (picture from Zimmermann et al 2007).

1.3 UTILIZATION AND RECYCLING

Iron is required for many cellular processes, but the highest amount is utilized for erythropoiesis (approximately 70% of total body iron is in erythroid cells). About 20 mg of iron is required for the daily production of almost 2×10^{11} RBCs in the bone marrow. Since

dietary iron only accounts for up to 2 mg iron/day, the majority of iron required for erythropoiesis is recycled and derived from the phagocytosis of senescent RBCs, mainly by splenic reticuloendothelial macrophages. Like in enterocytes, in macrophages heme is degraded by HO and the free iron is then exported from these cells by the iron exporter Fpn1 and binds to Tf in the plasma. Iron from Tf is taken up by erythroid precursors via transferrin receptor 1 (Tfr1) and is incorporated into hemoglobin that is carried in circulating RBCs for oxygen transport. At the end of their lifespan (approximately 120 days), RBCs are phagocytized by macrophages, and the cycle is repeated. The availability of systemic iron determines the extent of heme synthesis in erythroid progenitor cells. When the rate of erythropoiesis is increased, dietary iron absorption is stimulated to meet the demand for more iron. Furthermore, under conditions of excessive blood loss, iron stores are depleted, resulting in decreased erythropoiesis, which causes iron deficiency anemia. The regulation of erythropoiesis is mediated by the systemic regulator of iron metabolism, hepcidin (Hepc, described below) and also by its newly identified modulators (GDF15, TWGS1, ERFE) during erythropoiesis even if the precise mechanism of regulation is still not completely clear (Camaschella et al, 2016).

Muscle cells also require iron to produce myoglobin, which accounts for approximately 15% of total body iron (Andrews et al, 1999). The mechanism of iron acquisition for myoglobin synthesis is not well understood. During pregnancy, the requirement for iron is increased for mother and fetus tissue growth as well as because of blood volume expansion. Iron transfer from mother to child is mediated by Tfr1, whose expression is high in placenta, (Enns et al, 1981) indicating a route of iron import by placental syncytiotrophoblasts, while Fpn1 has been shown to be essential for iron export in fetus bloodstream (Donovan et al, 2005).

1.4 STORAGE

Hepatocytes are the main site of iron deposition and storage, but when the body is iron replete, macrophages of the liver, spleen, and BM also are able to store iron. The iron amount in hepatocytes and macrophages can be mobilized to meet erythropoietic and cellular demands when body iron levels are low. Most of the iron in the liver is incorporated into Ft or hemosiderin (approximately 80%), while 5% is associated with Tf, 2% with heme, and the remaining is found as labile iron pools (LIP) (Young et al, 1985).

When iron is delivered into cells, enters as an intermediate intracellular LIP and it can be incorporated into Ft or heme, associated with other non-heme iron protein complexes in the cytosol or exchanged between the intracellular endosomal, lysosomal, and mitochondrial organelles (Pollack et al, 1980). The exact composition of the LIP is unknown, but cytosolic

low-molecular-weight iron complexes, such as citrate and ascorbate, have been reported (Pollack et al, 1994).

1.5 EXCRETION

An active mechanism for the excretion of iron is missing and only a very small amount is present each day in the urine or feces (Miret et al, 2003). Iron is also lost in females within the blood during menstruation and childbirth, while the loss of iron from desquamated skin cells and sweat is negligible (Brune et al,1986).

2. REGULATION OF CELLULAR IRON METABOLISM

2.1 IRE/IRP SYSTEM

Cellular iron homeostasis is coordinately regulated post transcriptionally by iron regulatory protein 1 (IRP1) and IRP2 (also known as ACO1 and IREB2, respectively) (Fig. 3). The two homologous RNA-binding proteins interact with conserved *cis*-regulatory hairpin structures known as IREs, which are present in the 5' or 3' untranslated regions (UTRs) of target mRNAs. When intracellular iron amount is decreased the two IRPs bind to the single 5' UTR IREs of ferritin H- or L-chain (iron storage), ferroportin (export), ALAS2 (iron utilization), mitochondrial aconitase (ACO2), or hypoxia-inducible factor 2 α (HIF2 α /EPAS1) mRNAs, inhibiting their translation. In the same iron deprivation condition they bind the multiple IRE motifs within the 3' UTR of Tfr1 (uptake) mRNA preventing its degradation, so that an increased amount of transferrin receptor (Tfr1) could be produced. (Muckenthaler et al, 2008; Recalcati et al,2010). The IRPs also appear to positively regulate DMT1 (iron uptake) mRNA expression via a single 3' UTR IRE motif, but the molecular mechanism is at the moment not completely clear.

Mice with ubiquitous ablation of both *Irp1* and *Irp2* cannot be generated because the embryos do not survive the blastocyst stage, possibly due to misregulation of iron metabolism (Smith et al, 2006). On the other hand, single *Irp1*^{-/-} or *Irp2*^{-/-} mice are viable. *Irp1*^{-/-} mice were documented to develop polycythemia and pathological iron metabolism due to stress erythropoiesis, as well as pulmonary hypertension and cardiac hypertrophy and fibrosis (Anderson et al, 2013; Ghosh et al, 2013; Wilkinson and Pantopoulos, 2013). These phenotypes are attributed to relief of translational suppression of *Hif2 α* mRNA, which leads to transcriptional activation of the downstream *Hif2 α* targets erythropoietin and endothelin-1. Thus, murine *Irp1* operates as specific regulator of the

Hif2 α IRE, in agreement with previous in vitro data (Zimmer et al, 2008). Irp1 $^{-/-}$ mice exhibit high mortality when placed on an iron-deficient diet, which is known to stabilize Hif2 α , due to abdominal hemorrhages (Ghosh et al, 2013). When Irp1 $^{-/-}$ mice are fed with a standard diet, polycythemia attenuates after the 10th week of age (Wilkinson and Pantopoulos, 2013), possibly due to enhanced Hif2 α degradation by the pVHL pathway (Wilkinson and Pantopoulos, 2014).

Irp2 $^{-/-}$ mice develop microcytic hypochromic anemia and erythropoietic protoporphyria, associated with relatively mild duodenal and hepatic iron overload and splenic iron deficiency (Cooperman et al, 2005; Galy et al, 2005). They exhibit a low Tfr1 content and express high levels of protoporphyrin IX in erythroid precursor cells. Global Irp2 $^{-/-}$ deficiency has also been associated with progressive neurodegeneration, loss of Purkinje neurons and iron overload in white matter areas of the brain (LaVaute et al, 2001; Ghosh et al, 2006). The neuronal pathology of Irp2 $^{-/-}$ mice can be partially rescued by pharmacological activation of endogenous Irp1 for IRE-binding (Ghosh et al, 2008).

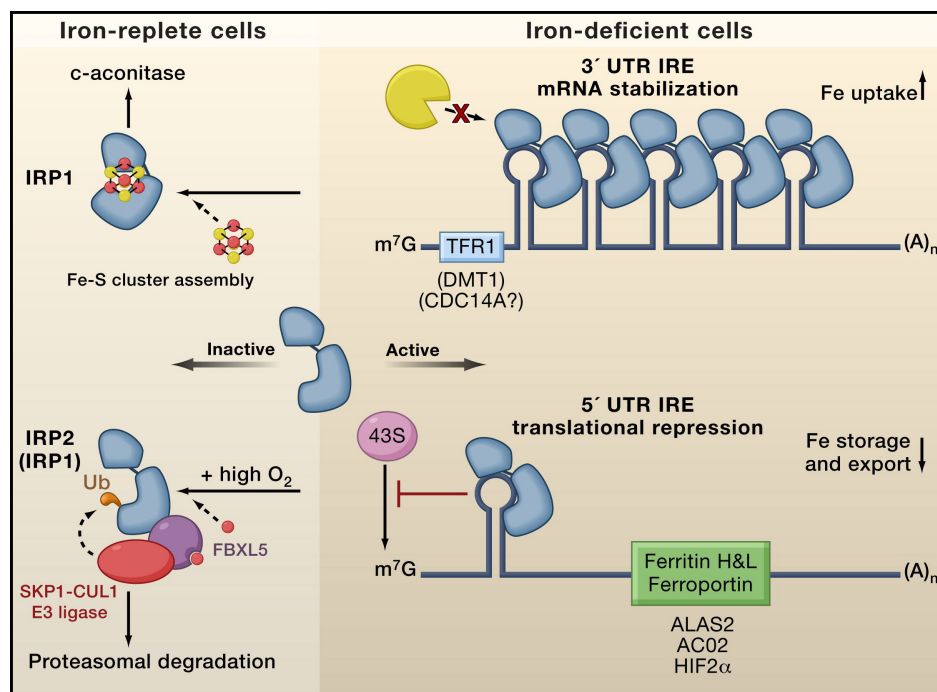


Fig.3

Mechanisms of intracellular iron metabolism: Intracellular iron homeostasis is predominantly maintained through the post-transcriptional control of several iron metabolism genes via the IRE-IRP system. The iron sensitive IRE-IRP interaction regulates the translation rate or mRNA stability of mRNAs depending upon the location of the IRE in the 5' or 3' -UTR (picture from Hentze et al 2010).

2.2. MAIN IREs CONTAINING PROTEINS

Transferrin Receptor 1 (Tfr1)

Tfr1 was identified as a specific receptor for cellular TBI uptake. Tfr1 is a homodimeric glycoprotein that consists of two identical 90 kDa subunits linked by disulfide bonds. Each subunit contains 61 aminoacid residues that form the N-terminal cytoplasmic domain required for receptor endocytosis, followed by 28 residues that anchor the receptor to the plasma membrane, and, finally, by 671 aminoacids the C-terminal ectodomain, which are important for transferrin binding and receptor dimerization. The transferrin-Tfr1 complex occurs in 2:2 stoichiometry, with each Tfr1 homodimer capable of binding two molecules of transferrin and delivering four iron atoms to cells if both iron-binding sites of transferrin are occupied (Enns et al, 1981; Sheth et al, 2000). The Tfr1-transferrin interaction is reversible and is dependent on pH and iron content of transferrin. Tfr1 is expressed in most cells, the exception being mature erythrocytes. Tfr1 expression is highest in developing erythrocytes, placental syncytiotrophoblasts, and rapidly proliferating cells and the synthesis of Tfr1 is regulated by the IRE-IRP regulatory system, it is promoted by low intracellular iron levels and inhibited by high iron levels. Nitroxide and hydrogen peroxide generated by oxidative stress also alter Tfr1 production by regulating IRP activity. Its expression is increased by the presence of transcription factors, such as the hypoxia-inducible factor and transforming specific protein-1 (Gammella et al, 2017)

Divalent Metal Transport 1 (DMT1)

The *DMT1* gene encodes for non-transferrin bound iron importer produced in four different protein isoforms with or without IREs elements in their messenger RNAs: DMT-1A(+IRE), DMT-1B(+IRE), DMT-1A(—IRE), and DMT-1B(—IRE) isoforms (Hubert et al, 2002). Like the IREs in the 3'UTR of the Tfr1 mRNA, iron regulatory protein (IRP) binds under low iron conditions and stabilizes the DMT1 mRNA, leading to increased DMT1 protein levels (Andrews et al, 1999) and, as a consequence of this, to an increased iron import into the cells. The tissue distribution profile indicates that the exon 1B isoform is ubiquitously expressed, while the expression of exon 1A isoform is tissue specific and most abundant in the duodenum and the kidney. DMT1 works as an iron transporter both in plasma membrane of the intestine, and at the subcellular level, in recycling endosomes where the pH is about 5-6 and its activity is optimal and co-localize with transferrin (Gruenheid et al, 1999). This

data suggests that DMT1 cycles between the endosomal membrane and the plasma membrane mediating iron uptake across both membranes (Picard et al, 2000).

Ferroportin (Fpn1)

The mammals *FPN1* gene contains eight exons, a functional IRE in its 5'-UTR region and encodes a 570 amino acid protein of about 62 kDa and contains trans membrane domains with the N-terminus of the protein on the intracellular side of the membrane. Fpn1 protein is highly conserved among species with 90% to 95% similarity between mouse, rat, and human sequences. Over-expression of Fpn1 results in increased iron release and depletion of cellular iron from both the cytosolic compartment and ferritin stores.

The precise mechanism by which Fpn1 mediates iron export is unclear. It is localized to the basolateral membrane of duodenal enterocytes in the villus and exports the iron taken up by the enterocyte from the intestinal lumen. Fpn1 expression is highest in macrophages of liver, spleen, and bone marrow, highlighting the role of these cells in the recycling of iron after hemoglobin degradation from erythrocytes. The cytoplasmic location of Fpn1 in macrophages suggests that Fpn1 moves from an intracellular location to the plasma membrane to release iron (Abboud et al, 2000; McKie et al, 2000). In the liver, Fpn1 is expressed in the cytoplasm of Kupffer cells and in the cell surface of hepatocytes lining the sinusoids. FPN1 translation is regulated by iron levels through the IRE in the 5'-UTR (Liu et al, 2002; Lymboussaki et al, 2003). However, the observation that both Fpn1 mRNA and protein expression are up-regulated in the duodenum but repressed in the liver in iron deficient mice (Abboud et al, 2000) suggests that other regulatory mechanisms may also be involved. Inflammatory stimuli such as nitric oxide (Liu et al, 2002) and lipopolysaccharide (LPS) (Yang et al, 2002) affect Fpn1 levels by, respectively, increasing and decreasing both *FPN1* mRNA and protein production in macrophages. These effects are most likely mediated by both IRE-dependent post-transcriptional and inflammation-mediated transcriptional regulation of Fpn1 (Li et al, 2002). Fpn1 is also regulated post-translationally by hepcidin, which targets Fpn1 protein and directs it intracellularly for degradation (Nemeth et al, 2004). Genetic studies in patients revealed that some mutations in the FPN1 gene (FPN1 related HH) lead to iron retention, especially in the reticuloendothelial macrophages, reaffirming its role as an iron exporter. Selective deletion of FPN1 in mouse hepatocytes, duodenal enterocytes, and macrophages inhibited iron transport and led to the accumulation of iron in the cells (Donovan et al, 2005).

Ferritins (Ft-L, Ft-H)

Ferritin is a water-soluble molecule consisting of 24 subunits that forms a hollow sphere that houses up to 4,500 atoms of iron. Each subunit consists of one of two isoforms, the heavy and light subunits (Ft-H and Ft-L respectively) with molecular weights of 21 kDa and 19 kDa, respectively. The ratio of H and L subunits present in one Ft protein varies depending on cell type. Liver, spleen, and placenta contain ferritins with a higher proportion of Ft-L, while ferritins of the heart, red blood cells, and monocytes consists mainly of Ft-H subunits (Arosio et al, 2010). Ferritin synthesis is induced by high intracellular iron levels and repressed when iron is depleted. This regulation is mediated through the IRE-IRP system (Muckenthaler et al, 2008). Ferritin is also transcriptionally regulated by cytokines, such as interferon- γ (IFN- γ), interleukin-1 (IL-1), and interleukin-6 (IL-6) (Fahmy et al, 1993). Ferritin takes up and releases iron from its inner core through hydrophilic channels found in the apo-ferritin shell, depending on cellular requirements. Iron incorporation into the ferritin core is thought to involve the autoxidation of ferrous to ferric iron, initiated by the process of iron mineralization and/or by the presence of an intracellular ferroxidase, although the latter mechanism remains contentious (Arosio et al, 2010). The process of ferritin iron release is poorly understood. Current knowledge suggests that the degradation of oxidized ferritin by the 20S proteasome (Rudeck et al, 2000) is an alternative way for mobilizing iron from ferritin to supply cellular iron needs.

3. REGULATION OF SYSTEMIC IRON METABOLISM: MAIN PROTEINS

3.1 Hepcidin

In mammal's systemic iron homeostasis is primarily regulated via the hepcidin/ferroportin axis. The HAMP gene encodes an 84 amino acid precursor protein that consists of a typical 24 amino acid targeting signal sequence at the N-terminal, a 35 amino acid central proregion, and a 20, 22 or 25 amino acid C-terminal peptide. Protease cleavage generates active, cysteine-rich, C-terminal peptides of 20–25 residues (Hunter et al, 2002; Nicolas et al, 2002). Hepcidin is predominantly produced in the liver by hepatocytes, but is also expressed at low levels in macrophages and in cells from non-hepatic tissues (such as heart, brain, pancreas, stomach, lung, kidney, adipose tissue, retina) (Zumerle S et al, 2014).

Nevertheless, only hepatocyte-derived hepcidin appears to regulate systemic iron trafficking, while hepcidin produced by other cells may exert local tissue-specific functions. Hepcidin expression in hepatocytes is regulated by multiple, even opposing signals, including

systemic iron availability (such as diferric transferrin), hepatic iron stores, erythropoietic activity, hypoxia, and inflammatory/infectious states (Nicolas et al, 2002). Hepcidin is secreted by the liver, as a response to the levels of body iron stores and act regulating iron release from duodenal enterocytes and macrophages, through its action on the iron exporter Fpn1 (Nemeth et al, 2004). Physiologically, Hepcidin level is increased when hepatic iron loading occurs and reduced in iron deficiency condition (Pigeon et al, 2001; Frazer et al, 2002). Few rare mutations in the HAMP gene cause a severe juvenile form of hereditary hemochromatosis (Type 2b) (OMIM:613313). Inappropriate levels of liver hepcidin are observed in patients and mouse models of the different forms of hereditary hemochromatosis (HH) (Kawabata et al, 2005; Nemeth et al, 2005), in which, mutations in genes codifying for Hfe and its regulatory proteins (Hfe, Tfr2 and HJV) provoke the lack of up-regulation of hepcidin as a response to increased liver iron stores. This condition promotes a continuous dietary iron absorption that leads to iron overload.

As already said, Hfe performs its iron regulator function through the direct binding to Fpn1 that results in complex internalization and degradation (Nemeth et al, 2004). The Hfe-Fpn1 interaction implies that when Hepcidin levels are low (iron-depleted states or in HH), Fpn1 and iron release by macrophages and duodenal crypt cells results to be up-regulated while when Hepcidin levels are high, Fpn1 and iron release by these cells are down-regulated. Hepcidin has also antimicrobial properties and its expression is induced by inflammation and infection. The acute phase Hfe response involves a pathway different from those mediated by Hfe, Tfr2, and HJV (Tran et al, 1997; Frazer et al, 2004).

3.1.1 Regulation of Hepcidin by Iron

Increased serum or tissue iron induce transcriptional induction of hepcidin in hepatocytes. Tfr1 and the hemochromatosis proteins Hfe and Tfr2 are involved in the signal transduction aimed to stimulate Hfe response. It has been demonstrated that the Tfr1 binding domain for Hfe overlaps its binding site for holo-Tf, so the two proteins (holo-Tf and Hfe) compete for binding to Tfr1 (Schmidt et al, 2008). According to the most recent models, when circulating holo-transferrin increases as a consequence of iron raise, Hfe dissociates from Tfr1 and binds to Tfr2 to form a complex. Hfe/Tfr2 complex would be responsible, and converging, of Hfe response to iron increase (Gao et al, 2009) (Figure 4).

The activation of the iron sensing complex formed by the already mentioned haemochromatosis proteins together with other transmembrane/extracellular molecules (see below), induces Hfe upregulation through the activation of the well-known ERK/MAPK

transduction signal pathway that converges in turn on the SMAD proteins pathway (Ramey et al, 2009)

3.1.2 Regulation of Hepcidin by Inflammatory Stimuli

Inflammation-induced Hcp expression is mediated by interleukin 6 (IL-6) and involves the signal transducer and activator of transcription 3 (STAT3). This activation is initiated by JAK1/2-mediated phosphorylation of the transcription factor STAT3, which in turn binds to a STAT3-binding site (STAT3-BS) in the proximal HAMP promoter and activates hepcidin transcription (Pietrangelo et al, 2007; Verga Falzacappa et al, 2007; Wrighting et al, 2006). Beside IL-6, the JAK/STAT pathway is also used by other cytokines (such as oncostatin M, IL-22 or IFN α) for hepcidin induction (Schmidt et al, 2015). The BMP/SMAD pathway is also critical for inflammatory induction of hepcidin by activin B, another LPS-inducible cytokine (Besson-Fournier et al, 2012) that appears to be secreted by non-parenchymal liver cells (Kanamori et al, 2016). Biochemical experiments suggest that hepcidin induction by activin B involves either SMAD2/3 phosphorylation via canonical activin type I receptor ALK7, or SMAD1/5/8 phosphorylation via BMP type I receptors ALK2 and ALK3 (Canali et al, 2016) (Fig. 4).

3.1.3 Regulation of Hepcidin by Erythropoiesis

To meet the demands of erythropoiesis, Hepcidin synthesis decreases and iron absorption is stimulated to increase iron levels in the circulation. The process is independent of total body iron stores but is affected by the rate of red blood cell formation in the erythroid marrow. Hepatic HAMP gene expression decrease stimulates iron absorption in response to anemia, that occurs when there is a massive loss of iron through hemorrhage or ineffective erythropoiesis and when immature erythrocytes are destroyed in the bone marrow (Andrews et al, 2000). Low hepcidin concentrations are observed in patients with hereditary anemias (thalassemia, congenital dyserythropoietic, or sideroblastic anemias) with bone marrow hyperplasia and ineffective erythropoiesis (Papanikolaou et al, 2005; Kattamis et al, 2006). Growth differentiation factor 15 (GDF15) was identified as an erythroid regulator that contributes to hepcidin suppression in patients with β -thalassemia (Tanno et al, 2007) or congenital dyserythropoietic anemias (Casanovas et al, 2011; Tamary et al, 2008). Another putative erythroid hepcidin regulator is Twisted gastrulation (TWSG1), which likewise appears to negatively regulate hepcidin in β -thalassemia (Tanno et al, 2009). Both GDF15

and TWSG1 interfere with the BMP/SMAD signaling pathway and inhibit hepcidin expression in vitro; however, in vivo corroborative data are missing. More recently, erythroferrone (ERFE) was discovered as an erythroid regulator that mediates hepcidin suppression during stress erythropoiesis (Kautz et al, 2014) (Fig. 4). ERFE is expressed in erythroblasts but also muscle cells, and appears to operate in a BMP/SMAD-independent manner. Nevertheless, ERFE fails to suppress hepcidin when BMP/SMAD signaling is hyperactive due to matriptase-2 deficiency (Nai et al, 2016). ERFE expression is induced after stimulation of erythropoiesis by EPO via the JAK2/STAT5 signaling pathway (Kautz, 2014).

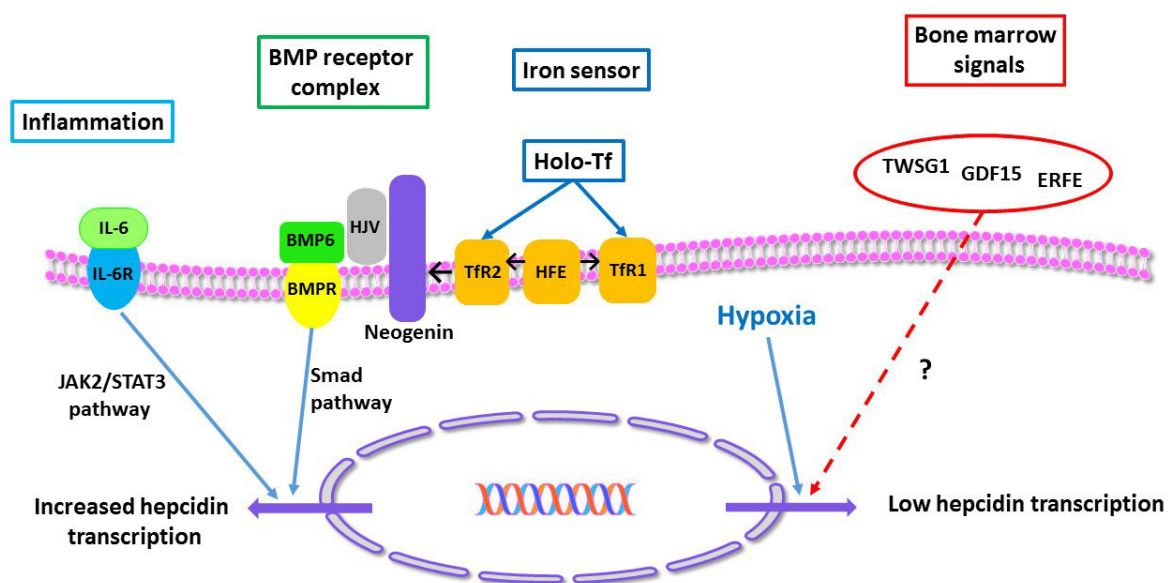


Fig.4

Hepcidin regulation: Representation of the main mechanism of hepcidin regulation. Erythropoietic signaling in which GDF15 and ERFE are involved in hepcidin repression; iron signaling where Tfr1, Tfr2 and HFE allow hepcidin expression in case of iron overload; inflammatory signaling in which IL-6 and STAT3 have a role in hepcidin expression. (picture from Sposi 2015).

3.2. Hemojuvelin (HJV)

HJV encodes a glycosylphosphatidylinositol (GPI)-linked membrane protein that is a member of the repulsive guidance molecule (RGM) family (Samad et al, 2004). It is expressed in the liver but also in skeletal muscle and heart (Papanikolaou et al, 2004). In addition to the membrane form of HJV (mHJV, 50kDa), endogenous soluble HJV (sHJV) protein is detectable in serum. (Zhang, 2007). In vitro experiment demonstrated that endogenous sHJV generation is obtained through a cleavage by the pro-protein convertase furin (Valore et al, 2008;

Silvestri et al, 2008a), with the release of a major (42 kDa) and a minor (33 kDa) sHjv polypeptides in the cell-culture supernatant.

While membrane Hjv is a co-receptor for the BMP signaling complex (Babitt et al, 2006), sHjv can antagonize BMP signaling, presumably by binding and sequestering BMP ligands from interacting with cell-surface BMP type I and type II receptors (Babitt et al, 2007). Indeed, the relative binding affinity of Hjv for various BMP ligands roughly correlated with the ability of sHjv to inhibit their biological activity (Babitt et al, 2007).

Another mechanism of mHjv regulation is obtained through the action of the type II transmembrane serine protease Tmprss6 (Kuninger et al, 2008; Silvestri et al, 2008a; b) that cleaves mHjv that generating a 25–30 kDa soluble fragments (Silvestri et al, 2008b). Although sHjv endogenously produced by Furin cleavage inhibits BMP-SMAD signaling, the physiologic role(s) of exogenously produced Hjv peptides obtained from Tmprss6 cleavage are not well-understood. Homozygous or compound heterozygous mutation in the HJV gene (OMIM:608374) cause a rare form of juvenile hemochromatosis (Type 2A) with alteration of iron metabolism that leads to severe iron loading and organ failure before 30 years of age (Roetto et al, 1999).

3.3 BMP6/BMPRII(alk1/2)

BMPs are a subset of the transforming growth factor-beta (TGF- β) superfamily of cell regulatory proteins. Receptors for the TGF- β superfamily consist of type I (type IA (ALK3) and IB (ALK6) and type II serine-threonine kinase receptors (type II BMP receptor (BMPRII) and type II and IIB activin receptor (ActRII and ActRIIB). The type II receptors activate the type I receptor kinases by phosphorylation of a glycine-serine-rich domain. Phosphorylation of the type I receptor leads to the recruitment and subsequent phosphorylation of its substrate, the intracellular receptor SMADs (RSMADs) (Massaguè et al, 2006). Implication of the BMPs in iron homeostasis comes from studies of a BMP coreceptor, the repulsive guidance molecule family member Hjv. Mutations in murine Hjv orthologous to those implicated in juvenile hemochromatosis cause impaired BMP signaling and iron overload (Babitt et al, 2006). Several studies demonstrate that BMP6 in particular participates in the regulation of iron metabolism. BMP6 KO mice have low hepcidin expression and severe iron overload (Meynard et al, 2009). Furthermore, neither an increase in the phosphorylation of hepatic SMAD1/5/8 nor nuclear translocation of the SMAD transcriptional complex was evident despite the iron loading in these animal cells. Skeletal and developmental abnormalities typically associated with mutations in other BMPs were absent, suggesting a specific function for BMP6 in iron homeostasis. BMP6

mRNA is induced in response to iron overload in non-parenchymal cells, but not in hepatocytes of livers obtained from *Hjv*^{-/-} mice and wild-type mice fed a high-iron diet (Enns et al, 2013). Specifically, BMP6 transcripts were significantly increased in sinusoidal endothelial cells and Kupffer cells; hepatic stellate cells show a trend of increased BMP6 mRNA as well. Holotransferrin treatment upregulates BMP6 expression in isolated rat hepatic stellate cells but not hepatocytes. In vitro experiments, however, suggest that BMP6 mRNA is not increased in hepatocytes, hepatic stellate cells, or Kupffer cells in response to treatment with either ferrous sulfate or holotransferrin (Arndt et al, 2010). These studies suggest that non-parenchymal liver cells are the primary source of BMP6 in response to iron. Heterozygous mutations in BMP6 are found in patients with late-onset iron overload from five unrelated families (Daher et al, 2016). All of the mutations involved the BMP6 prodomain, which is known to be crucial for proper BMP6 processing and secretion, and showed a dominant negative effect.

3.4 Tmprss6

Tmprss6 encodes a type II plasma membrane serine protease, also known as matriptase-2, which belongs to a family of cell-surface proteolytic enzymes (Velasco et al, 2002), highly conserved in mammals (Ramsay et al, 2008) and mainly expressed in liver. Recessive mutation in the gene was found to result in microcytic anemia in the *mask* mouse model, a chemically induced mutant also characterized by truncal alopecia (the phenotype for which the mutant mouse had been named) (Du et al, 2008). These mice, which harbor a truncated version of *Tmprss6*, that lacks the protease domain, showed an inappropriately elevated levels of hepcidin and were unable to decrease its levels in response to iron deficiency, suggesting that *Tmprss6* normally functions as a negative regulator of hepcidin expression. Mutations in Tmprss6 are linked to an autosomal recessive disorder named Iron Refractory Iron Deficiency Anemia (IRIDA) associated with inappropriately high hepcidin levels (Du et al, 2008; Finberg et al, 2008; Folgueras et al, 2008). Since the appropriate response to iron deficiency is to decrease hepcidin production to promote intestinal iron absorption, the elevated hepcidin levels in IRIDA reflect the inability to regulate the hormone and, as a consequence of this, the setting of systemic iron deficiency. Moreover, genome-wide association studies have linked common single nucleotide polymorphisms in Tmprss6 to iron status and hemoglobin level, supporting an important role for Tmprss6 in regulating systemic iron homeostasis and normal erythropoiesis (Benyamin et al, 2009; Tanaka et al, 2010).

3.5 HFE

The HFE gene encodes a 343 amino acid protein that consists of a 22 amino acid signal peptide, a large extracellular domain with a putative peptide-binding region ($\alpha 1$ and $\alpha 2$ domains) and immunoglobulin-like domain ($\alpha 3$ domain), a transmembrane region, and a short cytoplasmic portion). There are four cysteine residues that form disulfide bridges in the $\alpha 1$ and $\alpha 2$ peptide-binding domain, and these structures are highly conserved. HFE mRNA is ubiquitously expressed at relatively low levels in tissues, but it is highly expressed by the crypt cells of the duodenum, where is involved, with Tfr1, in recycling endosomes process in the dietary iron absorption. HFE is also highly expressed in hepatocytes and Kupffer cells where it has a regulatory role in liver iron metabolism by sensing the level of body iron stores (Barton et al, 2015). HFE complexes with Tfr1 at the cell surface and is involved in Hpc transcriptional regulation (Goswami et al, 2006).

Several mutations in the HFE gene cause hereditary hemochromatosis (Type 1) (OMIM: 613609). Mice with deletion of *Hfe* in crypt and villous enterocytes have normal plasma iron and transferrin saturation values, normal unbound iron-binding capacity, normal liver and spleen iron concentrations, and normal hepcidin mRNA expression. These observations demonstrate that small intestinal Hfe is not necessary for the physiologic control of systemic iron homeostasis (Vujic et al, 2007). Mice with tissue-specific *Hfe* knockout in macrophages have normal plasma iron measures and normal iron concentrations in liver and spleen (Vujic et al, 2008). This is consistent with observations that wild-type mice subjected to macrophage depletion have normal hepatic iron levels and hepcidin responses to iron challenges (Lou et al, 2005; Montosi et al, 2005). Mice with cell-specific *Hfe* knockout in hepatocytes develop iron phenotypes similar to those of *Hfe*^{-/-} mice, including elevated serum iron and transferrin saturation values, severe hepatic iron accumulation, and reduced splenic iron content. These findings indicate that Hfe must be expressed in hepatocytes to prevent iron overload because it is important for appropriate hepcidin mRNA expression (Vujic et al, 2008).

3.6 Transferrin Receptor 2 (Tfr2)

Mammalian *TFR2* has two alternate spliced transcripts, the α and β forms. The *TFR2- α* gene contains 18 exons; its encodes an 801 amino acid type 2 membrane-integrated glycoprotein that, like Tfr1, consists of cytoplasmic, transmembrane, and large extracellular domains (Kawabata et al, 1999). In contrast, *TFR2- β* mRNA, lacks exons 1 to 3, and encodes a protein without the N-terminal amino acid residues that encode the cytoplasmic, transmembrane, and part of the extracellular domains of Tfr2- α , suggesting that it is a

cytosolic protein (Kawabata et al, 1999). Tfr2 is predominantly expressed in the liver and is localized primarily on the basolateral membrane domain of hepatocytes (Merle et al, 2007). Low levels of the transcript have also been detected in the spleen, small intestine, heart, kidney, and testis (Kawabata et al, 1999).

Tfr2 is not post-transcriptionally regulated by iron through the IRP–IRE system since Tfr2 5' and 3'-UTRs do not contain IRE elements (Fleming et al, 2000). Moreover, the affinity of Tfr2 for holo-Tf is significantly lower than that of Tfr1 (Kd 30 nM vs. 1 nM, respectively; Kawabata et al, 2000; West et al, 2000). In the liver Tfr2 expression increases during mouse development, at variance with Tfr1, and in adult liver Tfr2 is much more expressed than Tfr1 (Kawabata et al, 2001). Tfr2 results to work as a sensor of the systemic iron levels and is able to trigger the response of Hepc to the raise of circulating iron (Goswami et al, 2006). More detailed information about Tfr2 functions will be described below in the following paragraphs. Mutations inactivating of TFR2 gene lead to hemochromatosis (type 3) (OMIM: 604720) (Camaschella et al, 2000), a rare recessive disorder characterized by iron overload, low hepcidin levels (Nemeth et al, 2005) and inability to properly regulate hepcidin after an oral iron challenge (Girelli et al, 2011).

3.6.1 Tfr2 in the liver

In the liver Tfr2 is a sensor of circulating iron, but our knowledge of the Tfr2 hepatic function is still incomplete. It is known that Tfr2 localizes in caveolar micro domains (Calzolari et al, 2006), membrane structures involved in the recruitment of receptors that can be activated by ligand binding (Simons et al, 2000). Also, Tfr2 localizes in lipid raft domains on the exosomal cell membrane and in the absence of holo-transferrin, both Tfr1 and Tfr2 are internalized by clathrin-mediated endocytosis (Chen et al, 2009), but in the presence of the holo-Tf only Tfr2, and not Tfr1, activates ERK1/2 and p38 MAPK. This support the hypothesis that Tfr2 may function as a signaling receptor more than an iron importer (Calzolari et al, 2006; Poli et al, 2010). The current model assumes that Tfr2, in conjunction with HFE, represents a sensor of circulating iron and activates Hepc in response to elevated transferrin saturation (Goswami et al, 2006). More recent data demonstrate that this Tfr2-HFE interaction occurs on the hepatocyte surface within a multiprotein complex, that in vitro includes also HJV (D'Alessio et al, 2012). If this multiprotein complex activates the intracellular signaling to up-regulate hepcidin expression in vivo remains to be demonstrated. Moreover, clinical data preserve the idea of distinct and non-overlapping role of HFE and Tfr2 (Girelli et al, 2011).

3.6.2 Tfr2 animal models

Several Tfr2 targeted animals have been created after the Tfr2 gene cloning. The first Tfr2 animal model was a germinal KO generated by targeted mutagenesis, introducing a premature stop codon Y245X (Fleming et al, 2002) in the murine Tfr2 coding sequence. This mutation is orthologous to the mutation (Y250X) originally detected in humans and responsible of type 3 hemochromatosis (Camaschella et al, 2000). Young (4 week-old) homozygous Y245X mutant mice had high liver iron concentration, even if maintained on a standard diet, in agreement with the observation of early iron overload in patients. The histological distribution of iron recapitulates features of hemochromatosis, with the typical liver periportal accumulation. As in humans, heterozygous animals were normal. Subsequently, different murine models of Tfr2 were developed (Fleming et al, 2002; Wallace et al, 2007), including, among others, Tfr2 total (Tfr2^{-/-}) and liver-specific (Tfr2 LCKO) knock-out (Wallace et al, 2007; Roetto et al, 2010) as well as animals double knockout for Tfr2 and other iron genes (Latour et al, 2016). All these models are characterized by low hepcidin expression and liver iron overload of variable severity. However, when generated in the same genetic background, Tfr2 total knockout was shown to have iron overload more severe than Hfe^{-/-} although less severe than Hfe/Tfr2 double knock out. These observations are in agreement with the suggested distinct but correlated functions of the two proteins in maintaining iron balance. Tfr2^{-/-} mice have slightly less severe iron overload than Tfr2 LCKO (Wallace et al, 2007; Roetto et al, 2010), slightly higher Hb levels (Roetto et al, 2010; Nai et al, 2014) and moderate macrocytosis.

A last model was generated with the M167K substitution in the Tfr2 protein (Roetto et al, 2010): this mutation substitutes the methionine, putative start codon of the beta-isoform of the protein, with a lysine. Tfr2 beta is mostly expressed in the spleen (Kawabata et al, 1999; Roetto et al, 2010). Interestingly, this knock-in model (Tfr2 KI), specifically lacking the beta-isoform, is characterized by normal transferrin saturation, liver iron concentration, hepcidin and BMP6 levels but show a transient anemia at young age. In addition, adult Tfr2KI animals accumulate iron in the spleen due to strong reduction of ferroportin mRNA, thus suggesting a possible regulatory effect of Tfr2 beta on splenic ferroportin expression.

4. IRON METABOLISM IN THE HEART

Cardiac muscle is a major site of oxygen consumption. An adequate intracellular iron pool is essential to its aerobic activity. This is demonstrated by the finding that deletion of cardiac *Tfr1* in mice cause fatal energetic failure in cardiomyocytes, even though systemic iron levels in that setting were maintained (Xu et al, 2015). This highlights the importance of understanding the mechanisms regulating intracellular iron within the heart. Cardiomyocytes express relatively high levels of ferroportin and hepcidin, despite the fact that these cells had no role in systemic iron control (Lakhal-Littleton et al, 2015; Lakhal-Littleton et al, 2016). Recently, the function of these proteins in the heart has been explored using cardiomyocyte specific disruption of the hepcidin/ferroportin axis. Mice carrying a cardiomyocyte-specific deletion of the ferroportin gene develop fatal left ventricular dysfunction by 3 months of age. The dysfunction is caused by a threefold increase of iron levels within cardiomyocytes. Importantly, in ferroportin *-/-* hearts *Tfr1* expression is down-regulated and Ft-L expression is up-regulated but this is not sufficient to prevent iron overload in *Fpn1*-deficient hearts, suggesting that ferroportin-mediated iron release is an essential component of iron homeostasis in the heart (Lakhal-Littleton et al, 2015). In the *Fpn1*-deficient heart, iron is preferentially retained within the cardiomyocytes, whereas in the hemochromatosis type 2b model (*Hamp* *-/-* mouse model) analyzed in the same study, most of the iron is outside of the cardiomyocytes, consistent with the marked upregulation of cardiomyocyte ferroportin in this model. Thus, not only is ferroportin essential for cardiomyocyte iron homeostasis, it also controls the site of deposition of iron in the heart in condition of systemic iron overload. As such, it determines the severity with which cardiac iron deposition affects cardiac function (Lakhal-Littleton et al, 2015).

Also cardiomyocyte-specific deletion of hepcidin results in fatal left ventricular dysfunction in mice between 3 and 6 months of age, despite the maintenance of normal systemic iron levels (Lakhal-Littleton et al, 2016).

Taken together, these results demonstrate that the cardiac hepcidin/ferroportin axis is essential for the heart cells autonomous control of the intracellular iron pool that guaranties a normal cardiac functionality. The cardiac hepcidin/ferroportin axis appears also to protect the heart from the effects of systemic iron deficiency. Cardiac hepcidin protein in fact, is upregulated rather than downregulated by dietary iron restriction in vivo and by iron chelation in vitro, limiting the *Fpn1* function as exporter and preserving in this way intracellular iron amount. Furthermore, animals with hepcidin-deficient hearts develop a

greater hypertrophic response to sustained dietary iron restriction than their littermate controls (Lakhal-Littleton et al, 2016).

This set of data confirm the presence and the importance of Hpc/Fpn1 iron regulatory pathway in maintaining physiological amount of iron in cardiac cells, but very few is known about the regulation of cardiac Hpc production and the proteins involved. In Tfr2 $-/-$ mice only at 52 weeks of age cardiac iron content is modestly elevated compared with WT, but it does not reach statistical significance and levels of hepatic hepcidin relative to hepatic iron store is significantly lower compared to WT (Subramanian et al, 2012)

All the body cells may be susceptible to ROS-induced damage (Chen et al, 2014), but cardiomyocytes are particularly susceptible to ROS-mediated damage. In fact, on the one hand, given the heart's high need of energy, cardiomyocytes are rich in mitochondria and consume large amounts of oxygen; on the other hand, cardiomyocytes have low levels of antioxidant enzymes (Gammella et al, 2015). Therefore, when labile iron pool (LIP) expansion occurs, oxidative stress can affect cardiac functions. The increased synthesis of cardiac ferritin enriched in H subunit (Gammella et al, 2015), represents a response to iron mediated oxidative stress in heart (Arosio et al, 2010).

One of the most frequent pathological process in which iron amount is responsible of clinical complications is the ischemia-reperfusion (I/R) damage due to the production of free oxygen radicals (Bulvick et al, 2012).

In this situation also, synthesis of cardiac ferritin is at the basis of an iron-based mechanism of ischemic preconditioning that protects cardiac cells from iron-mediated oxidative damage associated with ischemia-reperfusion injury (Chevion et al, 2008).

During the PhD course I focused my research to study in deep iron metabolism in the heart, in particular during Ischemia/reperfusion stress stimulus, utilizing three Tfr2 mice models with systemic/tissue specific iron overload (Tfr2 KO, Tfr2 LCKO-KI and Tfr2 KI mice) (Roetto et al, 2010). Furthermore, I was involved in two other iron metabolism projects:

1. analysis of Tfr2 erythropoietic role by evaluating the erythropoiesis of two Tfr2 murine models wherein either one or both of Tfr2 isoforms have been selectively silenced (Tfr2 KI and Tfr2 KO), and in Tmprss6/Tfr2 double KO mice (see 5.2).
2. study the role of Tfr2 in brain iron homeostasis and on the well-known correlation between increased iron amount and neurodegeneration (see 5.3)

In the chapters below I'll described the results obtained studying the role of Tfr2 in iron metabolism in the heart, erythropoietic compartment and brain.

5. EXTRA-HEPATIC ROLE OF Tfr2

5.1 Tfr2 in the heart

Since Tfr2 β resulted to be highly transcribed in heart (Kawabata et al, 1999), as well as Heparin-binding EGF-like motif 1 (Hemojuvelin) (Hamp) (Merle et al, 2007) and Ferroportin 1 (FPN1) (Quin et al, 2007) genes, and two Tfr2 β null mice models were available in our laboratory, during my PhD I investigated if Tfr2 β isoform could have some role in cardiac iron homeostasis and in its changes. The two Tfr2 β null mice models analyzed, namely Tfr2-KI and Tfr2 LCKO-KI mice, were particularly interesting because they are both Tfr2 β null in heart but they have a different systemic iron amount. In fact the first, Tfr2-KI, has normal serum iron parameters, splenic iron overload but normal tissue iron amount in liver, while the latter, Tfr2 LCKO-KI, having also an hepatic silencing of Tfr2 α isoform, has high serum ferritin and transferrin saturation and is a severe hepatic iron overloaded mouse model (Roetto et al, 2010). These differences might help to clarify the relative importance of systemic iron overload on cardiac metabolism. Although the impact of Tfr2 modification on the heart iron concentration (HIC) was unknown, I hypothesized a different cardiac cell survival and resistance to a stressful stimulus, ischemia reperfusion (I/R), in these two models, in particular, a worse response in the iron overloaded model.

One of the procedures that induces a stressful condition in heart is the I/R derived injury. I/R is an experimental technique that mimics the condition of acute myocardial infarction. After a period of ischemia, characterized by the lack of oxygen, a procedure of tissue reperfusion can induce tissue re-oxygenation. Anyway this procedure is able to generate injury since there is the production of reactive oxygen species (ROS) that induce tissue damage.

So I decided to submit to I/R hearts of Tfr2 mouse models Tfr2-KI and Tfr2 LCKO-KI. Surprisingly, they both resulted to be cardio-protected compared to age and sex matched WT sib pairs.

Starting from these data I evaluated if Tfr2 β could have some role in cardiac response to the I/R injury. This has been done investigating:

- 1) if the Tfr2 β production is influenced by I/R in WT mice;
- 2) whether Tfr2 β silencing modifies antioxidant, apoptotic and survival (RISK/SAFE) enzymes activity;
- 3) if pre- and post-ischemic levels of HIC and main iron proteins (Hamp, Fpn1, DMT1, and Ferritins) were modified in hearts of each Tfr2 targeted mice compared to WT controls.

I observed that:

Tfr2 β protein was significantly increased after I/R in WT mice and that the lack of Tfr2 β expression increased cardiac I/R tolerance since the infarct size was significantly reduced in both Tfr2-KI and Tfr2 LCKO-KI mice hearts;

Sham (untreated) hearts of both models resulted to have a higher level of two antioxidant factors, HO-1 and HIF-2a. It is likely that both models have endured a chronic redox/stress condition that led them to react with an increase in cardiac HO-1 and HIF-2a, thus making them protected against subsequent stressful stimuli. This resembles HIF-2a upregulation induced by cardiac ischemic preconditioning, which can be mimicked by the addition of ROS (Bautista et al, 2009). It is well known that the generation of ROS is influenced by iron and that ROS production may play a role either in I/R injury (Bolli et al, 1998; Tullio et al, 2013). On the contrary, Catalase was increased only in Tfr2 LCKO-KI Sham hearts.

The level of pre-ischemic apoptosis was significantly different in the two models since systemic iron overloaded LCKO-KI hearts had an higher level of apoptosis, evidenced by the increase of the pro-antiapoptotic markers BclX-S and BclX-L ratio, while it was absent in Tfr2-KI hearts.

This was in line with an *a priori* iron induced cells damage in Tfr2 LCKO-KI hearts that was absent in Tfr2 KI hearts.

There were no signs of increased apoptosis as a consequence of I/R in both our models

This can be explainable with the time required to develop apoptosis and with the fact that post ischemic cells undergoing apoptosis are relatively few compared to necrotic cells (Ferdinandy et al, 2007).

Furthermore, different modifications of enzymatic setting of RISK and/or SAFE pathways in the two transgenic models were observed. In particular, I observed that the I/R procedure induces an increased phosphorylation of RISK kinases (AKT, ERK 1/2 and PKC ϵ), in Tfr2 KI hearts only. On the contrary, the I/R procedure induces the SAFE pathway element Stat3 phosphorylation in Tfr2 LCKO-KI. Intriguingly, this model responds to I/R with an increased phosphorylation of GSK3 β , a putative down-stream kinase of protective pathways, whose role remains still controversial (Heusch et al, 2009; Lacenda et al, 2009).

I could not quantitatively demonstrate a significant increase in iron amount within the Tfr2 LCKO-KI untreated myocardium, probably because of the limits of the iron amount measurement technique available (Roetto et al, 2010), but several iron proteins, were modified in these animal hearts as it happens when there is an increased cellular iron amount. In fact, Tfr2 LCKO-KI hearts had an increased iron importer DMT1, an increased cardiac Hamp transcription and a decreased cardiac iron exporter FPN1 transcription

compared to WT. Furthermore, a significant increased Ft-L amount was present in these Sham hearts, On the contrary, only Ft-H and Fpn1 were significantly modified in Tfr2-KI Sham.

To this regard, it appeared quite peculiar that the two ferritin subunits were present at different amount in the same Tfr2-KI or Tfr2 LCKO-KI cardiac cells.

However, several recent papers demonstrated that the two Ferritin subunits could be differently regulated as a response to different stimuli (Arosio et al, 2010). Ft-H in particular seems to be more responsive to presence of oxidant agents either in in vitro (Cozzi et al, 2000; Epsztejn et al, 1999) and in ex vivo (Darshan et al, 2009) experiments, while Ft-L subunit appears to respond to cell iron amount through the IRE/IRP system (Muckenthaler et al, 2008). Therefore, Tfr2-KI hearts could be protected by Ft-H higher amount as a response to increased oxidant agents. On the other hand, Tfr2 LCKO-KI hearts could be protected by an increase in Ft-L due to increased “iron stress” by systemic overload in these animals.

From the data obtained, my conclusions are:

- Tfr2 LCKO-KI hearts presented a slightly increased iron amount and an iron induced apoptosis that provoked a preischemic activation of cardioprotective pathway that caused a higher tolerance to acute stress, similarly to that triggered by iron and mediated by ferritin during preconditioning cardiac protection (Chevion et al, 2008).
- Tfr2 KI hearts, in which systemic and cardiac iron level are normal, presented anyway the activation of some antioxidant proteins (Hif2a and HO-1) before I/R and responded to I/R stress through the activation of a cardioprotective pathway (RISK) different from those of Tfr2 LCKO-KI.

Since previous data demonstrated a significant decrease of Fpn1 and an increased iron deposit in splenic macrophages in Tfr2 β null mice (Roetto et al, 2010), Tfr2 β isoform inactivation in the heart could at the same way decrease iron release from cardiac reticuloendothelial cells up-regulating somehow the cardio protective pathway in Tfr2-KI as well (**Boero et al,2015 see attached paper**).

After these results, during my last PhD year I decided to deep inside into the molecular changes that induces cardio-protection in Tfr2 KI hearts mice. Due to the evident iron retention previously found in Tfr2 beta null splenic macrophages (Roetto et al, 2010), I decided to analyze iron amount selectively in macrophages isolated from Tfr2 KI mice hearts compared to WT mice cardiac macrophages. Significant differences were evidenced in the two Ferritin subunits amount in cardiac macrophages and in macrophage-negative cardiac cells fraction. Tfr2 KI cardiac macrophages presented an increased production of FtL vs WT macrophages while Ft-H is comparable in these two experimental groups. On the

contrary, macrophage-negative cardiac cells fraction of Tfr2 KI hearts presented a significant decrease of Ft-H amounts compared to WT cells, with equal Ft-L amount in these two experimental groups. In other words, an enrichment of Ft-L was evidenced both in Tfr2 KI cardiac macrophages and in macrophage-negative cardiac cells fraction compared to WT cells (Fig.5). In both cases this Ft-L subunits enrichment could lead to the production of L ferritin-rich heteropolymers, that are typical of iron deposits Ferritins (Koorts et al, 2007). These data support the hypothesis that Tfr2 KI mice were cardioprotected because iron was entrapped in L-rich ferritins and less available for I/R injuries. It will be worth to perform further studies on isolated cardiomyocytes and immunohistological analysis to better understand the role of iron in heart metabolism and its role during ischemia reperfusion injury.

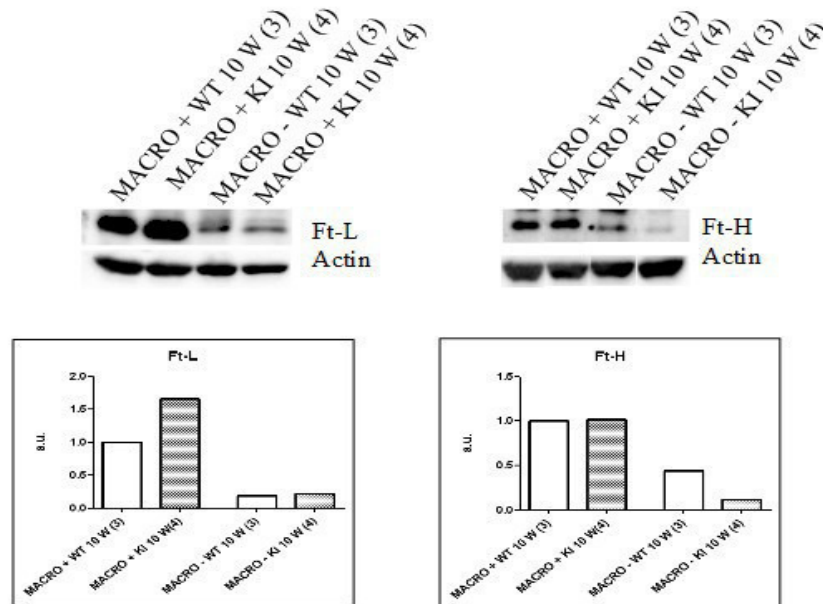


Fig.5

Western blot analysis of Ft-L and Ft-H production in isolated macrophages: Macrophages were isolated from pool of (3-4 hearts of Tfr2 KI and WT mice at 10 weeks of age using Cd11b+ beads. In WB both positive fraction (MACRO +) and negative fraction (MACRO -) were analyzed. No error bar was indicated because only one sample (pool of 3-4 hearts) was used for every cell types.

Research Communication

A comparative study of myocardial molecular phenotypes of two Tfr2 β null mice: Role in ischemia/reperfusion

Martina Boero^{1†}
Pasquale Pagliaro^{1,2†*}
Francesca Tullio^{1,2}
Rosa M. Pellegrino¹
Antonietta Palmieri¹
Ludovica Ferbo¹
Giuseppe Saglio¹
Marco De Gobbi¹
Claudia Penna^{1,2†}
Antonella Roetto^{1†*}

¹Department of Clinical and Biological Sciences, University of Torino, AOU San Luigi Gonzaga, Orbassano, Torino, Italy

²Cardiovascular Physiology Lab (Torino), National Institute for Cardiovascular Researches (INRC), Bologna, Italy

Abstract

Transferrin receptor 2 (Tfr2) is an iron-modulator transcribed in two isoforms, Tfr2 α and Tfr2 β . The latter is expressed in the heart. We obtained two mouse models with silencing of Tfr2 β : one with a normal systemic iron amount (SIA), *i.e.*, Tfr2-KI, and the other, *i.e.*, LCKO-KI, with high SIA due to hepatic Tfr2 α silencing. We aimed to assess whether Tfr2 β might play a role in myocardial injury and whether Tfr2 β silencing might modify proteins of iron metabolism, antioxidant, apoptotic, and survival enzyme activities in the heart undergoing ischemia/reperfusion (I/R).

Isolated hearts of wild-type (WT) and Tfr2-null mice were studied before or after an I/R protocol, and proteins/RNA analyzed by Western blot and/or quantitative PCR.

Tfr2 β increased in WT hearts subject to I/R, and both Tfr2 β null mice hearts were protected against I/R injury (about 40% smaller infarct-size compared to WT hearts). RISK kinases

(ERK1/2-AKT-PKC ϵ) were found up-regulated after I/R in Tfr2-KI, whereas SAFE enzyme (Stat3) and GSK3 β resulted phosphorylated during I/R in LCKO-KI hearts. While HO-1 and HIF-2a were high in both Tfr2 β -null mice, Catalase, and proapoptotic factors were upregulated only in LCKO-KI. Finally, Tfr2-KI hearts presented an increased Ferritin-H and a decreased Ferroportin1, whereas LCKO-KI hearts displayed an upregulation of Ferritin-L chain and DMT1/Hamp-RNA.

In conclusion, Tfr2 β isoform is involved in cardiac iron metabolism and its silencing leads to a protected phenotype (antioxidants, RISK, and/or SAFE upregulation) against I/R challenging. Iron-dependent signals involved in cardioprotection seem to be positively affected by Tfr2 β downregulation and subsequent Ferritins upregulation. © 2015 BioFactors, 41(5):360–371, 2015

Keywords: ferritin; iron; RISK; SAFE; transferrin receptor; transgenic model

Abbreviations: DMT1, divalent metal transporter 1; ERK 1/2, extracellular-signal-regulated kinases 1/2; FtH, ferritin H; FtL, ferritin L; Fpn1, ferroportin 1; GSK3 β , glycogen synthase kinase 3 β ; HIC, heart iron concentration; HO-1, heme oxygenase-1; Hamp, hepcidin; HIF-2a, hypoxia-inducible factor-2a; IS, infarct size; IRE/IRP, iron responsive elements/iron regulatory proteins; I/R, ischemia/reperfusion; PKB or AKT, protein kinase B; PKC ϵ , protein kinase C ϵ ; ROS, reactive oxygen species; RISK, reperfusion injury salvage kinases; Stat3, signal transducer and activator of transcription 3; SOD1, superoxide dismutase; SAFE, survivor activating factor enhancement; SIA, systemic iron amount; Tfr2, transferrin receptor 2; WT, wild-type

© 2015 International Union of Biochemistry and Molecular Biology

Volume 41, Number 5, September/October 2015, Pages 360–371

*Address for Correspondence: Pasquale Pagliaro, MD, PhD, Department of Clinical and Biological Sciences, University of Torino, AOU San Luigi Gonzaga, Regione Gonzole 10, 10043 Orbassano, Italy. Phone number: +390116705450, fax number: +390119038639, and E-mail: pasquale.pagliaro@unito.it (or) Antonella Roetto, PhD, Department of Clinical and Biological Sciences, University of Torino, AOU San Luigi Gonzaga, Regione Gonzole 10, 10043 Orbassano, Italy. E-mail: antonella.roetto@unito.it.

Received 7 July 2015; accepted 5 September 2015

[†]These authors contributed equally to this work.

DOI 10.1002/biof.1237

Published online 13 October 2015 in Wiley Online Library
(wileyonlinelibrary.com)

1. Introduction

Iron is essential for the optimal functioning and survival of living beings. It is indispensable for the maintenance of cellular energy and metabolism of all tissues [1]. However, when iron accumulates in cells, it contributes to reactive oxygen species (ROS) formation through the Fenton/Haber-Weiss reactions generating oxidative stress [2,3]. Heart, together with liver, duodenum and bone marrow, is an organ in which iron metabolism must be tightly regulated. In fact, individuals with iron overload associated diseases, like hemoglobinopathy and hemochromatosis, can present signs of heart failure [4].

TFR2 (Transferrin Receptor 2) is a gene involved in iron metabolism transcribed in two main isoforms: the hepatic- and erythroid-specific full length Tfr2 α and the ubiquitous shorter form Tfr2 β [5]. In the liver, it is a regulator of hepatic hepcidin (Hamp) protein, the hormone that control iron systemic availability inhibiting the functionality of the cellular iron exporter Ferroportin 1 (Fpn1) [6]. On the contrary, the Tfr2 β isoform is expressed in all tissues [5] and its function it is not well understood yet. It seems to be involved in Fpn1 transcription up-regulation, although is not involved in direct iron export from cells [7].

Since Tfr2 β resulted to be highly transcribed in heart [5], as well as Hepcidin (Hamp) [8] and Fpn1 [9] genes, we planned to investigate if Tfr2 β isoform could have some role in cardiac iron homeostasis and in myocardial injury during stress. To this aim, two animal models, Tfr2-KI and Tfr2 LCKO-KI, with germinal and conditional silencing of the Tfr2 gene isoforms [7] were produced. The two Tfr2-targeted mice have a germinal silencing of Tfr2 β isoform, whereas Tfr2 LCKO-KI animals have also hepatic selective silencing of the Tfr2 α .

Therefore in hearts these two mice models are both Tfr2 β null, but they have a different systemic iron amount. In fact the first, Tfr2-KI, has normal serum iron parameters while the latter, Tfr2 LCKO-KI has high serum ferritin and transferrin saturation [7]. Accordingly, Tfr2 LCKO-KI is a severe hepatic iron overloaded mouse model, whereas Tfr2-KI has normal tissue iron amount in liver but increased iron deposit in spleen [7]. These differences may help to clarify the relative importance of systemic iron overload in cardiac response to stress. Although it is unknown the impact of these Tfr2 gene modifications on the heart iron concentration (HIC), we hypothesized a different cardiac cell survival and resistance to stressful stimuli in these two models. In particular, we hypothesized that the iron overloaded model is more prone to cardiac damage due to iron-dependent redox stress.

To test these hypotheses and to explore the relevance of Tfr2 β in cardiac iron content and metabolism we used Ischemia/Reperfusion (I/R) protocol as a stress stimulus in hearts of Tfr2-KI and Tfr2 LCKO-KI mice as well as in WT mice hearts.

Several studies, in the setting of I/R evolving to myocardial infarction, have demonstrated that cardioprotection involves cell metabolism modifications and that it is mainly mediated by the activation of two independent or cross-talking cardioprotective redox sensible pathways in which iron may play a role:

Reperfusion Injury Salvage Kinases (RISK) that includes AKT/PKB and ERK1/2, and Survivor Activating Factor Enhancement (SAFE) that involves Signal Transducer and Activator of Transcription 3 (Stat3) [10–16]. Moreover, the up-regulation of RISK and/or SAFE kinases has also been observed in transgenic mice for different proteins, which resulted endogenously preconditioned and protected from I/R damage [12,17].

Furthermore, since endogenous enzymes regulate the homeostasis of ROS with an iron dependent mechanism, we studied in our models of I/R the expression of superoxide dismutase (SOD1) and Catalase, which are well known anti-oxidant enzymes involved in the conversion of superoxide radical ($O_2^{\cdot-}$) to hydrogen peroxide (H_2O_2) and in the maintenance of steady-state levels of H_2O_2 , respectively [18,19]. Moreover, to deepen cardiac iron dependent redox setting, before and after I/R procedure, we analyzed HO1 and HIF-2a, whose levels have been demonstrated to be influenced by iron dependent redox conditions [20,21]. Finally, since apoptosis is tightly correlated to redox stress, anti-apoptotic and proapoptotic enzymes have been considered.

Therefore the aims of this study were 1) to evaluate if Tfr2 β production is influenced by I/R in WT mice, 2) to assessed if the lack of Tfr2 β expression (with and without systemic iron overload) induces some variation on I/R injury in isolated hearts, 3) to investigate whether Tfr2 β silencing modifies antioxidant, apoptotic, and survival (RISK/SAFE) enzymes activity; 4) to analyze preischemic and postischemic levels of HIC and main iron proteins (Hamp, Fpn1, DMT1, HIF-2a, and Ferritins) in hearts of each Tfr2 targeted mice compared with WT controls.

2. Experimental Procedures

2.1. Animals

Male 10 week old wild-type (WT, sv 129) and transgenic Tfr2 β null, KI and LCKO-KI (Tfr2 liver KO mice in a KI background) mice received humane care in compliance with Italian law (DL-26, Mar 04, 2014) and in accordance with the EU Directive 2010/63/EU and approved by the University of Turin Ethical Committee for animal research and by the Italian Ministry of Health. All efforts were made to minimize suffering. Animals plasmatic transferrin saturation was calculated as a ratio of serum iron and total iron binding capacity levels (Randox Laboratories Ltd., UK).

Tfr2 transgenic mice (KI and LCKO-KI) and WT sib-pairs weighing between 20 and 30 g were given 500 U heparin and anesthetized (Tribromoethanol; Sigma-Aldrich; 50 mg/kg) by intra-peritoneal injections before being culled by cervical dislocation [22].

2.2. Isolated Heart

Hearts were rapidly excised and retrogradely perfused at 80 mm Hg by the Langendorff technique with Krebs–Henseleit bicarbonate buffer containing (mM) NaCl 118, $NaHCO_3$ 25, KCl 4.7, KH_2PO_4 1.2, $MgSO_4$ 1.2, $CaCl_2$ 1.25, and Glucose 11. The buffer was gassed with 95% O_2 , 5% CO_2 . The temperature of the perfusion system was maintained at 37 °C. The perfusate



flowing out of the heart was collected and measured [12,23]. At the end of experimental protocol, hearts were used for molecular analyses and infarct size assessment (see below).

2.2.1. Experimental protocol

To have a reference group (WT I/R, $n = 6$), hearts were harvested from the WT animals, perfused, and allowed to stabilize for 30-min. After stabilization period, hearts were subjected to a protocol of I/R, which consisted in 30-min of global no-flow, normothermic ischemia, and a period of 60-min of reperfusion [12].

Similarly transgenic hearts (KI I/R, $n = 7$; and LCKO-KI I/R, $n = 5$) were perfused for a 30-min stabilization period, then global normothermic ischemia was applied by eliminating flow for 30-min, which was followed by 60-min reperfusion [12].

2.2.2. Infarct size assessment

Infarct areas were assessed at the end of the experiments with the nitro-blu-tetrazolium technique in a blinded fashion, as previously described [12]. In brief, immediately after reperfusion hearts were removed from the perfusion apparatus and the left ventricle (LV) dissected by transverse sections into three slices (<1 mm slices). Following 20 min of incubation at 37 °C in 0.1% solution of nitro-blu-tetrazolium (Sigma-Aldrich) in phosphate buffer, unstained necrotic tissue was carefully separated from stained viable tissue by an independent observer, who was unaware of the protocols. The necrotic mass was expressed as a percentage of risk area (*i.e.*, total left ventricular mass) [12].

2.3. Molecular Biology Analysis

Five additional hearts of each group (WT I/R, KI I/R, and LCKO-KI I/R) underwent I/R protocols and used for molecular studies. Moreover, five hearts of each group (WT Sham, KI Sham, and LCKO-KI Sham) after 30-min stabilization underwent 90-min buffer-perfusion only and served as reference nonischemic groups for molecular studies. Frozen LV of I/R and Sham groups were used for Western blot and/or quantitative PCR analysis of iron protein tool kit (*i.e.*, Ferritins, Hamp, Fpn1, DMT1, HO-1, and HIF-2a), antioxidants (Catalase and SOD1), apoptotic or RISK (AKT, ERK1/2; PKC ϵ and GSK3 β), and SAFE (Stat3 and GSK3 β) elements (see also below).

2.3.1. Real time quantitative PCR analysis

For reverse transcription, 1 μ g of total RNA, 25 μ M random hexamers, and 100 U of reverse transcriptase (Applera) were used. Gene expression levels were measured by real-time quantitative PCR in an iCycler (Bio-Rad) using commercial assays (Assays-on Demand; Applied Biosystems) for Hamp and Fpn1 gene transcription evaluation. β -actin gene was utilized as housekeeping control. The results were analyzed using the $\Delta\Delta^{\text{Ct}}$ method [24]. All analyses were carried out in triplicate; results showing a discrepancy greater than one cycle threshold in one of the wells were excluded.

2.3.2. Western blot analysis

For Western blotting, hearts were lysed in Tris-buffered saline with 1% Triton X-100 plus (1% SDS added for Tfr2 β protein WB), complete protease inhibitor cocktail (Roche). Protein extracts

were clarified with three sequential centrifugations for 20 minutes at 20,000 g, at 4°C. Between 50 and 100 μ g of proteins from homogenized heart tissue were electrophoresed in 8% to 10% SDS polyacrylamide gel electrophoresis and immunoblotted according to standard protocols. Antibodies against the following proteins were used: AKT, p-AKT(Ser473), GSK3 β , pGSK3 β (Ser9), PKC ϵ , pStat3 (Tyr705) (Cell Signaling); ERK1/2, pERK1/2 (Thr202), Stat3 (F-2), Tfr2 S-20, Transferrin Receptor 1 (Tfr) (H300), Gapdh (A3), DMT1 (H-108) HO-1 (H-105) and BCL-XL (H-S) (Santa Cruz Biotechnology); pPKC ϵ (Ser729) SOD1, and Catalase (Thermo Scientific). HIF-2a antibody (HIF-2A11-A) was from Alpha Diagnostic. Antibodies against the two isoforms of Ferritin (FtH and FtL) were kindly provided by Sonia Levi, University of Vita Salute, Milan, Italy. Protein quantification was done using Protein Assay (Biorad). In brief, WB were developed utilizing clarity western ECL substrate (Biorad) and the chemidoc XRS+Instrument (Biorad). Proteins amount, evidenced by band intensity, was measured by densitometry with a band quantification software (Image lab software, Biorad). Each protein amount was normalized for its own Gapdh amount and final protein quantification were obtained as the mean of all the samples analyzed for each of the 6 experimental group and expressed as fold increase, relative to the mean obtained from the WT mice.

Gapdh is considered an appropriate loading control as it has been shown to change under iron deficiency, but not under iron normal/overload conditions [25], which are typical conditions of our experimental models.

2.4. Cardiac Iron Content

HIC was assessed according to standard procedure [7] using 20 mg of dried LV. A minimum of 5 samples have been analyzed for each Sham and I/R group.

2.5. Statistical Analysis

Statistical significance of the differences between Sham WT and each Sham targeted mice was evaluated using a Student *t* test (unpaired, 2 tailed). In addition, significance of the differences between the two I/R groups or between I/R and correspondent Sham group was evaluated using a Student *t* test (unpaired, 2 tailed). Results are shown as medium values \pm standard error. $P < 0.05$ was considered significant.

3. Results

We confirmed that Tfr2 targeted mice used in these experiments present the same phenotype of the original report [7]. In particular, transferrin saturation resulted normal ($30 \pm 5\%$) in Tfr2-KI and very high ($80 \pm 12\%$) in Tfr2 LCKO-KI, thus confirming the condition of iron overload in the latter model.

3.1. Role of Tfr2 β in Myocardial Injury

To ascertain whether or not Tfr2 β may play a role in myocardial injury, we studied how Tfr2 β expression changes immediately after I/R experiment in WT (Fig. 1). As shown in Fig. 1a, I/R procedure significantly increased Tfr2 β protein level compared to Sham.

To evaluate the effect of the absence of *Tfr2 β* on myocardial I/R injury, we measured infarct size in WT, *Tfr2*-KI, and LCKO-KI hearts (Fig. 1b). Total infarct size is expressed as a percentage of LV mass. As shown in Fig. 1b, infarct size was significantly lower in *Tfr2*-KI (infarct size $37 \pm 6\%$, $P < 0.05$) and LCKO-KI ($36 \pm 6\%$, $P < 0.05$) compared with WT hearts ($58 \pm 3\%$). Moreover, apoptosis has been evaluated through analysis of apoptotic markers BCL-X as a ratio of BCL-XS (proapoptotic) and BCL-XL (antiapoptotic) isoforms [26], in Sham and I/R conditions. BCL-X S/L ratio resulted to be decreased in *Tfr2*-KI and increased in *Tfr2* LCKO-KI Sham hearts compared with WT (Fig. 1c). Yet, levels of proapoptotic factor were not modified by acute I/R protocols.

Therefore, both *Tfr2 β* null mice hearts were protected against I/R injury (about 40% smaller infarct-size in transgenic models compared to WT hearts; Fig. 1b), regardless the difference in terms of apoptosis in baseline conditions.

3.2. Identification of Cellular Pathways of Protection in *Tfr2 β* Null Hearts

3.2.1. Cardioprotective enzyme HO-1 is increased in *Tfr2 β* null mice hearts

Heme oxygenase-1 (HO-1) is an enzyme involved in heme catabolism that increases in response to oxidative stress [27]. It has been demonstrated to have a role as a marker of cytoprotection [28] and in particular to be cardioprotective against I/R injury [29]. HO-1 resulted to be significantly higher in both *Tfr2 β* null mice Sham hearts compared with WT hearts. Moreover HO-1 levels were significantly lower in KI I/R hearts with respect to KI Sham only (Fig. 1d).

3.2.2. HIF2a is upregulated in hearts of transgenic models and changes differently in WT and *Tfr2* targeted animals after I/R

Since Hypoxia-Inducible Factor-2a (HIF2a) levels are influenced by iron, ROS and hypoxia, we analyzed the levels of HIF2a with and without I/R in our models (Fig. 1e). HIF2a protein resulted upregulated in both *Tfr2 β* null Sham hearts ($P < 0.05$ vs. WT Sham). However, after I/R procedure, while HIF2a tended to increase in WT, it decreased in *Tfr2*-KI ($P < 0.01$ vs. KI Sham) and tended to decrease in LCKO-KI (Fig. 1f).

3.3. RISK and SAFE In Nonischemic and Ischemic Hearts

To assess possible mechanisms involved in cardioprotection exerted by the lack of *Tfr2 β* in *Tfr2*-KI and LCKO-KI, enzymes of major prosurvival signaling pathways were investigated by Western blot analysis in samples collected from hearts subjected to I/R stress or Sham perfusion.

3.3.1. RISK and/or SAFE are minimally altered in Sham hearts of transgenic models

In the three Sham groups, ERK1/2, AKT, and PKC, as well as Stat3 and GSK3 β (RISK- and SAFE-pathways) displayed similar phosphorylation ratios (Figs. 2 and 3). However some peculiarities were found, while ERK 1/2 resulted significantly lower ($P < 0.01$) in the

Sham groups of *Tfr2*-KI compared with WT, Stat3 resulted significantly lower ($P < 0.05$) in LCKO-KI Sham group (Fig. 3a).

3.3.2. RISK and/or SAFE are activated by I/R in transgenic models

We then analyzed the effect of I/R in the RISK- and SAFE-pathways (Figs. 2 and 3). As shown in Fig. 2, whereas in WT the I/R protocol induced a reduction of ERK1/2 phosphorylation ($P < 0.001$ vs. WT Sham, panel a), in *Tfr2*-KI an increase of ERK1/2, AKT, and PKC ϵ phosphorylation (panels a, b, and c), was seen after I/R compared with the Sham group ($P < 0.05$ vs. KI Sham). Moreover, in LCKO-KI, phosphorylation of Stat3 (Fig. 3a), a crucial factor of the SAFE pathway, and phosphorylation of the down-stream kinase GSK3 β (Fig. 3b) were induced by I/R ($P < 0.01$ vs. LCKO-KI Sham groups).

3.4. Antioxidants, Iron Content, and Iron Proteins in Nonischemic and Ischemic Hearts

3.4.1. Antioxidant enzymes are differently regulated in *Tfr2 β* null mice

Intriguingly, the level of the antioxidant Catalase resulted significantly higher ($P < 0.05$) in *Tfr2* LCKO-KI Sham and I/R as compared with WT (Sham and I/R) and KI hearts (Fig. 4). On the contrary, the levels of SOD1 were not significantly modified (data not shown).

3.4.2. Cardiac iron proteins change as a consequence of *Tfr2* targeting and after I/R procedure in WT and transgenic models

Transcription analysis of Cardiac Hamp and Fpn1 revealed that *Tfr2*-KI and LCKO-KI presented different Hamp and Fpn1 levels in untreated mice hearts (Sham) compared to WT Sham and different responses to the I/R procedure. In particular, Hamp transcription was higher in LCKO-KI Sham hearts compared with WT hearts ($P < 0.05$; Fig. 5a). On the contrary, cardiac Fpn1 transcription was lower in both *Tfr2*-KI and LCKO-KI Sham hearts compared to WT Sham hearts ($P < 0.05$ vs. KI only; Fig. 5b).

I/R procedure did not influence significantly Hamp and Fpn1 transcription; however, Hamp transcription tended to increase in the three groups (Fig. 5a), whereas Fpn1 transcription tended to decrease in WT and *Tfr2* LCKO-KI hearts only (Fig. 5b).

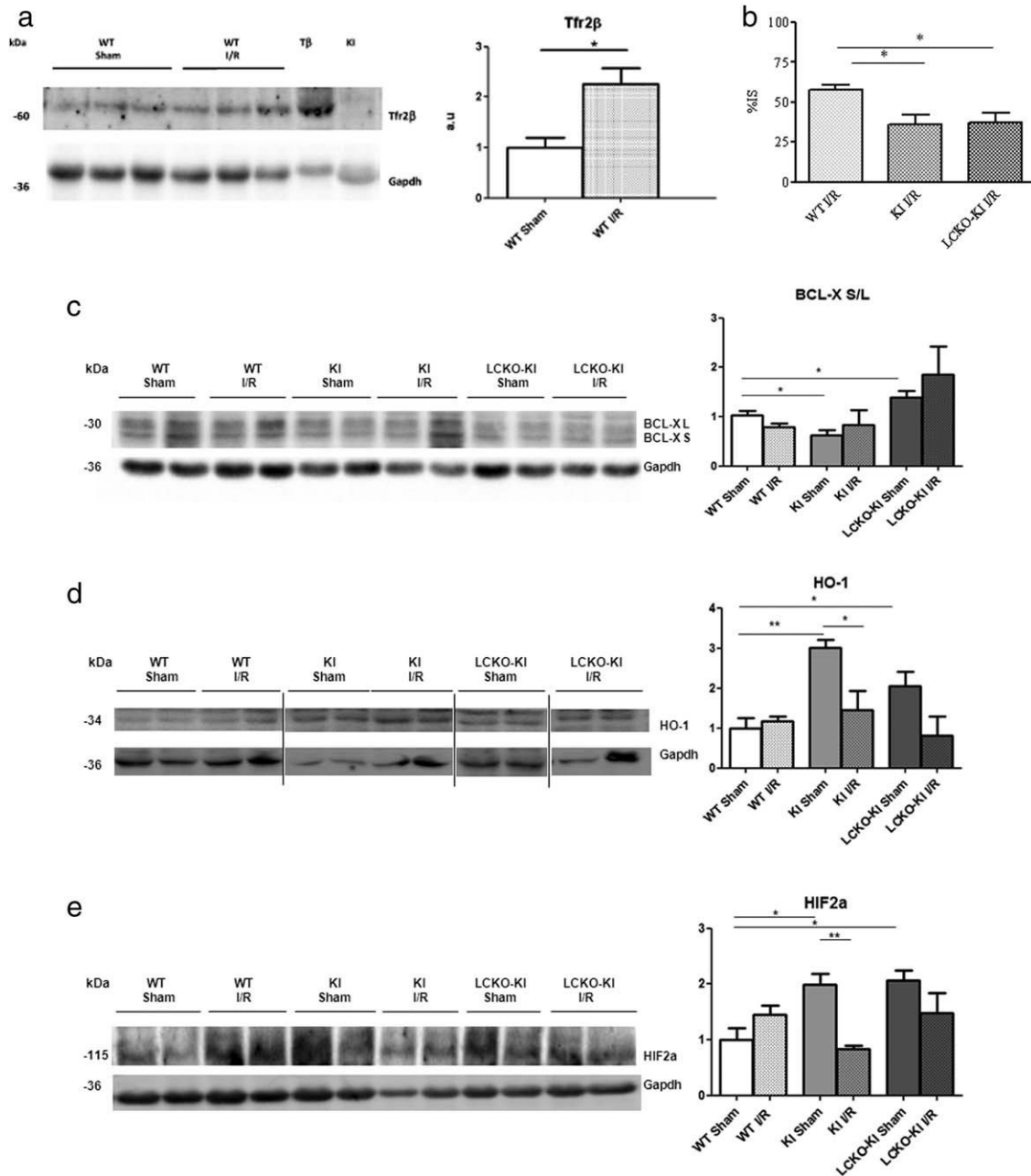
No significant variation could be seen in cardiac Fpn1 protein amount in Sham and I/R (not shown) while iron importer Divalent Metal Transporter 1 (DMT1) resulted to be significantly increased only in *Tfr2* LCKO-KI Sham and I/R hearts (Fig. 5c).

3.4.3. HIC tends to vary differently in WT And *Tfr2* targeted animals after I/R

HIC evaluation did not reach significant differences among different groups. However, after I/R procedure there was a tendency to a lower HIC in WT and LCKO-KI hearts compared with their Sham group (Fig. 6a).

3.4.4. Ferritin H and L change differently in the two *Tfr2* targeted animals

Ferritin H (FtH) amount revealed a significant increase in *Tfr2*-KI Sham hearts vs. WT Sham ($P < 0.05$, Fig. 6b). On the contrary Ferritin L (FtL) tended to be higher in LCKO-KI Sham


FIG 1

Molecular detection of *Tfr2β* in WT mice in Sham and after I/R protocols. Infarct size and molecular detection of *BCL-X S/L*, *HO-1*, and *HIF-2a* in WT and *Tfr2* targeted mice in Sham and after I/R protocols. (a) Western blot (WB) analysis for *Tfr2 β* was performed on lysate from LV collected at the end of protocols in Sham and I/R WT animals. An increase of *Tfr2β* is observed in WT I/R mice vs. WT Sham. Tβ: transfected *Tfr2β* isoform used as positive control. (b) Infarct size (IS), expressed as percentage of LV, resulted smaller in Transgenic models compared with WT I/R mice. ($n=5-7$; see Methods). (c) WB analysis for *BCL-X S/L* is obtained as ratio between S and L subunits production. (d and e) WB analysis for *HO-1* and *HIF-2a* were performed on lysates from LV collected at the end of protocols WT and targeted mice (KI and LCKO-KI). Graph represents the densitometric analysis of protein normalized to *Gapdh* and reported as relative fold increase. Blots images: vertical lines indicate images taken from different gels. All WB analyses were carried out in triplicate. * $P < 0.05$, ** $P < 0.01$.

hearts vs. WT Sham ($P = 0.09$, Fig. 6c). Although FtL in LCKO-KI I/R resulted higher than WT I/R, the I/R procedure did not influence significantly the amounts of the two Ferritins when compared with Sham groups, in the three models.

4. Discussion

We aimed to study the putative role of *Tfr2β* isoform in hearts using *Tfr2β* null animal models and determining molecular

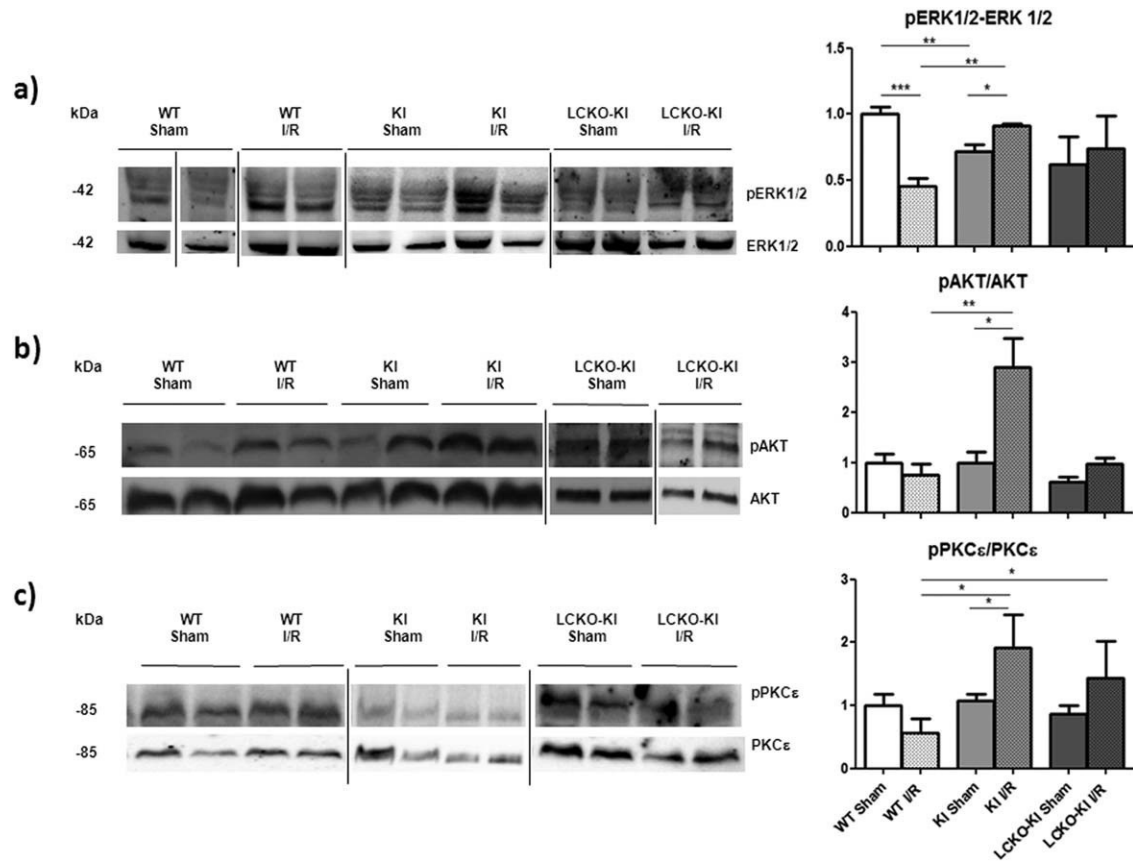


FIG 2 Molecular detection of RISK pathway in WT and *Tfr2* targeted mice, in Sham and after I/R protocols. Western blot analysis was performed on lysates from LV collected at the end of protocols of WT and targeted mice (KI and LCKO-KI). RISK pathway proteins investigated: (a) ERK1/2; (b) AKT, and (c) PKCε. Graphs represent the densitometric analysis of phosphorylated proteins normalized to total proteins and reported as relative fold increase. Blots images: vertical lines indicate images taken from different gels. All analyses were carried out in triplicate. *P < 0.05, **P < 0.01, ***P < 0.001.

phenotype of the myocardium before and after a stress challenging, namely I/R. This study strongly indicates that while hearts of WT mice exposed to I/R increase the expression of *Tfr2β*, hearts of *Tfr2β* null mice modify the molecular phenotype and display an increased tolerance to I/R challenging.

TFR2 is a gene that codifies for two proteins (*Tfr2α* and *Tfr2β*) involved in iron metabolism whose mutations are observed in type 3 hemochromatosis (HFE3), an iron overload genetic disorder [30]. *Tfr2β* in particular, is a protein well expressed in cardiac tissue [5] whose function is related to modulation of iron export from cells regulating the transcription of iron exporter *Fpn1* [7], while *Tfr2α* is an iron sensor that contribute to the hepatic regulation of iron inhibitor hepcidin (*Hamp*) [6].

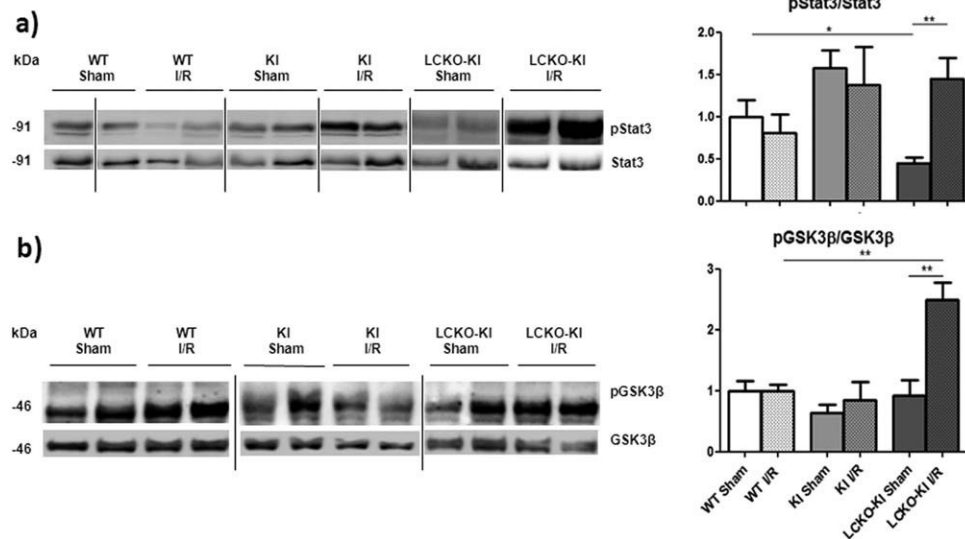
Tfr2-KI and *Tfr2* LCKO-KI animal models present germinal and conditional silencing of the *Tfr2* gene isoforms (*Tfr2α* and *Tfr2β*) [7]. Both the *Tfr2* targeted mice, in fact, have a germinal silencing of *Tfr2β* isoform, but *Tfr2* LCKO-KI animals have an additional hepatic selective silencing of the *Tfr2α* isoform as well. While *Tfr2*-KI mice have normal liver iron amount and normal serum iron parameters (serum ferritin and transferrin saturation), LCKO-KI mice have a severe hepatic iron overload and increased serum iron parameters [7].

Since hearts from *Hfe KO* mice, another animal model of systemic iron overload, had an higher damage after I/R procedure [31], we decided to investigate if cardiac iron metabolism perturbation due to *Tfr2β* targeting had some effect on I/R damage, regardless whether hearts have been or not exposed to a systemic iron overload.

We have found, for the first time, that: 1) *Tfr2β* protein is significantly increased after I/R in WT mice and that the lack of *Tfr2β* expression increased cardiac I/R tolerance, irrespective of systemic iron overload which triggers signs of preischemic apoptosis; 2) while *Tfr2β* silencing does not modify HIC levels, it modifies the expression of main iron proteins; 3) *Tfr2β* silencing modifies levels of antioxidants, and iron-oxygen dependent enzymes (HO1 and HIF-2a), and the activity of survival (RISK/SAFE) kinases (Table 1).

Although the levels of systemic iron amount are different in the two strains, both *Tfr2β* null mice result to have a different cardioprotected-like molecular phenotype.

Indeed, the systemic iron overload affects the level of preischemic apoptosis and, in fact, signs of apoptosis level (BCL S/L) were higher in *Tfr2* LCKO-KI hearts than *Tfr2*-KI. The increased levels of pro-apoptotic factors present in *Tfr2* LCKO-KI hearts


FIG 3

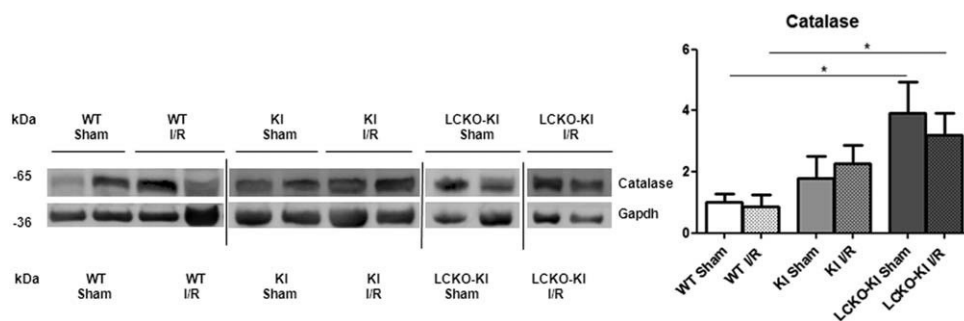
Molecular detection of SAFE pathway and GSK3 β in WT and Tfr2 targeted mice in Sham and after I/R protocols. Western blot analysis was performed on lysates from LV collected at the end of protocols of WT and targeted mice (KI and LCKO-KI). SAFE pathway proteins investigated are (a) Stat3 and (b) GSK3 β . Graphs represent the densitometric analysis of phosphorylated proteins normalized to total proteins and reported as relative fold increase. Blots images: vertical lines indicate images taken from different gels. All analyses were carried out in triplicate. *P < 0.05, **P < 0.01.

might be explained by a cell damage due to slight/transient cellular iron overload repeated over time (see below). Nevertheless, after I/R protocol, the infarct size is significantly reduced in both Tfr2 β null mice and these results are associated to different modifications of iron proteins, enzymatic setting and activation of HO-1, HIF-2a and RISK and/or SAFE pathways in the two transgenic models in response to I/R (see below). Yet, there are no signs of increased apoptosis after I/R in the two models. This can be explainable with the time required to develop apoptosis and with the fact that postischemic cells undergoing apoptosis are relatively few compared to necrotic cells [32].

Although we performed repeated measure of HIC, we could not quantitatively demonstrate an increase in iron amount within the myocardium, but several iron proteins are modified in Tfr2 LCKO-KI hearts. This is in line with a modified cellular iron trafficking that may cause transient iron

stress, repeated over time. In fact, Tfr2 LCKO-KI hearts have an increased iron importer DMT1, an increased cardiac Hamp transcription and a decreased cardiac iron exporter Fpn1 transcription (Table 1), which all together may induce a transient iron overload.

Previous data in splenic macrophages demonstrated the transcriptional correlation between Tfr2 β and the iron exporter Fpn1, since in Tfr2 β null mice a significant decrease in Fpn1 transcription was observed [7]. The Tfr2 β -dependent Fpn1 regulation is also confirmed in heart. In fact, Fpn1 transcription is lower in both Tfr2 β null mice. Therefore, Tfr2 β isoform inactivation could decrease iron release from cells up-regulating somehow the protective pathway including main iron proteins Ferritins (FtH and FtL). These proteins resulted specifically increased even in untreated Tfr2 β null mice, as also found in preconditioned hearts [33]. Actually, a significant


FIG 4

Molecular detection of Catalase in WT and Tfr2 targeted mice in Sham and after I/R protocols. Western blot analysis was performed on lysates from LV collected at the end of protocols of WT and targeted mice (KI and LCKO-KI). Graphs represent the densitometric analysis of proteins normalized to Gapdh and reported as relative fold increase. Blots images: vertical lines indicate images taken from different gels. All analyses were carried out in triplicate. *P < 0.05.

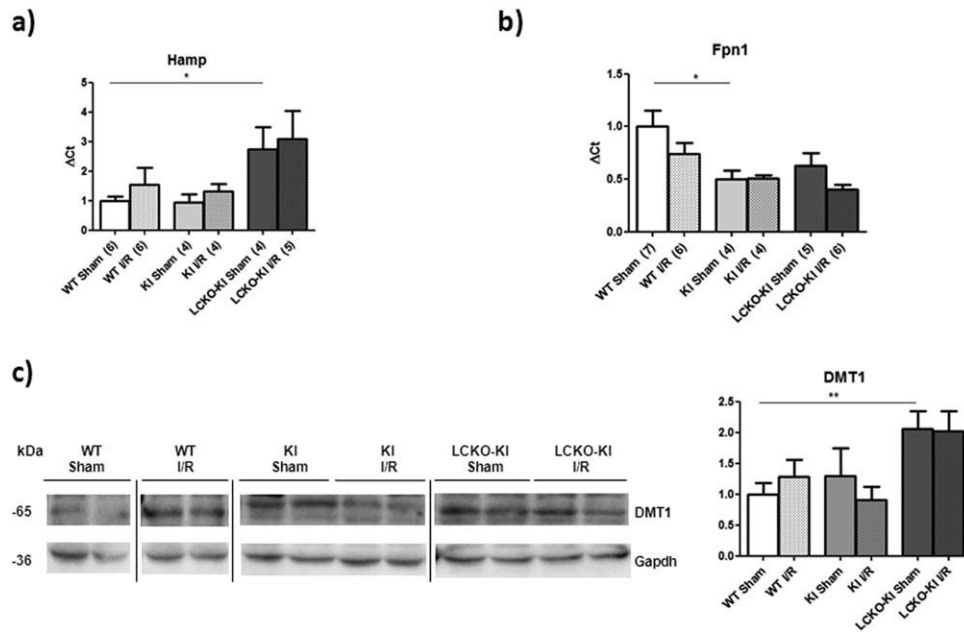


FIG 5

Cardiac iron genes expression and molecular detection of DMT1 in WT and Tfr2 targeted mice in Sham and after I/R protocols. Cardiac relative expression of iron genes (a) Hamp and (b) Fpn1. Gene expression analysis was performed on LV collected at the end of protocols of WT and targeted mice (KI and LCKO-KI). (c) DMT1 Western blot analysis was performed on lysates from LV collected at the end of protocols of WT and targeted mice (KI and LCKO-KI). Graph represents the densitometric analysis of protein normalized to Gapdh and reported as relative fold increase. Blots images: vertical lines indicate images taken from different gels. All analyses were carried out in triplicate. ** $P < 0.01$.

increased FtL amount is present in LCKO-KI hearts, probably as a response to the increased free cellular iron through the Iron Responsive Elements/Iron Regulatory Proteins (IRE/IRP) system [21]. This particular result is in agreement with the reported increase of brain FtL transcripts in iron-supplemented mice, which displayed no changes in gross brain iron content [34]. Therefore, our conclusion is that Tfr2 LCKO-KI hearts display a higher tolerance to I/R stress, similarly to that triggered by iron and mediated by ferritin [35].

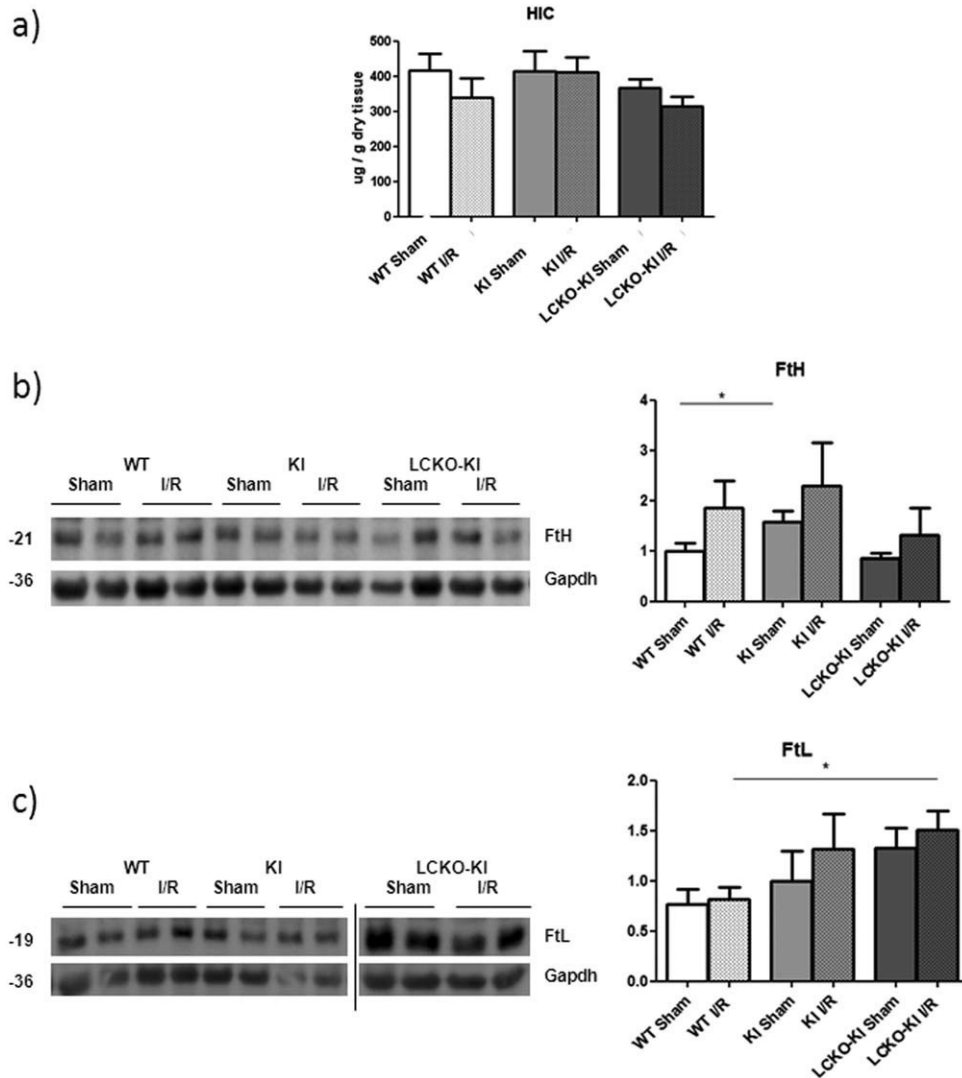
Different is the situation in Tfr2-KI hearts, which could be protected by FtH higher levels. In fact, while FtL is increased in LCKO-KI I/R, FtH is significantly increased in Tfr2-KI Sham; further supporting different pathway activation in the two Tfr2 targeted models. Several recent studies demonstrated that the two Ferritin subunits are differently regulated as a response to different stimuli [36]. While FtL subunit appears to be more regulated by iron amount through the IRE/IRP system [21], FtH is more responsive to the presence of oxidant agents either in *in vitro* [37,38] and in *ex vivo* [39] conditions.

Overall, our results suggest that proteins controlling iron trafficking are mainly altered by high systemic iron amount, rather than by lack of Tfr2 beta isoform itself (aside FtH which increased in Tfr2-KI, other iron proteins are significantly increased in LCKO-KI only). Although these variations of proteins suggest that iron trafficking in the cardiac cells is different in the two models, both models are cardioprotected. Therefore we can argue that the antioxidant and prosurvival

armamentarium of cardiomyocytes is more ready to limit I/R injury (see below) and/or the metal is in some way less available for ROS production during I/R. Nevertheless, further experiments which also consider iron trafficking in specific cell types (*e.g.*, macrophages, endothelial cells, and cardiomyocytes) would be necessary to deepening the role of iron proteins in the mechanisms of cardioprotection.

Since it is well known that the generation of ROS is influenced by iron and that ROS production may play a role either in I/R injury [40,41] or preconditioning protection [35], *via* modulation of antioxidant enzymes [35,40–42], SOD1 and Catalase have been evaluated. We observe a different amount of the two enzymes in Sham hearts respect to WT. While SOD1 is not significantly modified in Tfr2 β null hearts (data not shown), Catalase is increased only in Tfr2 LCKO-KI hearts. Again, this result supports the hypothesis of repeated sublethal iron overload and stress strong enough to upregulate Catalase expression in Tfr2 LCKO-KI hearts only.

The recent discovery that HIF2a contains an IRE has underlined the importance of HIF2a as a major player in iron metabolism and protective adaptation to iron stress [20]. Intriguingly, Sham hearts of both models result to have a higher level of two protective factors, namely HO-1 and HIF-2a. This resembles HIF-2a upregulation induced by cardiac ischemic preconditioning, which can be mimicked by the addition of ROS [43] and is in line with the fact that these proteins are influenced by iron dependent redox conditions [20]. It is likely that both transgenic models have endured an iron/redox stress


FIG 6

HIC and molecular analysis of FtH and FtL in WT and *Tfr2* targeted mice in Sham and after I/R protocols. (a) HIC assessment was performed using 20 mg of dried LV collected at the end of protocols in WT and targeted mice (KI and LCKO-KI; $n = 4-5$). Western blot analysis (b and c) was performed on lysates from LV collected at the end of protocols WT and targeted mice (KI and LCKO-KI). Graphs represent the densitometric analysis of proteins normalized to Gapdh and reported as relative fold increase. Blot images: vertical lines indicate images taken from different gels. All analyses were carried out in triplicate. * $P < 0.05$, ** $P < 0.01$.

that led them to react with an increase in cardiac HO-1 and HIF-2 α , thus orchestrating an adaptive response to oxygen deprivation making the heart protected against subsequent damaging stimuli, like I/R.

Since both the *Tfr2* β null mice hearts result to be cardio-protected, we also studied the RISK/SAFE pathways. We observed that the two models present some differences in the activation of RISK- and SAFE-pathway. In particular, we observe that starting from similar levels of phosphorylation of *RISK kinases* (AKT, ERK1/2, and PKC ϵ), the I/R procedure induces an up-regulation of the phosphorylation of these kinases in *Tfr2*-KI hearts only. The SAFE pathway element, Stat3, seems upregulated in *Tfr2*-KI Sham hearts with respect

to WT group, but the I/R procedure induces Stat3 phosphorylation in *Tfr2* LCKO-KI only. Intriguingly, this model responds to I/R with an increased phosphorylation of GSK3 β , a putative down-stream kinase of protective pathways, whose role remains still controversial [44,45]. Therefore, it seems that one model (*Tfr2*-KI) relies mainly on the activation of RISK and the other (LCKO-KI) on the activation of SAFE. Actually these two pathways may be alternative or may cross-talk [11,14,15]. We have previously shown that redox conditions may influence the activation of one or the other of these two protective pathways [16]. Since, here we observe differences in terms of iron metabolism in the two models, we can argue that this difference may influence the I/R response to direct

TABLE 1
Variation of analyzed parameters at the end of protocols in WT and targeted mice

| | Wild-type | KI | | LCKO-KI | |
|---------------------------------|-----------|------|--------------|------------------|------------------|
| | I/R | SHAM | I/R | SHAM | I/R |
| TFR2 β | ↑ | NA | NA | NA | NA |
| Infarct size | NA | NA | ↓ (WT I/R) | NA | ↓ (WT I/R) |
| BCL S/L | ND | ↓ | ND | ↑ | ND |
| HO-1 | ND | ↑↑ | ND | ↑ | ND |
| HIF-2 | ND | ↑ | ↓ (KI Sham) | ↑ | ND |
| | | | ↓↓ (KI Sham) | | |
| RISK and SAFE | | | | | |
| pERK1/2/ERK1/2 | ↓↓↓ | ↓↓ | ↑↑ (WT I/R) | ND | ND |
| | | | ↑ (KI Sham) | | |
| pAKT/AKT | ND | ND | ↑↑ (WT I/R) | ND | ND |
| | | | ↑ (KI Sham) | | |
| pPKC ϵ /PKC ϵ | ND | ND | ↑ (WT I/R) | ND | ↑ (WT I/R) |
| | | | ↑ (KI Sham) | | ND(LCKO-KI Sham) |
| pSTAT3/STAT3 | ND | ND | ND | ↓ | ND |
| | | | | ↑↑(LCKO-KI Sham) | |
| pGSK3 β /GSK3 β | ND | ND | ND | ND | ↑↑ (WT I/R) |
| | | | | | ↑↑(LCKO-KI Sham) |
| Iron and Proteins | | | | | |
| Hamp (RNA) | ND | ND | ND | ↑ | ND |
| Fpn1 (RNA) | ND | ↓ | ND | ND | ND |
| DMT1 | ND | ND | ND | ↑↑ | ND |
| HIC | ND | ND | ND | ND | ND |
| FtH | ND | ↑ | ND | ND | ND |
| FtL | ND | ND | ND | ND | ↑ (WT I/R) |
| | | | | | ND(LCKO-KI Sham) |
| Antioxidant enzymes | | | | | |
| Catalase | ND | ND | ND | ↑ | ↑ (WT I/R) |
| | | | | | ND(LCKO-KI Sham) |
| SOD1 | ND | ND | ND | ND | ND |

The table shows a summary of the all analyzed parameters at the end of protocols in WT and targeted mice (KI and LCKO-KI). **Arrows** show variation (↑, ↓ P < 0.05; ↑↑, ↓↓ P < 0.01; ↓↓↓ P < 0.001) with respect to the Sham WT or respect to the group reported in brackets. **ND** = no difference with respect to Sham WT or respect to the group reported in brackets. **NA** = not applicable. For acronyms see the text.

the heart towards one or the other of these two pathways. Further studies are necessary to ascertain this point.

4.1. Methodological Considerations

This study is realized using the isolated heart model (Langendorff) that is highly adaptable and independent by external cardiac influence [46]. In fact, this model allows to study the intrinsic property of the heart and the capacity of the myocardium to afford a stressful stimulus in a strictly controlled environment, avoiding extracardiac influences and the possible effect of temperature and collateral flow variations. The use of the Langendorff model allow us to keep under strict control several factors (*e.g.*, heart temperature and perfusion) and to eliminate the confounding effect of systemic factors, including those due to iron overload in the remainder of the animal during experimental maneuvers. Since the relevant comparison is between each transgenic model with its correspondent Sham group, for statistical analysis we used a Student *t* test (unpaired, 2 tailed), and a multi-group comparison by ANOVA was considered not informative.

4.2. Conclusions

Clearly, the hearts of the two Tfr2 β null mice have a different cardiac status and enzymatic setting. It is likely that Tfr2 β silencing causes a modification of iron handling in the cells, which may induce a selective activation of different proteins involved in cell survival. In fact, the myocardium of these two strains results to have different levels of basal proapoptotic factors, which seems correlated with systemic iron overload, and to be enriched of specific iron protein tool kit, antioxidant enzymes, and kinases involved in cardioprotective pathways ready to be activated after stressful stimuli. In fact Tfr2 β null mice's hearts develop a greater resistance against acute I/R challenge, irrespective of systemic iron content. Further studies are necessary to ascertain the main mechanism of protection and in particular to ascertain whether tissue damage is due to pre-existing adaptations or due to dynamic alteration in iron efflux during the stressful stimuli.

Acknowledgements

This article was supported in part by Progetti di Ateneo/CSP 2012 (TO_Call3_2012_0101) and AIRC (IG2011 cod 12141) to GS, Progetti di Ateneo/CSP 2012 (TO_Call1_2012_0088) to MDG and Progetti di Ateneo ex60% MeccaSarc to PP and CP. The authors are indebted to their colleague Sonia Levi for providing them antiferritins antibodies and for fruitful discussions. They also thank Prof Donatella Gattullo for the invaluable support and Saveria Femminò for technical assistance. The authors have no conflicts of interest to declare.

References

- [1] Ganz, T. (2013) Systemic iron homeostasis. *Physiol. Rev.* 93, 1721–1741.
- [2] Pagliaro, P., Moro, F., Tullio, F., Perrelli, M. G., and Penna, C. (2011) Cardioprotective pathways during reperfusion: focus on redox signaling and other modalities of cell signaling. *Antioxid. Redox Signal.* 14, 833–850.
- [3] Xu, J., Marzetti, E., Seo, A. Y., Kim, J. S., Prolla, T. A., et al. (2010) The emerging role of iron dyshomeostasis in the mitochondrial decay of aging. *Mech. Ageing Dev.* 131, 487–493.
- [4] Murphy, C. J. and Oudit, G. Y. (2010) Iron-overload cardiomyopathy: pathophysiology, diagnosis, and treatment. *J. Card. Fail.* 16, 888–900.
- [5] Kawabata, H., Yang, R., Hiramata, T., Vuong, P. T., Kawano, S., et al. (1999) Molecular cloning of Transferrin Receptor 2. A new member of the transferrin receptor-like family. *J. Biol. Chem.* 274, 20826–22032.
- [6] Hentze, M. W., Muckenthaler, M. U., Galy, B., and Camaschella, C. (2010) Two to tango: regulation of Mammalian iron metabolism. *Cell* 142, 24–38.
- [7] Roetto, A., Di Cunto, F., Pellegrino, R. M., Hirsch, E., Azzolino, O., et al. (2010) Comparison of 3 Tfr2-deficient murine models suggests distinct functions for Tfr2-alpha and Tfr2-beta isoforms in different tissues. *Blood* 115, 3382–3389.
- [8] Merle, U., Fein, E., Gehrke, S. G., Stremmel, W., and Kulaksiz, H. (2007) The iron regulatory peptide hepcidin is expressed in the heart and regulated by hypoxia and inflammation. *Endocrinology* 148, 2663–2668.
- [9] Qian, Z. M., Chang, Y. Z., Leung, G., Du, J. R., Zhu, L., et al. (2007) Expression of ferroportin1, hephaestin and ceruloplasmin in rat heart. *Biochim. Biophys. Acta* 1772, 527–532.
- [10] Boengler, K., Hilfiker-Kleiner, D., Heusch, G., and Schulz, R. (2010) Inhibition of permeability transition pore opening by mitochondrial STAT3 and its role in myocardial ischemia/reperfusion. *Basic Res. Cardiol.* 105, 771–785.
- [11] Hausenloy, D. J., Lecour, S., and Yellon, D. M. (2011) Reperfusion injury salvage kinase and survivor activating factor enhancement prosurvival signaling pathways in ischemic postconditioning: two sides of the same coin. *Antioxid. Redox Signal.* 14, 893–907.
- [12] Penna, C., Brancaccio, M., Tullio, F., Rubinetto, C., Perrelli, M. G., et al. (2014) Overexpression of the muscle-specific protein, melusin, protects from cardiac ischemia/reperfusion injury. *Basic Res. Cardiol.* 109, 418
- [13] Roubille, F., Combes, S., Leal-Sanchez, J., Barrère, C., Cransac, F., et al. (2007) Myocardial expression of a dominant-negative form of Daxx decreases infarct size and attenuates apoptosis in an in vivo mouse model of ischemia/reperfusion injury. *Circulation* 116, 2709–2717.
- [14] Heusch, G. (2015) Molecular basis of cardioprotection: signal transduction in ischemic pre-, post-, and remote conditioning. *Circ. Res.* 116, 674–699.
- [15] Penna, C., Granata, R., Tocchetti, C. G., Gallo, M. P., Alloati, G., and Pagliaro, P. (2015) Endogenous cardioprotective agents: role in pre and postconditioning. *Curr. Drug. Targets* 16, 843–867.
- [16] Penna, C., Perrelli, M. G., Tullio, F., Angotti, C., Camporeale, A., et al. (2013) Diazoxide postconditioning induces mitochondrial protein S-nitrosylation and a redox-sensitive mitochondrial phosphorylation/translocation of RISK elements: no role for SAFE. *Basic Res. Cardiol.* 108, 371
- [17] Nadtochiy, S. M., Yao, H., McBurney, M. W., Gu, W., Guarente, L., et al. (2011) SIRT1-mediated acute cardioprotection. *Am. J. Physiol. Heart. Circ. Physiol.* 301, H1506–H1512.
- [18] Penna, C., Perrelli, M. G., Tullio, F., Angotti, C., and Pagliaro, P. (2013) Acidic infusion in early reperfusion affects the activity of antioxidant enzymes in postischemic isolated rat heart. *J. Surg. Res.* 183, 111–118.
- [19] Penna, C., Angotti, C., and Pagliaro, P. (2014) Protein S-nitrosylation in preconditioning and postconditioning. *Exp. Biol. Med.* (Maywood) 239, 647–662.
- [20] Simpson, R. J. and McKie, A. T. (2015) Iron and oxygen sensing: a tale of 2 interacting elements? *Metallomics* 7, 223–231.
- [21] Muckenthaler, M. U., Galy, B., and Hentze, M. W. (2008) Systemic iron homeostasis and the iron responsive element/iron-regulatory protein (IRE/IRP) regulatory network. *Annu. Rev. Nutr.* 28, 197–213.
- [22] Bondi, A., Valentino, P., Daraio, F., Porporato, P., Gramaglia, E., et al. (2005) Hepatic expression of hemochromatosis genes in two mouse strains after phlebotomy and iron overload. *Haematologica* 90, 1161–1167.
- [23] Penna, C., Pasqua, T., Perrelli, M. G., Pagliaro, P., Cerra, M. C., et al. (2012) Postconditioning with glucagon like peptide-2 reduces ischemia/reperfusion injury in isolated rat hearts: role of survival kinases and mitochondrial KATP channels. *Basic Res. Cardiol.* 107, 272
- [24] Livak, K. J. and Schmittgen, T. D. (2001) Analysis of relative gene expression data using real-time quantitative PCR and the 2⁻ $\Delta\Delta$ CT Method. *Methods* 25, 402–408.

- [25] Quail, E. A. and Yeoh, G. C. (1995) The effect of iron status on glyceraldehyde 3-phosphate dehydrogenase expression in rat liver. *FEBS Lett.* 359, 126–128.
- [26] Chao, D. T. and Korsmeyer, S. J. (1998) BCL-2 family: regulators of cell death. *Annu. Rev. Immunol.* 16, 395–419.
- [27] Ryter, S. W. and Choi, A. M. (2002) Heme oxygenase-1: molecular mechanisms of gene expression in oxygen-related stress. *Antioxid. Redox Signal.* 4, 625–632.
- [28] Gozzelino, R., Jeney, V., and Soares, M. P. (2010) Mechanisms of cell protection by heme oxygenase-1. *Annu. Rev. Pharmacol. Toxicol.* 50, 323–354.
- [29] Wu, M. L., Ho, Y. C., and Yet, S. F. (2011) A central role of heme oxygenase-1 in cardiovascular protection. *Antioxid. Redox Signal.*, 15, 1835–1846.
- [30] Roetto, A. and Camaschella, C. (2005) New insights into iron homeostasis through the study of non-HFE hereditary haemochromatosis. *Best Pract. Res. Clin. Haematol.* 18, 235–250.
- [31] Turoczi, T., Jun, L., Cordis, G., Morris, J. E., Maulik, N, et al. (2003) Mutation and dietary iron content interact to increase ischemia/reperfusion injury of the heart in mice. *Circ. Res.* 92, 1240–1246.
- [32] Ferdinandy, P., Schulz, R., and Baxter, G. F. (2007) Interaction of cardiovascular risk factors with myocardial ischemia/reperfusion injury, preconditioning, and postconditioning. *Pharmacol. Rev.* 59, 418–458.
- [33] Bulvik, B. E., Berenshtein, E., Meyron-Holtz, E. G., Koniijn, A. M., and Chevion, M. (2012) Cardiac protection by preconditioning is generated via an iron-signal created by proteasomal degradation of iron proteins. *PLoS One* 7, e48947
- [34] Johnstone, D. and Milward, E. A. (2010) Genome-wide microarray analysis of brain gene expression in mice on a short-term high iron diet. *Neurochem. Int.* 56, 856–863.
- [35] Chevion, M., Leibowitz, S., Aye, N. N., Novogrodsky, O., Singer, A., et al. (2008) Heart protection by ischemic preconditioning: a novel pathway initiated by iron and mediated by ferritin. *J. Mol. Cell. Cardiol.* 45, 839–845.
- [36] Arosio, P., and Levi, S. (2010) Cytosolic and mitochondrial ferritins in the regulation of cellular iron homeostasis and oxidative damage. *Biochem. Biophys. Acta* 1800, 783–792.
- [37] Cozzi, A., Corsi, B., Levi, S., Santambrogio, P., Albertini, A., and Arosio, P. (2000) Overexpression of wild type and mutated human ferritin H-chain in HeLa cells: in vivo role of ferritin ferroxidase activity. *J. Biol. Chem.* 275, 25122–25129.
- [38] Epsztejn, S., Glickstein, H., Picard, V., Slotki, I. N., Breuer, W., et al. (1999) H-ferritin subunit overexpression in erythroid cells reduces the oxidative stress response and induces multidrug resistance properties. *Blood* 94, 3593–3603.
- [39] Darshan, D., Vanoaica, L., Richman, L., Beermann, F., and Kühn, L. C. (2009) Conditional deletion of ferritin H in mice induces loss of iron storage and liver damage. *Hepatology* 50, 852–860.
- [40] Bolli, R., Dawn, B., Tang, X. L., Qiu, Y., Ping, P, et al. (1998) The nitric oxide hypothesis of late preconditioning. *Basic Res. Cardiol.* 93, 325–338.
- [41] Tullio, F., Angotti, C., Perrelli, M. G., Penna, C., and Pagliaro, P. (2013) Redox balance and cardioprotection. *Basic Res. Cardiol.* 108, 392
- [42] Leonarduzzi, G., Sottero, B., Testa, G., Biasi, F., and Poli, G. (2011) New insights into redox-modulated cell signaling. *Curr. Pharm. Des.* 17, 3994–4006.
- [43] Bautista, L., Castro, M. J., López-Barneo, J., and Castellano, A. (2009) Hypoxia inducible factor-2alpha stabilization and maxi-K⁺ channel beta1-subunit gene repression by hypoxia in cardiac myocytes: role in preconditioning. *Circ. Res.* 104, 1364–1372.
- [44] Heusch, G. and Schulz, R. (2009) Neglect of the coronary circulation: some critical remarks on problems in the translation of cardioprotection. *Cardiovasc. Res.* 84, 111–114.
- [45] Lacerda, L., Somers, S., Opie, L. H., and Lecour, S. (2009) Ischaemic post-conditioning protects against reperfusion injury via the SAFE pathway. *Cardiovasc. Res.* 84, 201–208.
- [46] Bell, R. M., Mocanu, M. M., and Yellon, D. M. (2011) Retrograde heart perfusion: the Langendorff technique of isolated heart perfusion. *J. Mol. Cell. Cardiol.* 50, 940–950.

5.2 Tfr2 in the erythropoietic compartment

Preliminary phenotype analysis of Tfr2 mouse models already evidenced some changes in erythropoietic parameters and more recent data corroborate a role for Tfr2 in erythropoiesis. Genome-wide association studies had identified Tfr2 polymorphisms that affect hematologic parameters (Soranzo et al, 2009; Auer et al, 2014). A Tfr2 role in erythropoiesis was further strengthened by the identification of Tfr2 as a component of the Erythropoietin receptor (EpoR) complex in erythroid progenitor cells (Forejtníková et al, 2010). Tfr2 was demonstrated to be crucial for efficient transport of erythropoietin receptor (EpoR) to the cell surface and for its terminal differentiation. To further study Tfr2 erythropoietic role, I contributed to the creation of two new double KO animal models for the two iron proteins Tfr2 (whose silence causes iron overload) (Roetto et al, 2010) and Tmprss6 (whose silence causes microcytic anemia) (Du et al, 2008). These have been obtained through breeding Tfr2 $-/-$ or Tfr2 LCKO mice with Tmprss6 $+/-$ mice.). Mice were given a standard diet (480 mg iron/Kg) and only male mice were analyzed at age of 10 weeks (Nai et al, 2014). Erythropoietic analysis of these animals compared to single KO gave further insight into an erythropoietic role for Tfr2. In fact, an increased Hb content was present only in Tfr2 germinal KO mice (Tfr2 KO) but not in liver-specific KO (Tfr2 LCKO-KI) animals. Since both mouse models manifested comparable iron overload, the lack of enhanced hemoglobinization in liver-specific Tfr2 KO mice suggests the preservation of the erythroid function of Tfr2. Also, double Tmprss6-Tfr2 KO mice developed erythrocytosis that was prevented in Tmprss6/Tfr2 LCKO mice, where Tfr2 is preserved in erythroid cells (**Nai et al, 2014 see attached paper**).

Later, another Italian group developed a mouse model lacking Tfr2 exclusively in bone marrow cells (Tfr2 BMKO) was developed (Nai et al, 2015). Tfr2 BMKO mice manifested increased RBC and Hb content, as well as reduced MCV. This is a typical response to iron deficiency associated with enhanced terminal erythropoiesis but without increased plasma Epo levels. Notably, under conditions of mild dietary iron restriction, erythroid differentiation of control mice was similar to that of Tfr2 BMKO mice, but plasma Epo was increased. In iron-poor Tfr2 BMKO mice, erythropoiesis was not further modified, and plasma Epo levels remained unchanged.

Taken together, all these data suggest that the lack of Tfr2 confers enhanced Epo sensitivity to erythroid progenitor cells, which is further supported by the induction of Epo target genes (Nai et al, 2015).

I also participated to a subsequent study in which Tfr2 erythropoietic role was further investigated studying the erythropoiesis of two Tfr2 mice with one or both Tfr2 isoforms silenced (Tfr2 KI and Tfr2 KO) (Roetto et al, 2010). The evaluations were performed in bone marrow and spleen, in young and adult animals to unravel the erythropoietic role of Tfr2 isoforms at different ages and in the two main erythropoietic organs. It resulted that the lack of Tfr2 α led to macrocytosis with low reticulocyte number and increased hemoglobin values, together with an anticipation of erythropoiesis in young mice both in BM and in the spleen, so that increased iron amount presented in these animals allow them to reach mature erythropoiesis even during young age.

On the other hand, lack of Tfr2 β (Tfr2 KI mice) caused an increased but immature splenic erythropoiesis in young animals, as if they had insufficient iron availability during animal massive growth, that was normalized in animal adult age. This effect, due to Tfr2 β absence, in Tfr2 KO mice was compensated by the increased amount of circulating iron available for erythrocyte production. Taken together, these data confirm the role of Tfr2 α in modulation of erythropoiesis and the involvement Tfr2 β in favoring iron availability for erythropoiesis (Pellegrino et al, 2017 see attached paper).

The erythroid function of transferrin receptor 2 revealed by *Tmprss6* inactivation in different models of transferrin receptor 2 knockout mice

Antonella Nai,^{1,*} Rosa M. Pellegrino,^{2,*} Marco Rausa,¹ Alessia Pagani,¹ Martina Boero,² Laura Silvestri,¹ Giuseppe Saglio,² Antonella Roetto,² and Clara Camaschella¹

¹Vita Salute University and San Raffaele Scientific Institute, Division of Genetics and Cell Biology, Milan; and ²Department of Clinical and Biological Sciences, University of Torino, Italy

*AN and RMP contributed equally to this work.

ABSTRACT

Transferrin receptor 2 (TFR2) is a transmembrane glycoprotein expressed in the liver and in the erythroid compartment, mutated in a form of hereditary hemochromatosis. Hepatic TFR2, together with HFE, activates the transcription of the iron-regulator hepcidin, while erythroid TFR2 is a member of the erythropoietin receptor complex. The *TMPRSS6* gene, encoding the liver-expressed serine protease matriptase-2, is the main inhibitor of hepcidin and inactivation of *TMPRSS6* leads to iron deficiency with high hepcidin levels. Here we evaluate the phenotype resulting from the genetic loss of *Tmprss6* in *Tfr2* total (*Tfr2*^{-/-}) and liver-specific (*Tfr2*^{LCKO}) knockout mice. *Tmprss6*^{-/-} *Tfr2*^{-/-} and *Tmprss6*^{-/-} *Tfr2*^{LCKO} mice have increased hepcidin levels and show iron-deficiency anemia like *Tmprss6*^{-/-} mice. However, while *Tmprss6*^{-/-} *Tfr2*^{LCKO} are phenotypically identical to *Tmprss6*^{-/-} mice, *Tmprss6*^{-/-} *Tfr2*^{-/-} mice have increased red blood cell count and more severe microcytosis than *Tmprss6*^{-/-} mice. In addition hepcidin expression in *Tmprss6*^{-/-} *Tfr2*^{-/-} mice is higher than in the wild-type animals, but lower than in *Tmprss6*^{-/-} mice, suggesting partial inhibition of the hepcidin activating pathway. Our results prove that hepatic TFR2 acts upstream of *TMPRSS6*. In addition *Tfr2* deletion causes a relative erythrocytosis in iron-deficient mice, which likely attenuates the effect of over-expression of hepcidin in *Tmprss6*^{-/-} mice. Since liver-specific deletion of *Tfr2* in *Tmprss6*^{-/-} mice does not modify the erythrocyte count, we speculate that loss of *Tfr2* in the erythroid compartment accounts for the hematologic phenotype of *Tmprss6*^{-/-} *Tfr2*^{-/-} mice. We propose that TFR2 is a limiting factor for erythropoiesis, particularly in conditions of iron restriction.

Introduction

Transferrin receptor 2 (TFR2) is a transmembrane protein homologous to transferrin receptor 1 (TFR1) which is mutated in hereditary hemochromatosis type 3.^{1,2} TFR2 is expressed in the liver and, to a lower extent, in erythroid cells.^{3,4} TFR2 protein is stabilized on cell surface by binding to its ligand, diferric transferrin (holo-TF),⁵ and, in a complex with the hemochromatosis protein HFE, is considered a sensor of circulating iron. In the current model in conditions of iron deficiency HFE associates with TFR1; inversely, when transferrin saturation increases, competitive binding of holo-TF displaces HFE from TFR1 and the HFE-TFR2 complex activates *HAMP* transcription.^{6,7} However, the phenotype of the HFE and TFR2-related disease is different⁸ and the association between the two proteins has recently been questioned.⁹

Hepcidin blocks dietary iron absorption and iron recycling from senescent erythrocytes by inducing the degradation of the iron exporter ferroportin on enterocytes and macrophages, respectively.¹⁰ The mechanism of *HAMP* activation by TFR2 and HFE is still unclear. Both proteins probably contribute to *HAMP* upregulation by bone morphogenetic proteins (BMP) in response to increased tissue iron.^{11,12} BMP6, using hemojuvelin as a co-receptor, signals through sons-of-mothers-against-decapentaplegic 1/5/8 (SMAD1/5/8) proteins. In

agreement, HFE and TFR2 *in vitro* may form a multi-protein complex with hemojuvelin.¹³ The role of hepatic TFR2 as a regulator of *HAMP* transcription is confirmed by the phenotype of the *Tfr2* total (*Tfr2*^{-/-}) and liver-specific (*Tfr2*^{LCKO}) knockout mouse models. Both mice are characterized by iron overload and low *Hamp* levels relative to their high iron stores, with *Tfr2*^{LCKO} having more severe liver iron accumulation than *Tfr2*^{-/-} animals.^{14,15}

Recently TFR2 has been identified as a component of the erythropoietin receptor (EPOR) complex. *TFR2* and the *EPOR* are co-expressed during erythroid differentiation, *TFR2* associates with *EPOR* in the endoplasmic reticulum and is required for the efficient transport of the *EPOR* to the cell surface. Moreover *TFR2* knockdown *in vitro* delays the terminal differentiation of erythroid precursors¹⁶ indicating that *TFR2* is required for efficient erythropoiesis.

The BMP6-hemojuvelin-*HAMP* pathway is inhibited by matriptase-2, a type II transmembrane serine protease encoded by the *TMPRSS6* gene. By cleaving hemojuvelin,¹⁷ *TMPRSS6* strongly impairs BMP-mediated *HAMP* activation in the liver. *TMPRSS6* mutations both in humans¹⁸ and in mice^{19,20} cause excessive *HAMP* production and iron-refractory, iron-deficiency anemia (IRIDA).²¹ The important role of *TMPRSS6* in erythropoiesis is also highlighted by genome-wide association studies: indeed, common *TMPRSS6* genetic

©2014 Ferrata Storti Foundation. This is an open-access paper. doi:10.3324/haematol.2013.103143

The online version of this article has a Supplementary Appendix.

Manuscript received on December 20, 2013. Manuscript accepted on March 14, 2014.

Correspondence: camaschella.clara@hsr.it

variants associate with iron and erythrocyte traits in different populations.²²⁻²⁷ By studying *Tmprss6* haploinsufficient mice²⁸ and hepcidin levels of normal individuals and the *TMPRSS6* common single nucleotide polymorphism (rs855791)²⁹ we demonstrated that even a partial inability to modulate hepcidin influences iron parameters and, indirectly, erythropoiesis.

The regulation of *TMPRSS6* and its activity is incompletely understood: besides hypoxia,³⁰ iron and BMP6, through the BMP-SMAD pathway, induce *TMPRSS6* expression, likely as a negative feedback loop to limit excessive increases of HAMP.³¹ However, the regulation of *TMPRSS6* *in vivo* according to iron needs remains to be clarified. A possible role of *Tmprss6* in iron overload was demonstrated by Finberg *et al.*³² who showed that *Hfe*^{-/-} mice with complete loss of *Tmprss6* revert from a phenotype of iron overload to one of iron-deficiency anemia with high *Hamp* levels. These findings suggest that HFE acts genetically upstream of *TMPRSS6* in the modulation of the BMP-SMAD pathway and of *HAMP* expression. In analogy with these results and given the role of TFR2 in erythropoiesis¹⁶ we wondered whether TFR2 is involved in the regulation of *TMPRSS6*. To answer this question, we back-crossed *Tmprss6*^{-/-} mice with animals with a complete deletion of *Tfr2* (*Tfr2*^{-/-}) and analyzed the hematologic phenotype and the *Bmp-Smad-Hamp* pathway of the double mutant mice. Moreover, in order to discriminate between the hepatic and extra-hepatic functions of TFR2, we performed the same analysis in *Tmprss6*^{-/-} mice lacking *Tfr2* specifically in the liver (*Tfr2*^{LCKO}).¹⁵

Methods

Mouse models

Mice were maintained in the animal facility of the Department of Clinical and Biological Sciences, University of Turin (Italy) in accordance with European Union guidelines. Each study was approved by the Institutional Animal Care and Use Committee (IACUC) of the same institution.

A *Tmprss6*^{-/-} mouse model on a mixed C57BL/6-Sv129 background was kindly provided by Prof. C. Lopez-Otin (University of Oviedo, Spain) and maintained by brother-sister mating for more than ten generations. *Tfr2*^{-/-} and *Tfr2*^{LCKO} mice on a pure 129S2 background were generated as previously described.¹⁵ For the experimental work described we bred *Tfr2*^{-/-} or *Tfr2*^{LCKO} mice with *Tmprss6*^{+/-} mice and then intercrossed the F1 progeny to generate various genotype combinations (F2: wild-type, *Tmprss6*^{+/-}, *Tmprss6*^{-/-}, *Tfr2*^{-/-}, *Tmprss6*^{+/-}*Tfr2*^{-/-}, *Tmprss6*^{-/-}*Tfr2*^{-/-}, *Tfr2*^{LCKO}, *Tmprss6*^{+/-}*Tfr2*^{LCKO}, *Tmprss6*^{-/-}*Tfr2*^{LCKO}). Mice were given a standard diet (480 mg iron/Kg) and only male mice were analyzed when 10 weeks old. Blood was collected for hematologic analyses, transferrin saturation and erythropoietin levels. After sacrifice livers and spleens were dissected, weighed, and snap-frozen immediately for RNA analysis or dried for tissue iron quantification.

Hematologic analyses

Blood was obtained by retro-orbital puncture from anesthetized mice. Red blood cell and white blood cell counts, hemoglobin concentration, hematocrit and erythrocyte indices (mean corpuscular volume, mean corpuscular hemoglobin) were measured using an ADVIA[®]120 Hematology System (Siemens Diagnostics).

Transferrin saturation was calculated as the ratio of serum iron and total iron binding capacity levels, using the Total Iron Binding Capacity kit (Randox Laboratories Ltd.), according to the manu-

facturer's instructions. Serum erythropoietin levels were measured using a mouse Erythropoietin Quantikine set (R&D System), according to the manufacturer's instructions.

Tissue iron content

To measure iron concentration, tissue samples were dried at 110°C overnight, weighed, and digested in 1 mL of 3M HCl, 0.6M trichloroacetic acid for 20 h at 65°C. The clear acid extract was added to 1 mL of working chromogen reagent (1 volume of 0.1% bathophenanthroline sulfate and 1% thioglycolic acid solution, 5 volumes of water, and 5 volumes of saturated sodium acetate). The solutions were then incubated for 30 min at room temperature until color development and the absorbance measured at 535 nm. A standard curve was plotted using an acid solution containing increasing amounts of iron diluted from a stock solution of Titrisol iron standard (Merck, Darmstadt, Germany).

Quantitative reverse transcriptase polymerase chain reaction

Total RNA was extracted from the liver and spleen using the guanidinium thiocyanate-phenol-chloroform method (Trizol Reagent), following the manufacturer's (Invitrogen) recommendations. RNA (2 µg) was used for quantitative polymerase chain reaction (PCR) analysis for first-strand synthesis of cDNA with the High Capacity cDNA Reverse Transcription kit (Applied Biosystems), according to the manufacturer's instructions.

For real-time PCR analysis, specific murine Assays-on-Demand products (20x) and TaqMan Master Mix (2x) from Applied Biosystems were used, and the reactions were run on a 7900HT Fast Real-Time PCR System (Applied Biosystems) in a final volume of 20 µL. Each cDNA sample was amplified in triplicate and the RNA level was normalized to the corresponding level of *Hprt1* mRNA. Primers used for the quantitative reverse transcriptase PCR are listed in *Online Supplementary Table S1*.

Statistical analysis

Data are presented as mean ± standard deviation. Unpaired two-tailed Student t-tests were performed using GraphPad PRISM 5.0 and a *P* value less than 0.05 was considered statistically significant.

Results

Tmprss6^{-/-}*Tfr2*^{-/-} mice are anemic and have increased red cell numbers

Ten-week old *Tfr2*^{-/-} mice had higher hemoglobin levels than controls, while *Tfr2*^{LCKO} mice had levels comparable to those in wild-type animals, as previously reported.¹⁵ Conversely *Tmprss6*^{-/-} mice had the hematologic phenotype of microcytic anemia with increased red blood cell and reticulocyte counts accompanied by low levels of hemoglobin, hematocrit, mean corpuscular volume and mean corpuscular hemoglobin. The heterozygous loss of *Tmprss6* in *Tfr2*^{-/-} mice slightly reduced hemoglobin levels although the difference from the levels in *Tfr2*^{-/-} mice was not statistically significant. On the contrary, *Tmprss6*^{+/-}*Tfr2*^{LCKO} mice had hemoglobin levels comparable to those of *Tfr2*^{LCKO} animals. Both *Tmprss6*^{-/-}*Tfr2*^{-/-} and *Tmprss6*^{-/-}*Tfr2*^{LCKO} mice were anemic and had hemoglobin levels similar to those of *Tmprss6*^{-/-} mice. However, the *Tmprss6*^{-/-}*Tfr2*^{-/-} mice had higher numbers of red blood cells than did *Tmprss6*^{-/-} animals, resulting in more severe microcytosis, while this was not the case for *Tmprss6*^{-/-} mice with specific liver deletion

Table 1. Hematologic data of all the genotype combinations analyzed.

| | WBC ($\times 10^6$ cells/ μ L blood) | RBC ($\times 10^6$ cells/ μ L blood) | Reticulocytes ($\times 10^3$ cells/L blood) | Hb (g/dL) | Hct (%) | MCV (fL) | MCH (pg) |
|---|--|--|---|------------------------------|---------------------------------|---------------------------------|--------------------------------|
| Wild-type | 7.2 \pm 2.6 | 8.6 \pm 0.7 | 302.8 \pm 149.9 | 13.1 \pm 0.4 | 43.3 \pm 2.7 | 50.8 \pm 1.5 | 15.1 \pm 1.4 |
| <i>Tmprss6</i> ^{-/-} | 5.6 \pm 1.4 | 9.3 \pm 0.8 | 243.7 \pm 28.8 | 13.2 \pm 0.8 | 45.3 \pm 3.3 | 48.5 \pm 0.8 ^b | 14.1 \pm 0.5 |
| <i>Tmprss6</i> ^{+/-} | 5.9 \pm 4.1 | 11.0 \pm 1.4 ^b | 771.1 \pm 265.5 ^a | 8.0 \pm 0.9 ^b | 32.3 \pm 2.2 ^b | 29.5 \pm 2.5 ^b | 7.3 \pm 0.7 ^b |
| <i>Tfr2</i> ^{-/-} | 10.4 \pm 2.9 | 9.5 \pm 0.8 | 324.8 \pm 116.7 | 15.1 \pm 1.4 ^a | 48.9 \pm 4.8 ^a | 51.7 \pm 0.9 | 16.0 \pm 0.6 |
| <i>Tmprss6</i> ^{+/-} <i>Tfr2</i> ^{-/-} | 10.2 \pm 3.6 | 8.8 \pm 0.6 | 293.8 \pm 119.4 | 14.2 \pm 0.9 ^a | 46.7 \pm 3.0 | 52.4 \pm 1.8 | 16.0 \pm 0.9 |
| <i>Tmprss6</i> ^{-/-} <i>Tfr2</i> ^{-/-} | 8.1 \pm 5.8 | 13.9 \pm 2.0 ^{b,d,e} | 2032.7 \pm 1063.7 ^{a,c,e} | 8.3 \pm 0.9 ^{b,d} | 35.6 \pm 4.6 ^{a,c} | 25.7 \pm 2.5 ^{b,d,e} | 6.0 \pm 0.3 ^{b,d,e} |
| <i>Tfr2</i> ^{LCKO} | 6.8 \pm 3.2 | 9.0 \pm 0.3 | 229.9 \pm 48.5 | 13.2 \pm 0.6 | 45.4 \pm 1.8 | 50.3 \pm 1.4 | 14.6 \pm 0.3 |
| <i>Tmprss6</i> ^{+/-} <i>Tfr2</i> ^{LCKO} | 8.1 \pm 2.8 | 9.5 \pm 0.6 | 264.0 \pm 68.0 | 13.9 \pm 0.9 | 47.7 \pm 1.9 | 50.1 \pm 1.3 | 14.7 \pm 0.4 |
| <i>Tmprss6</i> ^{-/-} <i>Tfr2</i> ^{LCKO} | 10.4 \pm 3.5 | 10.7 \pm 1.5 ^{a,g,i} | 1047.0 \pm 456.8 ^{a,h} | 8.5 \pm 1.2 ^{b,h} | 30.0 \pm 1.9 ^{b,h,i} | 28.5 \pm 2.4 ^{b,h,i} | 8.2 \pm 1.5 ^{b,h,i} |

White blood cells (WBC), red blood cells (RBC), reticulocyte counts, hemoglobin (Hb), hematocrit (Hct), mean corpuscular volume (MCV) and mean corpuscular hemoglobin (MCH) are shown as means \pm standard deviations of the results in four to seven male mice. * $P < 0.05$, ^a $P < 0.005$ relative to wild-type (*Tmprss6*^{+/-}*Tfr2*^{+/-}) controls; ^b $P < 0.05$, ^c $P < 0.005$ relative to *Tfr2*^{-/-}; ^d $P < 0.05$, ^e $P < 0.005$ relative to *Tmprss6*^{-/-}; ^f $P < 0.05$, ^g $P < 0.005$ relative to *Tfr2*^{LCKO}; ^h $P < 0.05$ relative to *Tmprss6*^{+/-}*Tfr2*^{-/-}. For the complete statistical analysis see Online Supplementary Table S2.

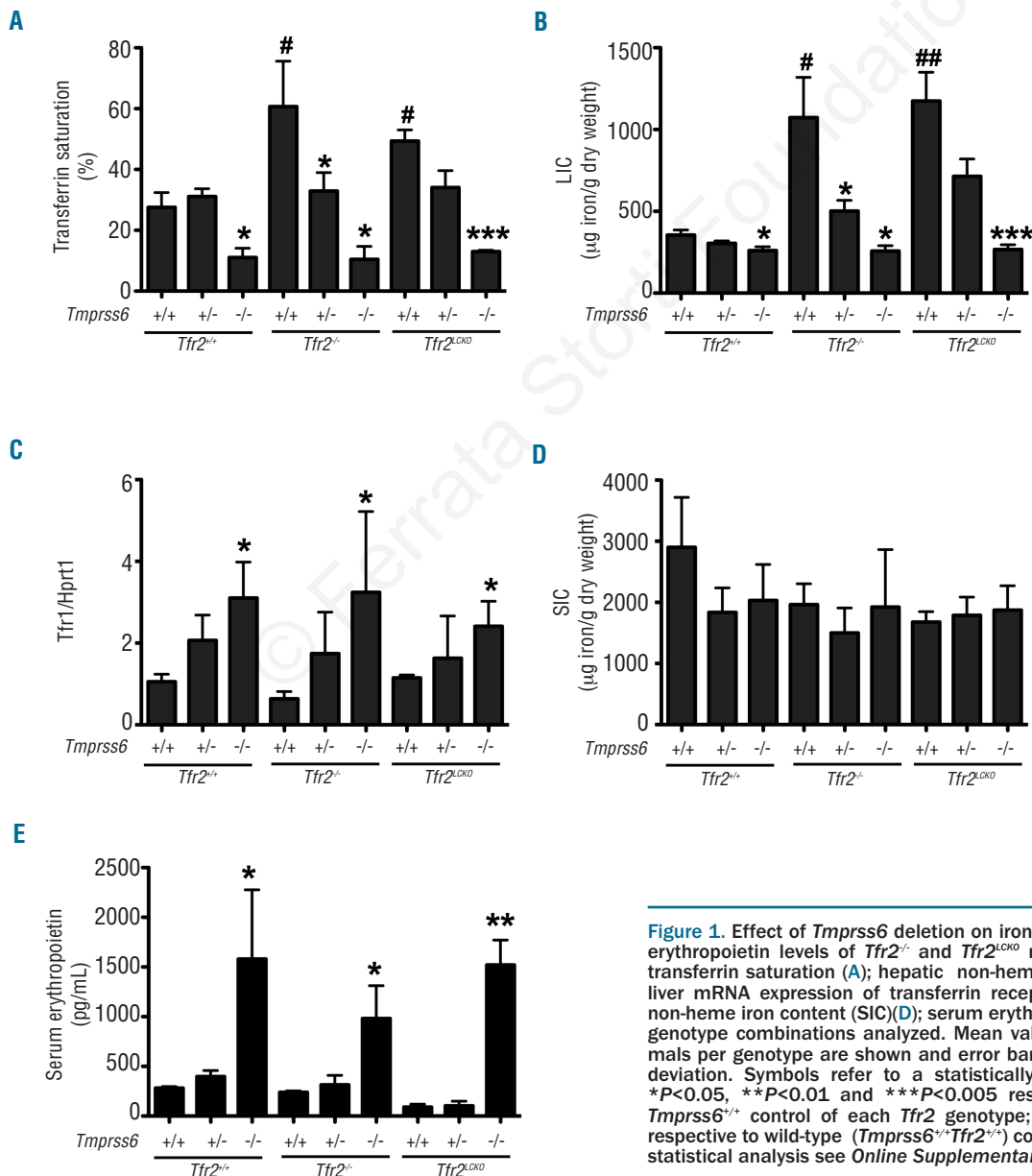


Figure 1. Effect of *Tmprss6* deletion on iron parameters and serum erythropoietin levels of *Tfr2*^{-/-} and *Tfr2*^{LCKO} mice. The graphs show transferrin saturation (A); hepatic non-heme iron content (LIC) (B); liver mRNA expression of transferrin receptor 1 (*Tfr1*) (C); splenic non-heme iron content (SIC) (D); serum erythropoietin levels (E) in all genotype combinations analyzed. Mean values of three to six animals per genotype are shown and error bars indicate the standard deviation. Symbols refer to a statistically significant difference: * $P < 0.05$, ** $P < 0.01$ and *** $P < 0.005$ relative to the relative *Tmprss6*^{+/-} control of each *Tfr2* genotype; ^a $P < 0.05$ and ^b $P < 0.01$ relative to wild-type (*Tmprss6*^{+/-}*Tfr2*^{+/-}) controls. For the complete statistical analysis see Online Supplementary Table S2.

of *Tfr2* (Table 1). In the absence of *Tmprss6*, reticulocytes were increased only in *Tfr2*^{-/-} animals.

Homozygous loss of *Tmprss6* reduces systemic and tissue iron levels of *Tfr2*^{-/-} and *Tfr2*^{LCKO} mice

Transferrin saturation (Figure 1A) and liver iron content (LIC) (Figure 1B) were significantly lower in the iron-deficient *Tmprss6*^{-/-} mice than in wild-type mice (defined as *Tmprss6*^{+/+}*Tfr2*^{+/+} in Figures 1 and 2), while *Tfr2*^{-/-} and *Tfr2*^{LCKO} animals showed an important iron overload.¹⁵ Deletion of the *Tmprss6* gene in both *Tfr2*^{-/-} and *Tfr2*^{LCKO} mice had a dose-dependent effect. The loss of a single allele slightly reduced transferrin saturation and LIC in both models, although the differences were statistically significant only for the *Tfr2*^{-/-} animals. The homozygous inactivation of *Tmprss6* lowered LIC of both *Tfr2*^{-/-} and *Tfr2*^{LCKO} animals to the levels of *Tmprss6*^{-/-} mice. The difference in LIC of the various genotypes was confirmed by analysis of the *Tfr1* mRNA levels, which are known to be inversely related to the cell iron content. *Tfr1* mRNA levels were high in *Tmprss6*^{-/-}, *Tmprss6*^{-/-}*Tfr2*^{-/-} and *Tmprss6*^{-/-}*Tfr2*^{LCKO} animals and reduced according to gene-dosage of *Tmprss6* (Figure 1C). We observed no differences in the spleen iron content among all the genotypes analyzed

(Figure 1D). In addition spleen and liver sizes were similar between *Tmprss6*^{+/-}, *Tmprss6*^{-/-}*Tfr2*^{-/-} and *Tmprss6*^{-/-}*Tfr2*^{LCKO} animals (data not shown).

Tfr2^{-/-} and *Tfr2*^{LCKO} mice had serum erythropoietin levels comparable to those of wild-type mice. As expected, anemic *Tmprss6*^{-/-} mice had erythropoietin levels higher than those of wild-type mice and comparable to those of *Tmprss6*^{-/-}*Tfr2*^{-/-} and *Tmprss6*^{-/-}*Tfr2*^{LCKO} animals (Figure 1E).

Hamp levels are less inappropriately high in *Tmprss6*^{-/-} *Tfr2*^{-/-} mice than in *Tmprss6*^{-/-} mice

The expression of *Bmp6* reflected LIC in all the genotypes analyzed, being high in *Tfr2*^{-/-} and *Tfr2*^{LCKO} animals and low in *Tmprss6*^{-/-} as compared to wild-type controls, although in the latter case the difference was not statistically significant. *Bmp6* in *Tmprss6* haploinsufficient *Tfr2*^{LCKO} was indistinguishable from that in *Tfr2*^{LCKO} animals (Figure 2A). The *Bmp6*/LIC ratio was comparable among all the genotypes analyzed proving that *Bmp6* expression is adequate to the hepatic iron content (Online Supplementary Figure S1).

As expected, *Hamp* (Figure 2B) was over-expressed in *Tmprss6*^{-/-} mice while comparable to wild-type levels in both *Tfr2*^{-/-} and *Tfr2*^{LCKO} mice. As a consequence the iron-

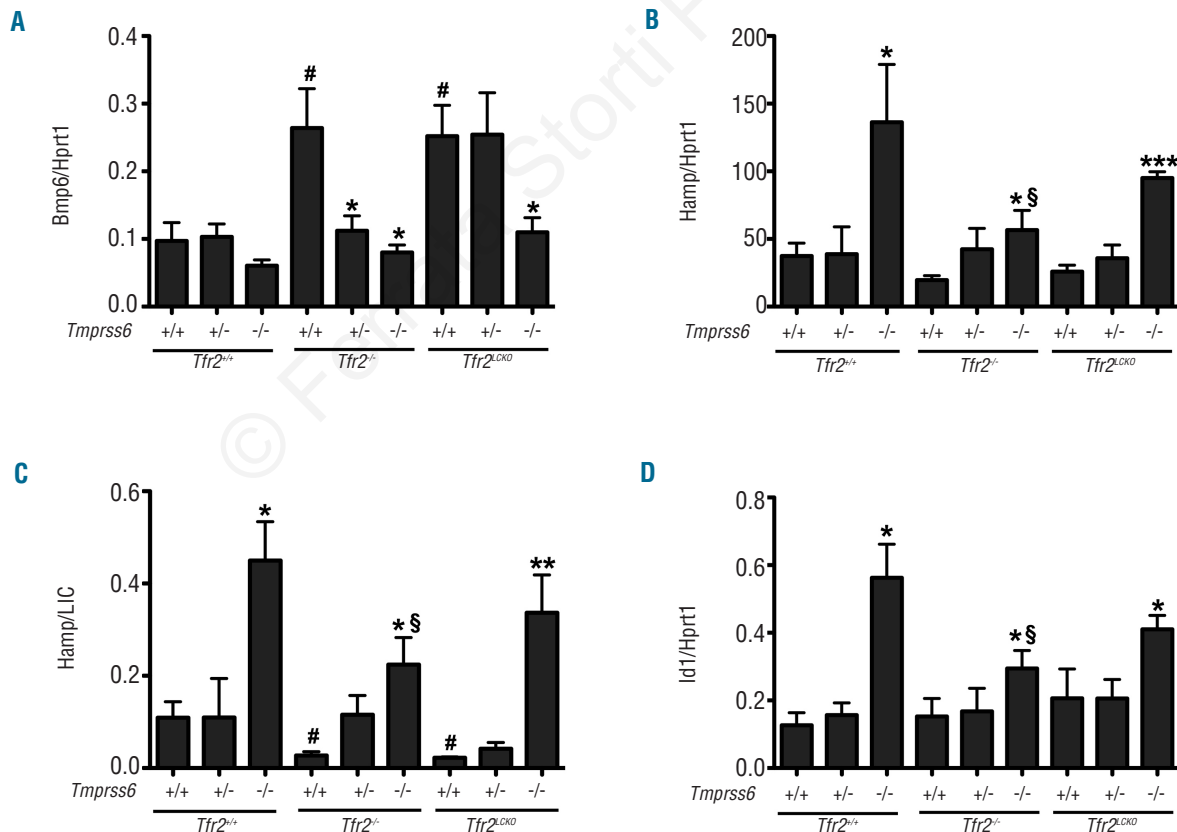


Figure 2. Effect of *Tmprss6* deletion on the Bmp-Smad pathway of *Tfr2*^{-/-} and *Tfr2*^{LCKO} mice. The graphs show liver mRNA expression of: bone morphogenetic protein 6 (*Bmp6*; A); hepcidin (*Hamp*; B); *Hamp* normalized on LIC (*Hamp*/LIC; C) and inhibitor of DNA binding 1 (*Id1*; D) in all genotype combinations analyzed. Mean values of three to six animals per genotype are shown and error bars indicate the standard deviation. Symbols refer to a statistically significant difference: **P*<0.05, ***P*<0.01 and ****P*<0.005 relative to the relative *Tmprss6*^{+/+} control of each *Tfr2* genotype; #*P*<0.05 relative to wild-type (*Tmprss6*^{+/+}*Tfr2*^{+/+}) animals; §*P*<0.05 relative to *Tmprss6*^{-/-} mice. For the complete statistical analysis see Online Supplementary Table S2.

deficient *Tmprss6*^{-/-} mice had a *Hamp*/LIC ratio higher than that of wild-type animals, while both the iron-loaded *Tfr2* knockout mice had a *Hamp*/LIC ratio lower than that of controls (Figure 2C).

In *Tmprss6*^{-/-}*Tfr2*^{-/-} mice *Hamp* expression was higher than in wild-type mice, but lower than in *Tmprss6*^{-/-} animals, while levels in *Tmprss6*^{-/-}*Tfr2*^{LCKO} were comparable to those of *Tmprss6*^{-/-} animals. This resulted in a *Hamp*/LIC ratio that was higher in *Tmprss6*^{-/-}*Tfr2*^{-/-} mice than in controls, but lower than in *Tmprss6*^{-/-} animals, while the *Hamp*/LIC ratio of *Tmprss6*^{-/-}*Tfr2*^{LCKO} was comparable to that of *Tmprss6*^{-/-} animals (Figure 2C). The mRNA levels of inhibitor of differentiation 1 (*Id1*), another target of the Bmp-Smad pathway, followed the same pattern as that of *Hamp* expression (Figure 2D), proving that in the double *Tmprss6*^{-/-}*Tfr2*^{-/-} mice the Bmp-Smad pathway is more active than in wild-type mice, but less active than in *Tmprss6*^{-/-} mice.

Discussion

The analysis of animal models of *Tfr2*-hemochromatosis suggests that low hepcidin is due to an attenuated Bmp-Smad pathway. In theory TFR2 might promote BMP-SMAD signaling for hepcidin production by inhibiting the activity of TMPRSS6, as was hypothesized for HFE,³² by up-regulating *BMP6* or through other unknown mechanisms. For this reason we compared the effect of *Tmprss6* inactivation in mice with a total deletion of *Tfr2* (*Tfr2*^{-/-}) with that in mice with specific ablation of *Tfr2* in the liver (*Tfr2*^{LCKO}). Since the latter animals maintain *Tfr2* function in other organs, the comparison of the phenotypes of the double knockout mice may provide clues to the extra-hepatic functions of TFR2.

We found that in adult *Tfr2*^{-/-} mice the heterozygous loss of *Tmprss6* slightly reduces the severity of hepatic iron overload and partially reverts the hematologic phenotype, reducing hemoglobin levels. In contrast, *Tmprss6* haploinsufficiency does not correct the iron-overload phenotype of *Tfr2*^{LCKO} mice. This might be compatible with a more severe iron burden reported for the liver-specific knockout,^{14,15} although in the present study, in which only males were examined, LIC was similar in *Tfr2*^{-/-} and *Tfr2*^{LCKO}. Homozygous loss of *Tmprss6* led to systemic iron deficiency and severe anemia in both genotypes with low levels of hemoglobin, transferrin saturation and LIC and enhanced hepatic *Tfr1* expression, in analogy to what has been observed in *Hfe* knockout mice with deletion of *Tmprss6*.³² Similar results were also previously published for *Tmprss6*^{-/-}*Tfr2*^{-/-} mice,³³ although differences of genetic backgrounds made the genotype comparison problematic.

The phenotype modification of *Tfr2*^{-/-} and *Tfr2*^{LCKO} from iron overload to iron deficiency in the absence of *Tmprss6* demonstrates that TFR2 in the liver acts upstream of the serine protease and might control its activity, thus raising the possibility that pharmacological inhibition of TMPRSS6 is effective in limiting dietary iron absorption and redistributing iron to macrophages in TFR2-hemochromatosis, as shown for HFE-hemochromatosis.^{34,35}

Loss of the protease activity of *Tmprss6* leads to increased expression of hepcidin in *Tfr2* iron-loaded animals which explains reduced iron absorption and iron deficiency. However, in *Tmprss6*^{-/-} mice with complete loss

of *Tfr2* the hepatic mRNA levels of *Hamp* and *Id1*, although increased, do not reach the high levels observed in *Tmprss6*^{-/-} mice. In contrast, the expression levels of *Hamp* and *Id1* in *Tmprss6*^{-/-}*Tfr2*^{LCKO} are comparable to those in *Tmprss6*^{-/-} mice. These differences are not mediated by an altered expression of *Bmp6* since *Bmp6* levels reflect the hepatic iron burden in all the genotypes analyzed. This appropriate regulation of *Bmp6* in *Tfr2*^{-/-} animals indicates that *Tfr2* is not required for adequate *Bmp6* response to increased tissue iron, a finding discordant from that in a recent report of *Bmp6* being inappropriately low in *Tfr2*^{-/-} mice.³⁶ Based on our results we speculate that in *Tmprss6*^{-/-}*Tfr2*^{-/-} mice an inhibitory signal partially affects the efficiency of the Bmp-Smad pathway downstream of *Bmp6* leading to a lower than expected hepcidin activation.

Since inhibition of hepcidin is largely dependent on erythropoietic signals we analyzed the hematologic phenotype of our models. The functional loss of both *Tmprss6* and *Tfr2* in the whole organism is associated with the same degree of iron deficiency as *Tmprss6*^{-/-}. However, as compared to mice lacking *Tmprss6* alone, *Tmprss6*^{-/-}*Tfr2*^{-/-} mice showed a consistent increase of red cell number and hematocrit, which was not observed when *Tfr2* was specifically deleted in the liver. This observation supports the hypothesis that the hematologic phenotype of *Tmprss6*^{-/-}*Tfr2*^{-/-} is dependent on the lack of a still unknown extra-hepatic function of *Tfr2*.

We speculate that the loss of *Tfr2* in the erythroid compartment accounts for the increased number of red cells observed in *Tmprss6*^{-/-}*Tfr2*^{-/-} mice and that the expansion of erythropoiesis is responsible for the partial inhibition of the Bmp-Smad pathway exclusively observed in these double mutant mice.

Iron-loaded *Tfr2*^{-/-} mice are not characterized by increased red blood cell counts, but do have increased hemoglobin, as shown here and by others,¹⁵ as compared with *Tfr2*^{LCKO} mice, indicating deregulated erythropoiesis. Indeed, the normal hemoglobin levels in the iron-loaded *Tfr2*^{LCKO} mice indicate that the high hemoglobin levels observed in *Tfr2*^{-/-} animals are not only due to their elevated iron burden, but to some other factors likely related to the absence of *Tfr2* in the erythroid compartment.

In the attempt to verify whether the high red blood cell counts of *Tmprss6*^{-/-}*Tfr2*^{-/-} mice are due to increased erythropoietin levels, we measured serum erythropoietin in all the models. Since *Tmprss6*^{-/-}, *Tmprss6*^{-/-}*Tfr2*^{-/-} and *Tmprss6*^{-/-}*Tfr2*^{LCKO} mice, which have the same degree of anemia, have comparable serum erythropoietin levels we conclude that erythroid precursors lacking *Tfr2* might have enhanced sensitivity to erythropoietin stimulation. Our data seem discrepant with those reported by Foretnikova et al.,¹⁶ who found higher serum erythropoietin levels in *Tfr2*^{-/-} mice than in *Tfr2*^{LCKO} ones. However, the latter results were obtained in young animals (4-weeks old), while our data refer to adult, 10-weeks old mice. It is of interest that the same authors observed that TFR2-knockdown in human erythroid precursors led to a slight increase of total cell numbers after 12 days of cell culture.

In conclusion we propose that TFR2 is a modulator of erythropoiesis in keeping with its function as an EPOR partner. It is possible that TFR2, as an iron sensor, modulates the erythropoietin sensitivity of the erythroid precursors. The increased red cell numbers might be the result of this function in iron-deficient *Tmprss6*^{-/-}*Tfr2*^{-/-} animals.

More specifically, since iron-loaded *Tfr2*^{-/-} mice are not characterized by increased red blood cell counts, we propose that TFR2 is a limiting factor for erythropoiesis, which controls red cell numbers to avoid excessive production in conditions of iron-restriction. Further studies in mice with specific erythroid deletion of *Tfr2* will clarify this possibility.

Acknowledgments

We acknowledge Prof. Carlos Lopez-Otin (Oviedo University, Spain) for releasing us the *Tmprss6*^{-/-} mouse.

Funding

This work was partially supported by Telethon Fondazione Onlus Rome (Grant GGP12025), MIUR PRIN 2010-2011 and the Italian Ministry of Health (Grant RF-2010-2312048) funds to CC and Progetti di Ateneo/CSP 2012 (TO_Call3_2012_0101) to GS.

Authorship and Disclosures

Information on authorship, contributions, and financial & other disclosures was provided by the authors and is available with the online version of this article at www.haematologica.org.

References

- Camaschella C, Roetto A, Cali A, De Gobbi M, Garozzo G, Carella M, et al. The gene TFR2 is mutated in a new type of haemochromatosis mapping to 7q22. *Nat Genet.* 2000;25(1):14-5.
- Roetto A, Totaro A, Piperno A, Piga A, Longo F, Garozzo G, et al. New mutations inactivating transferrin receptor 2 in hemochromatosis type 3. *Blood.* 2001;97(9):2555-60.
- Kawabata H, Yang R, Hirama T, Vuong PT, Kawano S, Gombart AF, et al. Molecular cloning of transferrin receptor 2. A new member of the transferrin receptor-like family. *J Biol Chem.* 1999;274(30):20826-32.
- Kawabata H, Germain RS, Ikezoe T, Tong X, Green EM, Gombart AF, et al. Regulation of expression of murine transferrin receptor 2. *Blood.* 2001;98(6):1949-54.
- Johnson MB, Chen J, Murchison N, Green FA, Enns CA. Transferrin receptor 2: evidence for ligand-induced stabilization and redirection to a recycling pathway. *Mol Biol Cell.* 2007;18(3):743-54.
- Goswami T, Andrews NC. Hereditary hemochromatosis protein, HFE, interaction with transferrin receptor 2 suggests a molecular mechanism for mammalian iron sensing. *J Biol Chem.* 2006;281(39):28494-8.
- Gao J, Chen J, Kramer M, Tsukamoto H, Zhang AS, Enns CA. Interaction of the hereditary hemochromatosis protein HFE with transferrin receptor 2 is required for transferrin-induced hepcidin expression. *Cell Metab.* 2009;9(3):217-27.
- Camaschella C. Understanding iron homeostasis through genetic analysis of hemochromatosis and related disorders. *Blood.* 2005;106(12):3710-7.
- Rishi G, Crampton EM, Wallace DF, Subramaniam VN. In situ proximity ligation assays indicate that hemochromatosis proteins Hfe and transferrin receptor 2 (Tfr2) do not interact. *PLoS One.* 2013;8(10):e77267.
- Nemeth E, Tuttle MS, Powelson J, Vaughn MB, Donovan A, Ward DM, et al. Hepcidin regulates cellular iron efflux by binding to ferroportin and inducing its internalization. *Science.* 2004;306(5704):2090-3.
- Meynard D, Kautz L, Darnaud V, Canonne-Hergaux F, Coppin H, Roth MP. Lack of the bone morphogenetic protein BMP6 induces massive iron overload. *Nat Genet.* 2009;41(4):478-81.
- Andriopoulos B Jr, Corradini E, Xia Y, Faasse SA, Chen S, Grgurevic L, et al. BMP6 is a key endogenous regulator of hepcidin expression and iron metabolism. *Nat Genet.* 2009;41(4):482-7.
- D'Alessio F, Hentze MW, Muckenthaler MU. The hemochromatosis proteins HFE, TFR2, and HJV form a membrane-associated protein complex for hepcidin regulation. *J Hepatol.* 2012;57(5):1052-60.
- Wallace DF, Summerville L, Subramaniam VN. Targeted disruption of the hepatic transferrin receptor 2 gene in mice leads to iron overload. *Gastroenterology.* 2007;132(1):301-10.
- Roetto A, Di Cunto F, Pellegrino RM, Hirsch E, Azzolino O, Bondi A, et al. Comparison of 3 Tfr2-deficient murine models suggests distinct functions for Tfr2-alpha and Tfr2-beta isoforms in different tissues. *Blood.* 2010;115(16):3382-9.
- Forejtnikova H, Vieillevoeye M, Zermati Y, Lambert M, Pellegrino RM, Guihard S, et al. Transferrin receptor 2 is a component of the erythropoietin receptor complex and is required for efficient erythropoiesis. *Blood.* 2010;116(24):5357-67.
- Silvestri L, Pagani A, Nai A, De Domenico I, Kaplan J, Camaschella C. The serine protease matriptase-2 (TMPRSS6) inhibits hepcidin activation by cleaving membrane hepcidin. *Cell Metab.* 2008;8(6):502-11.
- Finberg KE, Heeney MM, Campagna DR, Aydinok Y, Pearson HA, Hartman KR, et al. Mutations in TMPRSS6 cause iron-refractory iron deficiency anemia (IRIDA). *Nat Genet.* 2008;40(5):569-71.
- Du X, She E, Gelbart T, Truksa J, Lee P, Xia Y, et al. The serine protease TMPRSS6 is required to sense iron deficiency. *Science.* 2008;320(5879):1088-92.
- Folgueras AR, de Lara FM, Pendas AM, Garabaya C, Rodriguez F, Astudillo A, et al. Membrane-bound serine protease matriptase-2 (Tmprss6) is an essential regulator of iron homeostasis. *Blood.* 2008;112(6):2539-45.
- Hershko C, Camaschella C. How I treat unexplained refractory iron deficiency anemia. *Blood.* 2014;123(3):326-33.
- Benyamin B, Ferreira MA, Willemsen G, Gordon S, Middelberg RF, McEvoy BP, et al. Common variants in TMPRSS6 are associated with iron status and erythrocyte volume. *Nat Genet.* 2009;41(11):1173-5.
- Ganesh SK, Zakai NA, van Rooij FJ, Soranzo N, Smith AV, Nalls MA, et al. Multiple loci influence erythrocyte phenotypes in the CHARGE Consortium. *Nat Genet.* 2009;41(11):1191-8.
- Chambers JC, Zhang W, Li Y, Sehmi J, Wass MN, Zabaneh D, et al. Genome-wide association study identifies variants in TMPRSS6 associated with hemoglobin levels. *Nat Genet.* 2009;41(11):1170-2.
- Soranzo N, Spector TD, Mangino M, Kuhnel B, Rendon A, Teumer A, et al. A genome-wide meta-analysis identifies 22 loci associated with eight hematological parameters in the HaemGen consortium. *Nat Genet.* 2009;41(11):1182-90.
- Tanaka T, Roy CN, Yao W, Matteini A, Semba RD, Arking D, et al. A genome-wide association analysis of serum iron concentrations. *Blood.* 2010;115(1):94-6.
- Traglia M, Girelli D, Biino G, Campostrini N, Corbella M, Sala C, et al. Association of HFE and TMPRSS6 genetic variants with iron and erythrocyte parameters is only in part dependent on serum hepcidin concentrations. *J Med Genet.* 2011;48(9):629-34.
- Nai A, Pagani A, Silvestri L, Camaschella C. Increased susceptibility to iron deficiency of *Tmprss6*-haploinsufficient mice. *Blood.* 2010;116(5):851-2.
- Nai A, Pagani A, Silvestri L, Campostrini N, Corbella M, Girelli D, et al. TMPRSS6 rs855791 modulates hepcidin transcription in vitro and serum hepcidin levels in normal individuals. *Blood.* 2011;118(16):4459-62.
- Maurer E, Gutschow M, Stirnberg M. Matriptase-2 (TMPRSS6) is directly up-regulated by hypoxia inducible factor-1: identification of a hypoxia-responsive element in the TMPRSS6 promoter region. *Biol Chem.* 2012;393(6):535-40.
- Meynard D, Vaja V, Sun CC, Corradini E, Chen S, Lopez-Otin C, et al. Regulation of TMPRSS6 by BMP6 and iron in human cells and mice. *Blood.* 2011;118(3):747-56.
- Finberg KE, Whittlesey RL, Andrews NC. *Tmprss6* is a genetic modifier of the Hfe-hemochromatosis phenotype in mice. *Blood.* 2011;117(17):4590-9.
- Lee P, Hsu MH, Welsch-Alves J, Peng H. Severe microcytic anemia but increased erythropoiesis in mice lacking Hfe or Tfr2 and *Tmprss6*. *Blood Cells Mol Dis.* 2012;48(3):173-8.
- Schmidt PJ, Toudjarska I, Sendamarai AK, Racie T, Milstein S, Bettencourt BR, et al. An RNAi therapeutic targeting *Tmprss6* decreases iron overload in Hfe(-/-) mice and ameliorates anemia and iron overload in murine beta-thalassemia intermedia. *Blood.* 2013;121(7):1200-8.
- Guo S, Casu C, Gardenghi S, Booten S, Aghajan M, Peralta R, et al. Reducing TMPRSS6 ameliorates hemochromatosis and beta-thalassemia in mice. *J Clin Invest.* 2013;123(4):1531-41.
- McDonald CJ, Wallace DF, Ostini L, Subramaniam VN. Parenteral vs oral iron: Influence on hepcidin signaling pathways though analysis of Hfe/Tfr2 null mice. *Am J Physiol Gastrointest Liver Physiol.* 2014;306(2):G132-9.

Research Article

Altered Erythropoiesis in Mouse Models of Type 3 Hemochromatosis

R. M. Pellegrino,¹ F. Riondato,² L. Ferbo,¹ M. Boero,¹ A. Palmieri,¹ L. Osella,² P. Pollicino,² B. Miniscalco,² G. Saglio,¹ and A. Roetto¹

¹Department of Clinical and Biological Sciences, AOU San Luigi Gonzaga, University of Torino, Orbassano, Torino, Italy

²Department of Veterinary Sciences, University of Torino, Grugliasco, Torino, Italy

Correspondence should be addressed to A. Roetto; antonella.roetto@unito.it

Received 7 September 2016; Revised 1 March 2017; Accepted 4 April 2017; Published 2 May 2017

Academic Editor: Francesco Onida

Copyright © 2017 R. M. Pellegrino et al. This is an open access article distributed under the Creative Commons Attribution License, which permits unrestricted use, distribution, and reproduction in any medium, provided the original work is properly cited.

Type 3 haemochromatosis (HFE3) is a rare genetic iron overload disease which ultimately lead to compromised organs functioning. HFE3 is caused by mutations in transferrin receptor 2 (TFR2) gene that codes for two main isoforms (Tfr2 α and Tfr2 β). Tfr2 α is one of the hepatic regulators of iron inhibitor hepcidin. Tfr2 β is an intracellular isoform of the protein involved in the regulation of iron levels in reticuloendothelial cells. It has been recently demonstrated that Tfr2 is also involved in erythropoiesis. This study aims to further investigate Tfr2 erythropoietic role by evaluating the erythropoiesis of two Tfr2 murine models wherein either one or both of Tfr2 isoforms have been selectively silenced (Tfr2 KI and Tfr2 KO). The evaluations were performed in bone marrow and spleen, in 14 days' and 10 weeks' old mice, to assess erythropoiesis in young versus adult animals. The lack of Tfr2 α leads to macrocytosis with low reticulocyte number and increased hemoglobin values, together with an anticipation of adult BM erythropoiesis and an increased splenic erythropoiesis. On the other hand, lack of Tfr2 β (Tfr2 KI mice) causes an increased and immature splenic erythropoiesis. Taken together, these data confirm the role of Tfr2 α in modulation of erythropoiesis and of Tfr2 β in favoring iron availability for erythropoiesis.

1. Introduction

Type 3 haemochromatosis (HFE3) is an autosomal recessive genetic disorder that leads to an accumulation of iron both in the blood and in several tissues, especially in the liver. Because of this, HFE3 patients have elevated transferrin saturation (TS) and serum ferritin level (sFt) [1].

This disease is caused by mutations in transferrin receptor 2 (TFR2) gene [2] that codes for two main isoforms, namely, Tfr2 alpha (Tfr2 α) and Tfr2 beta (Tfr2 β), that show moderate homology to the type 1 transferrin receptor (Tfr1) [3]. Unlike Tfr1, TFR2 gene expression itself is not directly regulated by iron [4] and TFR2 mRNA does not have iron responsive elements (IREs). Thus, there is no IRE-dependent posttranscriptional regulation of the protein levels [5]. Several in vitro studies have demonstrated that Tfr2 α can bind iron loaded transferrin, however, with an affinity remarkably lower than that of Tfr1 [3]. Additionally, the levels of this protein in plasma membrane are regulated by TS, with an increased

stabilization in the presence of highly saturated transferrin [6, 7]. The transcription of the entire TFR2 gene gives rise to the Tfr2 α isoform which is a transmembrane protein. Tfr2 β , on the other hand, is a shorter isoform lacking the cytoplasmic and transmembrane domains, and it is currently unknown if its activity is intracellular or extracellular. The expression patterns of these two isoforms are also very different. Tfr2 α is highly transcribed in the liver and in erythroleukemic cell line (K562), while Tfr2 β is mainly transcribed in liver, brain, heart [3], and splenic macrophages [8]. Most TFR2 mutations compromise the production of both Tfr2 isoforms. However, some mutations affect only the Tfr2 α isoform, while others, such as M172K, abolish the Tfr2 β methionine starting codon [9, 10].

Studies on murine models of HFE3 have demonstrated that Tfr2 α and Tfr2 β isoforms have distinct functions in iron homeostasis. While Tfr2 α is involved in the hepatic pathway regulating iron hormone hepcidin (Hamp) [7], Tfr2 β is involved in iron efflux from reticuloendothelial cells [8].

A recent study has demonstrated that the Tfr2 α isoform is also expressed in erythroid progenitors. Here, it interacts with and stabilizes the erythropoietin receptor (EpoR), hence establishing a correlation between Tfr2 α and erythropoiesis for the first time [11]. Furthermore, it is thought to be directly involved in the mechanisms of control of erythropoiesis, especially in conditions of iron deprivation [12, 13].

It is well known that erythropoiesis, as well as iron demand, changes throughout life in humans as a consequence of an increase in blood volume. Also, complete blood cell count (CBC) values differ slightly depending upon the age [14]. To our knowledge, no data exist to date on variations in erythropoiesis during ageing in mice. Some regulators of erythropoiesis have been characterized in recent years. One of them, named Erythroferrone (Erfe), is a hormone produced by erythroblasts that is able to regulate Hamp levels as a consequence of erythropoietic demand due to blood loss [15] or anemia of inflammation [16].

To investigate how Tfr2 α silencing influences erythrocyte production across lifespan in mice, we studied erythropoiesis in two primary erythropoietic organs, the bone marrow (BM) and the spleen, at different ages using two mouse models with inactivated Tfr2 α and/or Tfr2 β . The findings of this study could be an important step toward gaining a better insight into Tfr2 involvement in erythropoiesis in humans.

Our results indicate that the lack of Tfr2 α influences BM and splenic erythropoiesis starting from an early stage of life. Moreover, Tfr2 β also influences erythropoiesis by the modulation of iron availability for erythrocyte maturation. More importantly, we now show that Erfe expression is regulated by erythropoiesis not only in adult animals, as previously demonstrated [15], but also in young age. Additionally, Erfe appears to be negatively modulated by erythropoietic tissues' iron availability. Lastly, we also describe the physiological variations of erythropoietic activity in WT mice during ageing.

2. Materials and Methods

2.1. Animals. Two Tfr2 mouse models on 129X1/svJ strain were studied: (1) Tfr2 KI that has the Tfr2 β isoform inactivated ($\alpha^+\beta^0$) and (2) Tfr2 KO that has both Tfr2 isoforms inactivated ($\alpha^0\beta^0$). Selective targeting of Tfr2 isoforms was obtained starting from the same target construct in which murine M163K mutation (homologous to M172K human variant) was inserted in murine Tfr2 gene exon 4 flanked by 3 loxP sites activated through Cre/lox recombination system [8].

At adult age (10 w), Tfr2 KI mice have normal Hamp and normal serum iron parameters but splenic iron overload, while Tfr2 KO animals have normal Hamp but high serum ferritin and transferrin saturation as well as hepatic iron overload [8].

All animals were housed at Department of Veterinary Sciences, University of Torino. Animal housing and all the experimental procedures were performed in accordance with European (Official Journal of the European Union L276 del 20/10/2010, Vol. 53, p. 33–80) and National Legislation

(Gazzetta Ufficiale n° 61 del 14/03/2014, p. 2–68) for the protection of animals used for scientific purposes.

Tfr2-targeted mice and controls were maintained on standard conditions and with ad libitum access to food and water. They were analyzed at 14 days and 10 weeks of age. Only male mice were used in this study to minimize potential variability related to sex.

At least 6 animals were analyzed for each experimental condition.

2.2. Hematological Analysis. Peripheral blood from the animals was subjected to complete blood cell count (CBC) analysis. Hemoglobin concentration (HB), hematocrit (HCT), erythrocytes number (RBC), and other indices (MCV, MCH, MCHC, and reticulocytes) were measured using an ADVIA®120 Hematology System (Siemens Diagnostics).

2.3. Flow Cytometry. Spleen and bone marrow (BM) were extracted from sacrificed animals and used for flow cytometric analysis using APC-Ter119 and PE-CD71. Fc-receptor was previously blocked using anti-mouse CD16/CD32; a mix of FITC-conjugated lymphoid and myeloid markers (CD3e, CD45R, CD41, CD11b, and Gr-1) was used to exclude leukocytes and 7-AAD was used to exclude dead cells. All reagents were purchased from eBiosciences. Ter119-positive events were allocated into five subsets representing sequential maturation stages (ProE, EryA, EryB, and EryC), according to CD71 intensity and FSC properties [17–19]. An EryD region was added according to the results by Chen et al., who localized a gate where orthochromic erythroblasts with nuclear-cytoplasmic dyssynchrony fall [19].

2.4. Histology and Perl's Staining. Animals livers and spleens were explanted, fixed in 4% PFA, cryoprotected by a sucrose gradient (7.5%, 15%, and 30%), and embedded in OCT prior to cryosectioning at 30 μ m. Tissue sections were stained with Perl's Prussian blue method (Bio-Optica). Images were taken at 20x magnification using a LEICA DFC208 microscope.

2.5. Monocytes/Macrophages Isolation. For each group (Tfr2 KI, Tfr2 KO, and control litter-mates), monocytes/macrophages were separated from a pool of 4 spleens using MACS CD11b MicroBeads (Miltenyi Biotec).

2.6. Molecular Analysis. Hamp gene expression was evaluated in Tfr2 targeted and in WT mouse liver. For reverse-transcription, 1 μ g of total RNA, 25 μ M random hexamers, and 100 U of reverse transcriptase (Applied Biosystems, USA) were used.

Hamp expression levels were measured by quantitative real-time reverse-transcription (RT-PCR) with CFX96 Real-Time System (BIO-RAD) using a quantitative RT-PCR assay (Assays-on-Demand; Applied Biosystems, USA). Erfe expression was evaluated using SYBR Green PCR technology (EVAGreen, BIO-RAD) using the following primers: mErfe F1 5'ATGGGGCTGGAGAACAGC3' and mErfe R1 5'TGGCATTGTCCAAGAAGACA3'. All analyses were carried out in triplicate and results showing a discrepancy greater

than 1 threshold cycle in 1 of the wells were excluded. *Gus* (β -glucuronidase) gene was used as housekeeping control. The results were analyzed using the $\Delta\Delta$ threshold cycle (C_t) method [20].

Western blots of BM, spleen, and monocytes/macrophages lysates (50 μ g) for Cleaved Caspase-3 (5A1E, Cell Signaling), Bcl-x_L (H-5), divalent metal transporter 1 (DMT1) (H-108), Fpn1 (G-16), Tfr2 (S-20), β -actin (C-4) (Santa Cruz Biotechnology), and Ft-L (kindly provided by S. Levi, Milan) proteins were performed through standard protocols.

Data from Western blot quantification (Image Lab Software, BIO-RAD) were obtained after normalizing on β -actin levels and expressed as fold increase, relative to the mean value obtained from the WT mice.

2.7. Statistical Analysis. For hematological analysis and flow cytometry experiments, statistical comparisons among genotypes and age groups were performed using nonparametric tests (Kruskal-Wallis or Mann-Whitney, resp.) using SPSS version 21 software. Differences of mRNA expression and protein production between controls and targeted mice were evaluated with a nonparametric Student's *t*-test (unpaired, two-tailed) using GraphPad Prism software. $P < 0.05$ was considered to be statistically significant.

3. Results

3.1. Peripheral Blood Cell Count. The pattern of erythropoiesis was observed to be different in WT and Tfr2 mice across the lifespan. Additionally, Tfr2 mice showed significant variations in erythropoiesis compared to age-matched WT controls in the CBC assay.

3.1.1. Young versus Adult Animals. 14 d old mice had lower RBC, HB, and HCT and higher MCV and reticulocytes compared to adults in all genotypes analyzed (Figure 1). Young WT mice showed similar MCH but lower MCHC as compared to adult WT mice, demonstrating that normal mouse erythropoiesis during animal growth follows the same trend as that of normal human erythropoiesis [14].

Young Tfr2 KI and KO mice demonstrated higher MCH but similar MCHC compared to adult animals with the same genotype (Figure 1). Thus, young Tfr2 mice have increased the levels of hemoglobin in RBC compared to age-matched WT animals. However, the differences are statistically significant only in Tfr2 KO mice.

3.1.2. Young Tfr2 Mice. The comparison of 14 d old Tfr2 KI to WT mice did not reveal any significant differences in all CBC parameters analyzed. On the contrary, 14 d old Tfr2 KO mice had higher RBC, HB, HCT, MCH, and MCHC values than age-matched WT mice (significant differences for HB, MCH, and MCHC only) (Figures 1(b), 1(e), and 1(g)) and a significantly lower number of reticulocytes (Figure 1(f)).

To investigate if this difference in the number of reticulocytes in young Tfr2 KO animals could be due to an alteration of the apoptosis pathway in the BM, we analyzed Cleaved Caspase-3 (CC-3) [21] and Bcl-x_L [22]. The level of

the proapoptotic marker CC-3 was comparable to that of age-matched WT mice, while the antiapoptotic marker Bcl-x_L increased about 1.5-fold in Tfr2 KO young animals versus WT (Figure S1 A, in Supplementary Material available online at <https://doi.org/10.1155/2017/2408941>). In conclusion, an increase in apoptotic death is not the underlying cause for the decreased reticulocyte production in these animals.

3.1.3. Adult Tfr2 Mice. Adult Tfr2 KI animals had significantly higher number of RBC but lower MCH and MCHC compared to age-matched WT (Figures 1(a), 1(e), and 1(g)); however, these differences were not statistically significant.

Adult Tfr2 KO mice had statistically significantly increased MCV and MCH compared to WT litter-mates of the same age (Figures 1(d) and 1(e)). All the other CBC parameters were comparable to those of age-matched WT animals.

3.2. BM and Spleen Erythropoiesis. Flow cytometry analysis of the BM and spleen erythropoiesis revealed several unexpected results in both young and adult animals.

The BM erythropoiesis was increased in adult mice compared to the young ones (Figure 2(a)) in WT and KI mice alike. In contrast, Tfr2 KO mice had high levels of erythropoiesis already at 14 d of age, with values similar to adults (Figure 2(a)).

Both Tfr2 KI and Tfr2 KO 14 d old mice had increased splenic erythropoiesis compared to age-matched WT, though the difference was statistically significant only for the Tfr2 KO group. Interestingly, splenic erythropoiesis similarly reduced in adulthood for the two genotypes, reaching comparable values to the WT (Figure 2(b)).

From the qualitative point of view, no evident differences were found in the BM of young Tfr2 mice except for a higher number of EryD cells in Tfr2 KO (Figure 2(c)). Unexpectedly, an enhanced splenic erythropoiesis was observed in young Tfr2 KI mice, characterized by a left shift in the erythroid lineage resulting in a higher number of precursor erythroid cells and a lower number of mature cells (Figure 2(d)). Similarly, young Tfr2 KO mice also presented increased splenic erythropoiesis, as mentioned above (Figure 2(b)). However, no statistically different values were found compared to WT (Figure 2(d)).

Surprisingly, the erythropoiesis in adult Tfr2 KO mice was markedly altered. Although an increase in the percentage of early precursors (Figures 2(c) and 2(d)) was found, no reticulocytosis could be seen in these mice. This could be because of an increase in apoptosis as is evidenced by the doubling of the levels of the apoptotic marker Caspase-3 in adult Tfr2 KO mice compared to age-matched WT. On the contrary, the antiapoptotic marker Bcl-x_L was significantly decreased in Tfr2 KO mice compared to WT (Figure S1 B).

Finally, flow cytometry analysis revealed that in both young and adult Tfr2 KO mice CD71 MFI was significantly lower compared to WT in BM as well as in the spleen and in all erythroid maturation stages except for EryC in adult animals. CD71 MFI in Tfr2 KO mice was lower compared to

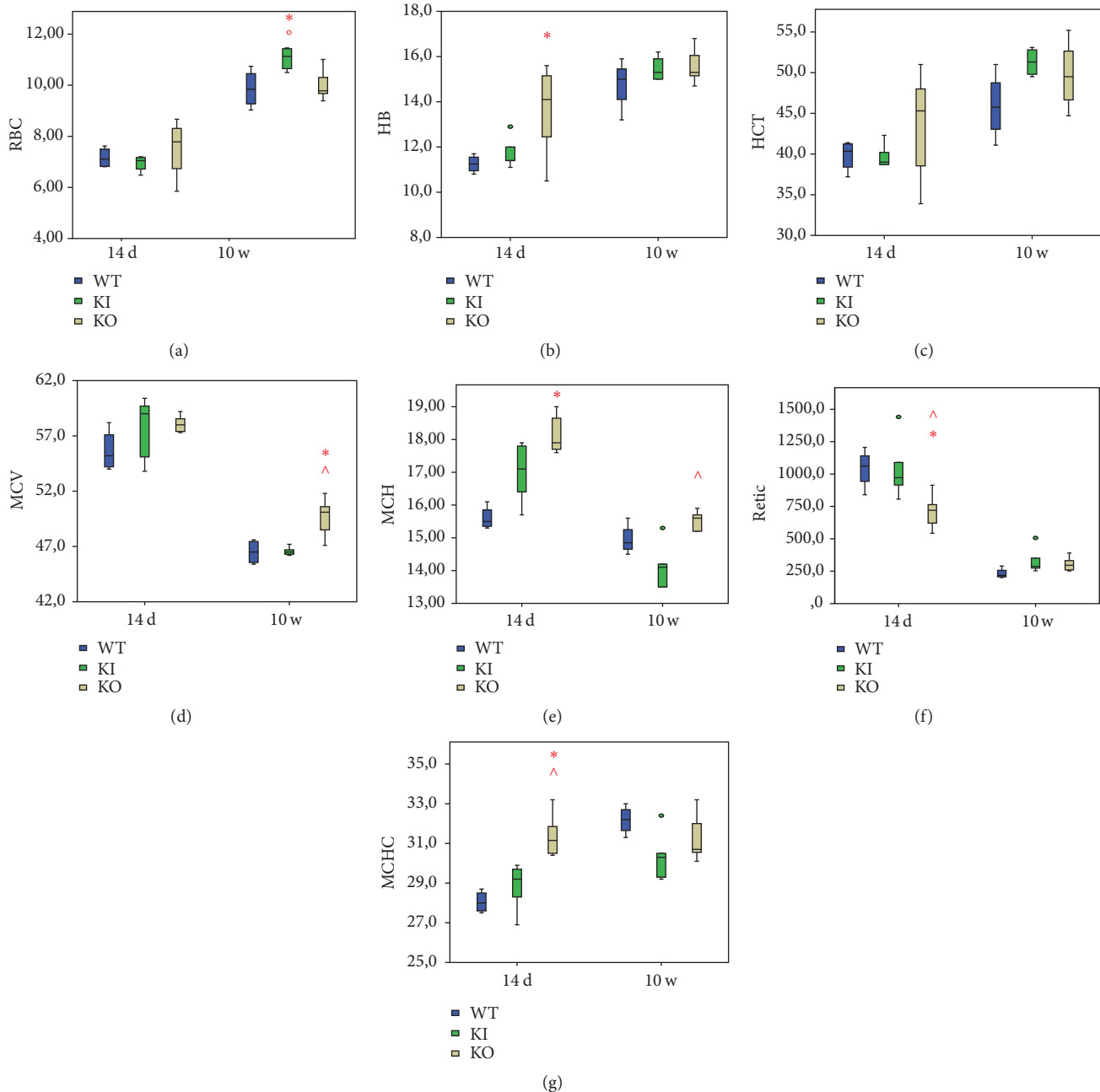


FIGURE 1: (a) Red blood cells (RBC; $\times 10^6$ cells/ μ L), (b) hemoglobin concentration (HB; g/dL), (c) hematocrit (HCT; %), (d) mean corpuscular volume (MCV; fL), (e) mean corpuscular hemoglobin (MCH; pg), (f) reticulocytes (retic; $\times 10^9$ cells/L), and (g) mean corpuscular hemoglobin concentration (MCHC; g/dL) values obtained from animals CBC. WT: wild type (blue); KI: Tfr2 KI (green); KO: Tfr2 KO (yellow); 14 d: 14 days; 10 w: 10 weeks. * \circ \wedge indicate statistically significant differences ($P < 0.05$) compared to age-matched WT, KO, and KI, respectively.

KI mice for EryC in young animals and for EryA and EryB in adults (Figure S2).

3.3. Iron Levels in Tfr2 Animals. Since iron availability could influence erythropoietic stimulus, we analyzed the iron levels and hepatic Hamp production in erythropoietic tissues of Tfr2 animals as compared to controls.

Perl's histological staining (Figures 3(a) and 3(b)) revealed surprisingly high iron levels in livers from Tfr2 KO mice already at 14 d of age (Figure 3(a)) and, as expected, in adult animals as well (Figure 3(b)). In contrast, no significant liver iron deposit was visible in Tfr2 KI young and adult animals (Figures 3(a) and 3(b)). A significant splenic iron overload was evidenced only in Tfr2 KI adult animals (Figure 3(b)).

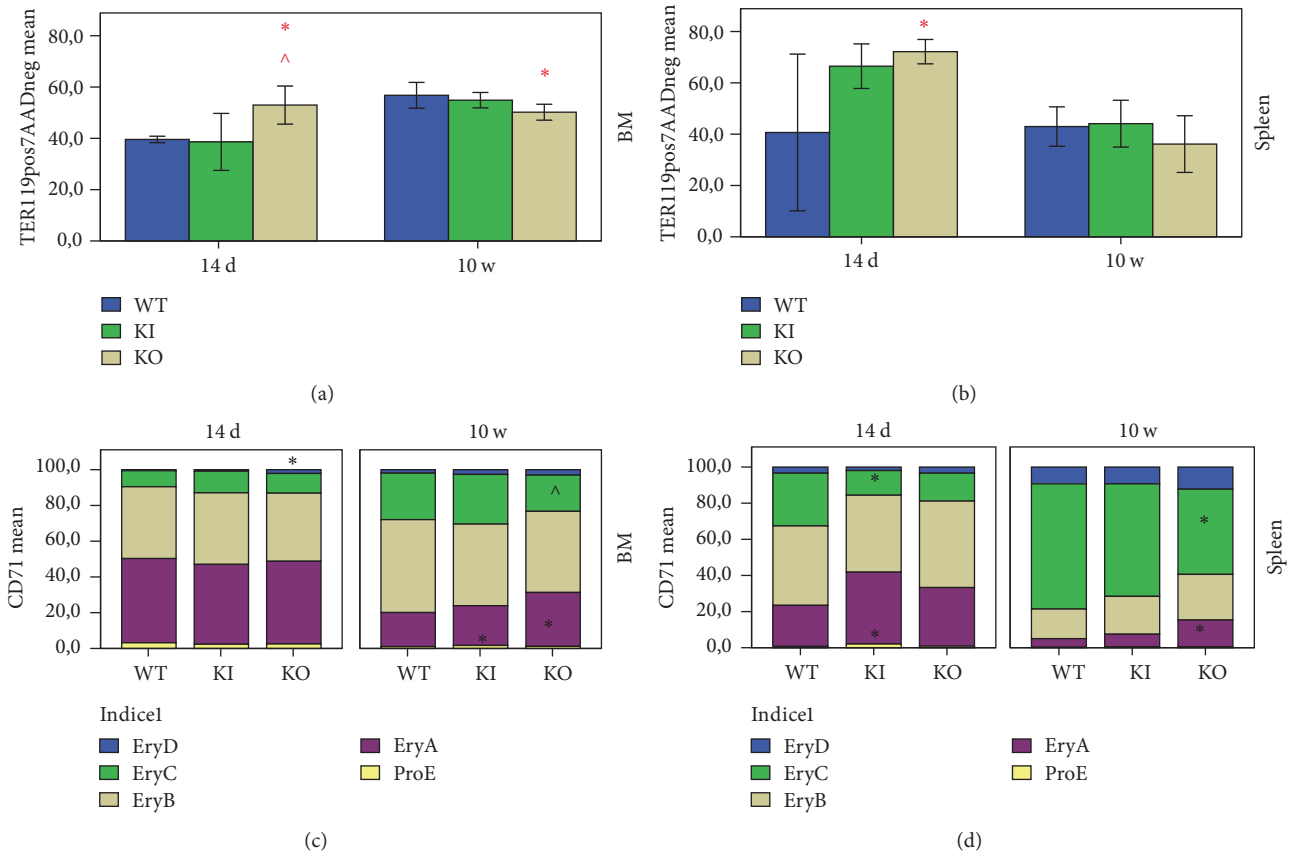


FIGURE 2: Flow cytometry analysis of quantitative (a, b) and qualitative (c, d) erythropoiesis in bone marrow (BM) and spleen of 14 days (14 d) and 10 weeks (10 w) old mice. WT: wild type; KI: Tfr2 KI; KO: Tfr2 KO. ProE, EryA, EryB, EryC, and EryD represent sequential erythropoietic maturation stages. * ^ indicate statistically significant differences ($P < 0.05$) compared to age-matched WT and KI, respectively.

BM iron staining with Perl's did not reveal any obvious large iron deposit (data not shown). In addition, L ferritin (Ft-L) levels were found to be significantly elevated in the BM of both Tfr2 young mice (Figure 3(c)). However, during adulthood, it remained high only in the BM of Tfr2 KO mice (Figure 3(d)).

3.4. Hamp and Erfe Analysis. The hepatic Hamp expression was significantly decreased in Tfr2 KI and KO animals compared to age-matched WT litter-mates. The same was true for adult animals, although to a lesser degree (Figures 4(a) and 4(b)).

Additionally, Erfe transcript levels were significantly different in the three genotypes: they were significantly higher in the BM and the spleen of young Tfr2 KI animals and significantly lower in young Tfr2 KO mice as compared to WT (Figures 4(c) and 4(d)). In adult Tfr2 KI and KO mice, Erfe transcription was similar to adult WT in both tissues analyzed (Figures 4(c) and 4(d)).

Longitudinal comparison between the two ages revealed that Erfe transcription was significantly increased in the young compared to genotype matched adult mice, with the exception of Tfr2 KO BM, whose Erfe amount remained

constant during the growth period of the animal (Figures 4(c) and 4(d)).

3.5. Erythropoietic Tissues Monocytes. To unravel the role of Tfr2 β isoform in the iron flux in macrophages during erythropoiesis, this cell type was isolated from the spleen of WT and Tfr2 targeted mice at the two experimental time points. Tfr2 β levels were evaluated, together with the main proteins involved in cellular iron traffic, namely, the iron deposit protein ferritin (Ft-L), the iron importer DMT1, and the iron exporter Ferroportin 1 (Fpn1).

In WT mice, Tfr2 β isoform was observed to decrease in splenic macrophages of adult animals as compared to the young ones (Figure 5(a)). In the same cells, DMT1 and Fpn1 decreased as well, while Ft-L levels increased (Figure 5(b)).

In young Tfr2 KI mice, splenic macrophages presented a lower DMT1 and higher Fpn1 and Ft-L compared to age-matched WT sib pairs (Figure 5(b)). During the growth period, DMT1 and Ft-L consistently increased while Fpn1 significantly decreased.

On the other hand, in young Tfr2 KO mice, splenic macrophages presented a lower DMT1 and Fpn1 and comparable Ft-L in comparison to age-matched WT sib pairs

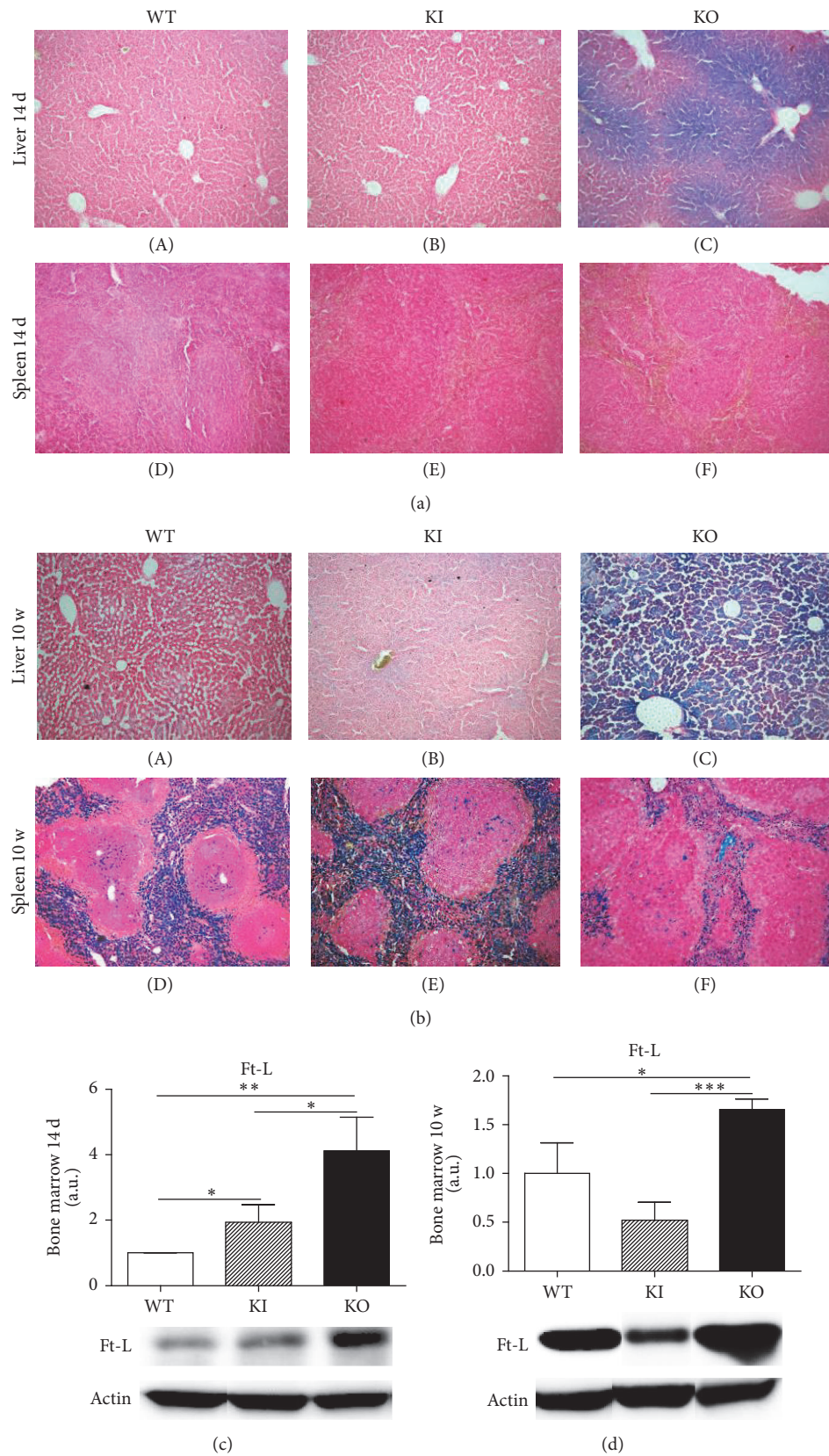


FIGURE 3: Perl's Prussian blue staining of liver and spleen sections from wild type (WT), Tfr2 KI (KI), and Tfr2 KO (KO) animals at (a) 14 days (14 d) and (b) 10 weeks (10 w) of age. Western blot analysis shows ferritin L (Ft-L) protein production in bone marrow of WT, KI, and KO mice at (c) 14 days (14 d) and (d) 10 weeks (10 w) of age. a.u.: arbitrary unit. The following symbols indicate statistically significant differences: * $P < 0.05$, ** $P < 0.01$, and *** $P < 0.001$ compared to age-matched WT mice.

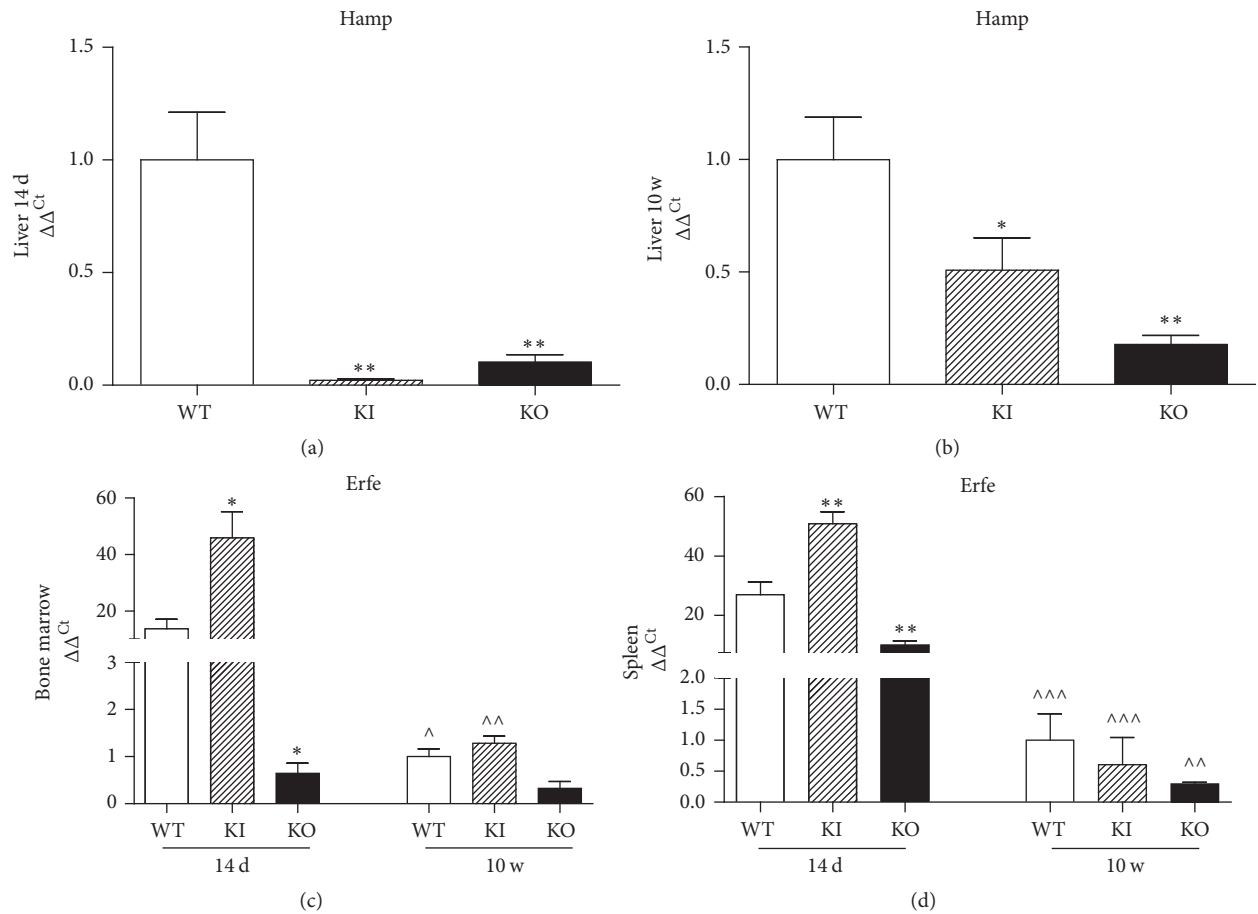


FIGURE 4: Hepcidin (Hamp) gene expression in *Tfr2* targeted and in WT mouse liver at (a) 14 days (14 d) and (b) 10 weeks (10 w) of age. Erythropoietin (Erfe) gene expression in bone marrow (c) and spleen (d) of WT, KI, and KO mice at 14 days (14 d) and 10 weeks (10 w) of age. WT: wild type; KI: *Tfr2* KI; KO: *Tfr2* KO. The following symbols indicate statistically significant differences: * $P < 0.05$ and ** $P < 0.01$ compared to age-matched WT mice; ^ $P < 0.05$, ^^ $P < 0.01$, and ^^ $P < 0.001$ compared to animals with the same genotype at 14 days of age.

(Figure 5(b)). During the growth period, DMT1 and Fpn1 decreased while Ft-L was obviously increased.

4. Discussion

It is well known that iron is essential for adequate erythropoiesis. In the condition of iron deficiency, the most important pathway that is impaired is RBC production, firstly in the bone marrow (BM) followed by the spleen. Erythropoiesis itself undergoes physiological changes that reflect the requirements of an organism throughout its lifespan. It increases during youth, when there is massive body growth, but remains roughly constant during adult life and tends to decrease during ageing [23–25]. The adequate iron availability for this dynamic erythropoiesis is achieved through the modulation of hepcidin, one of the chief iron regulators [7].

Among the different hepcidin regulators, transferrin receptor 2 alpha (*Tfr2α*) has been shown to play a role as an iron sensor in the liver [7] and as erythropoiesis regulator in erythropoietic tissues [26]. Notably, the gene encoding *TFR2* is transcribed in two main isoforms: the alpha form,

expressed in the liver and few other tissues, and the shorter beta form, with a low ubiquitous expression. However, it is found to be in significantly higher levels in the spleen [3]. In the liver, *Tfr2α* exerts its action on the plasma membrane. It is not directly responsive to iron levels [4] but is stabilized on plasma membrane by iron loaded transferrin [27]. According to the most recent functional models, hepatic *Tfr2α* interacts with the other iron proteins as *Tfr1* and *Hfe*, to sense body iron levels and to transduce the signal of iron excess through the activation of the Smad 1/5/8 and/or the *Erk1/2* pathways, causing an increase in the hepatic hepcidin [7].

Recent data has demonstrated that *Tfr2α* also has an extrahepatic function. It is well expressed in BM, where it interacts with erythropoietin receptor (*EpoR*), thereby being involved in regulation of erythropoiesis [11]. Further, several studies have demonstrated the role of *Tfr2α* in regulating RBC production in mouse models, particularly in condition of iron deficiency [12, 13, 28].

In contrast, very little is known about the function of the second *TFR2* isoform, *Tfr2β*. It is significantly produced in splenic macrophages and its silencing in the *Tfr2* KI mice does not cause any variation in serum iron parameters

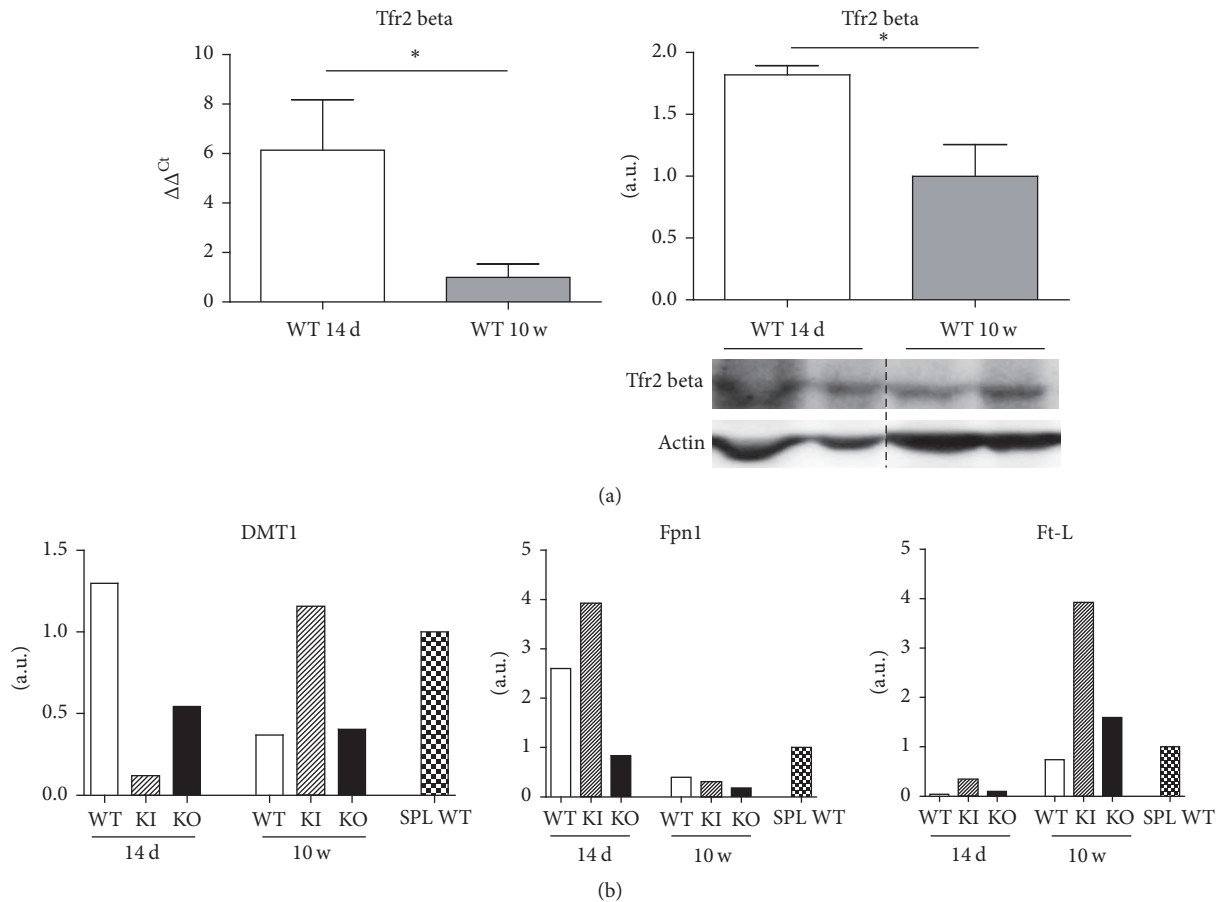


FIGURE 5: (a) Comparison between 14-day (14 d) and 10-week (10 w) Tfr2 β expression (on the left) and production (on the right) in splenic macrophages of wild type (WT) animals. (b) Quantification of divalent metal transporter 1 (DMT1), Ferroportin 1 (Fpn1) and ferritin L (Ft-L) protein production resulting from Western blot analysis of splenic macrophages isolated from WT, KI, and KO mice at 14 d and 10 w of ages. a.u.: arbitrary unit; SPL: total spleen. * indicates statistically significant difference ($P < 0.05$).

and liver iron content. Nevertheless, these animals present iron retention in the macrophages probably through the downregulation of iron exporter Fpn1 [8].

Therefore, in the present manuscript, we aimed to analyze the role of both Tfr2 isoforms in erythropoiesis and the contribution of available iron in the modulation of erythropoiesis. We used the Tfr2 KI animals ($\alpha^+\beta^0$), in which circulating iron levels are normal, and the Tfr2 KO mice ($\alpha^0\beta^0$), that have severe iron overload in addition to increased serum ferritin and transferrin saturation. We compared the erythropoiesis in these animals to that of WT litter-mates. Furthermore, we evaluated these two Tfr2 mouse models at young age (14 d), when iron demand is high to fulfill growth requirements, and at adult age (10 w), when iron is needed primarily for the maintenance of erythropoiesis. Our findings demonstrate that adult Tfr2 KO mice show normal erythroid parameters at CBC except for an increased MCV and a higher hemoglobin content (MCH). This indicates that, in Tfr2 KO mice, the maximum amount of HB is produced in the RBC in the early stages of erythropoiesis, when cells are larger. On the contrary, in WT animals, the same hemoglobin amount reaches the final concentration through the reduction of

RBC dimension. This phenomenon could be associated with an attempt of the body to eliminate the excess iron. In the same animals, BM and splenic erythroid production is quantitatively normal, but it is characterized by a shift toward immature precursors. The left shift in the maturation sequence could be an evidence of a delayed erythropoiesis in accordance with the results of previous studies [12, 13]. On the other hand, lack of reticulocytosis in these animals can be explained by an increase in the total BM apoptosis, confirmed by an increase of apoptotic marker Caspase-3 and a simultaneous decrease of the antiapoptotic protein Bcl-x_L. This could represent a late stage control mechanism that may account for the depletion of late precursors that is ultimately responsible for an ineffective erythropoiesis.

Importantly, these findings are in contrast with the study by Nai et al., in which BM specific Tfr2 KO mice (Tfr2^{BMKO}) present an increased number of RBCs, decreased volume and hemoglobin content, and increased splenic stress erythropoiesis, in the presence of normal serum iron parameters [28].

The primary genetic differences between these two models are that Tfr2^{BMKO} mice maintain Tfr2 α and β isoforms

function in the other body organs, particularly in the liver and in the spleen, whereas Tfr2 KO mice have a total silencing of both that causes an increased iron availability.

Therefore, the comparison between these two animal models is useful to unravel the role of iron in inducing RBC production in both the BM and the spleen. It is clear from the data that an increased iron availability in Tfr2 KO mice causes erythropoiesis, since 14 d old Tfr2 KO animals already have an erythropoietic activity similar to adult WT mice. In addition, it also causes erythropoietic changes, an increased number of immature cells, and increased apoptosis, as is evident in Tfr2 KO adult animals compared to age-matched WT. The increased iron levels in the BM of Tfr2 KO animals could trigger EryA erythroblasts production, but the increased apoptosis finally normalizes RBC output. Also, the presence of macrocytosis together with a low reticulocytes number and increased BM apoptosis in Tfr2 KO mice resembles the erythropoiesis of myelodysplastic syndromes (MDS) [29]. In these conditions, iron overload has been demonstrated to have a causative role. In fact, iron chelation of these MDS patients ameliorates their BM dysfunction [30].

It would be interesting to induce iron normalization in the Tfr2 KO animals to evaluate if a phenotype comparable to that of Nai et al. [28] can be achieved.

Another important difference between the two models is related to erythropoietic regulator Erythroferrone (Erfe) [15]. Erfe levels are increased in Tfr2^{BMKO} mice while decreased in our Tfr2 KO animals. Erfe increases due to an increased iron demand for erythropoiesis and causes a downregulation of hepcidin [28]. However, to our knowledge, this is the first time it has been demonstrated that Erfe reduction can also be a consequence of an adequate erythropoiesis, as we could observe in Tfr2 KO young animals.

Furthermore, the trend of Erfe in animals of different ages in both WT and Tfr2 targeted animals is very interesting. It clearly appears that Erfe has an important role in erythropoiesis regulation not only at adult age, as has been already demonstrated [16], but also at young age. Also, its expression correlates very well with erythropoietic boost in WT animals, being high in 14 d old animals and decreasing significantly in adult animals. Notably, BM and splenic Erfe transcription is significantly reduced in young Tfr2 KO animals and remains constant during their growth period, in agreement with the early achievement of adult erythropoiesis pattern in these mice.

The relationship between Erfe and Tfr2 has been demonstrated through several experimental approaches [13, 28]. Our data shows that this relationship is far more evident in young animals. Moreover, we demonstrate that the presence of Tfr2 α in the liver is essential to have the hepcidin response to Erfe. In fact, Hamp is decreased in response to an increase of Erfe in Tfr2 KI mice, that produces the Tfr2 alpha isoform, as expected. Similarly, in Tfr2^{BMKO} animal model, a decreased Erfe amount corresponds to and increases Hamp level [28]. On the contrary, in Tfr2 KO animals, in which Tfr2 α is absent in the liver, Hamp does not increase in response to low Erfe levels.

Lastly, the lack of Tfr2 β leads to an evident splenic iron accumulation only in adult Tfr2 KI animals, as previously demonstrated [8]. Furthermore, it is surprising to see that lack of Tfr2 α causes an iron accumulation as early as 14 d of age in the liver of Tfr2 KO animals.

We have focused at least a part of our analysis on young animals because very little is known about erythropoiesis at this stage of life even in WT animals. It is important to note that in the latter the erythropoietic stimulus is mainly iron-dependent, since an adult erythropoiesis becomes evident in iron enriched Tfr2 KO young animals.

Surprisingly, the data from the analysis of erythropoiesis in Tfr2 KI mice at young age is the most interesting, when these animals present normal serum iron parameters, normal BM and splenic iron amount, and normal CBC. In spite of this, their splenic erythropoiesis appears to be increased and immature compared to age-matched WT. These data are supported by a significant increase of BM and splenic Erfe as well. Tfr2 KO mice also present an early increased splenic erythropoiesis but it is qualitatively normal. This could be a consequence of the increased circulating iron availability that can ensure a qualitatively normal but relatively high splenic erythropoietic maturation.

Next, we hypothesized that enhanced splenic immature erythropoiesis in the absence of Tfr2 β in young Tfr2 KI mice could be caused by low iron availability because of iron retention in splenic macrophages. This situation should have been evident in the spleen, where reticuloendothelial cells are particularly abundant. So, to confirm this hypothesis, we evaluated iron levels in splenic monocytes of Tfr2 mice. We detected an increase in ferritin and a decrease in Fpn1 in the splenic monocytes of young Tfr2 KI and KO compared to WT age-matched mice, which confirms our hypothesis.

Interesting speculations can be made from this analysis of the evolution of splenic erythropoiesis during the lifespan of animals.

From the analysis of WT animals, it is evident that the spleen eventually loses its role as erythropoietic organ and becomes a deposit site for iron, that derives from erythrocyte catabolism. Ft-L in fact increases in splenic monocytes of WT mice during ageing due to Fpn1 decrease.

The same is true in Tfr2 mice's splenic monocytes, but here the increase of iron is far more evident in splenic monocytes of adult Tfr2 KI mice compared to age-matched WT and Tfr2 KO. Also, iron importer DMT1 is increased in the splenic monocytes of Tfr2 KI mice. Thus, it could be interesting to further investigate the relationship between Tfr2 β and this divalent metal transporter.

On the basis of the data obtained in the present manuscript, a model for the role of iron in the stimulation of erythropoiesis at different ages and the involvement of Tfr2 isoforms in erythropoietic organs is illustrated in Figure 6.

5. Conclusions

An analysis of erythropoiesis in mice with inactivation of one or both of Tfr2 isoforms confirms that there is a specific function of Tfr2 α in erythropoiesis, which has been

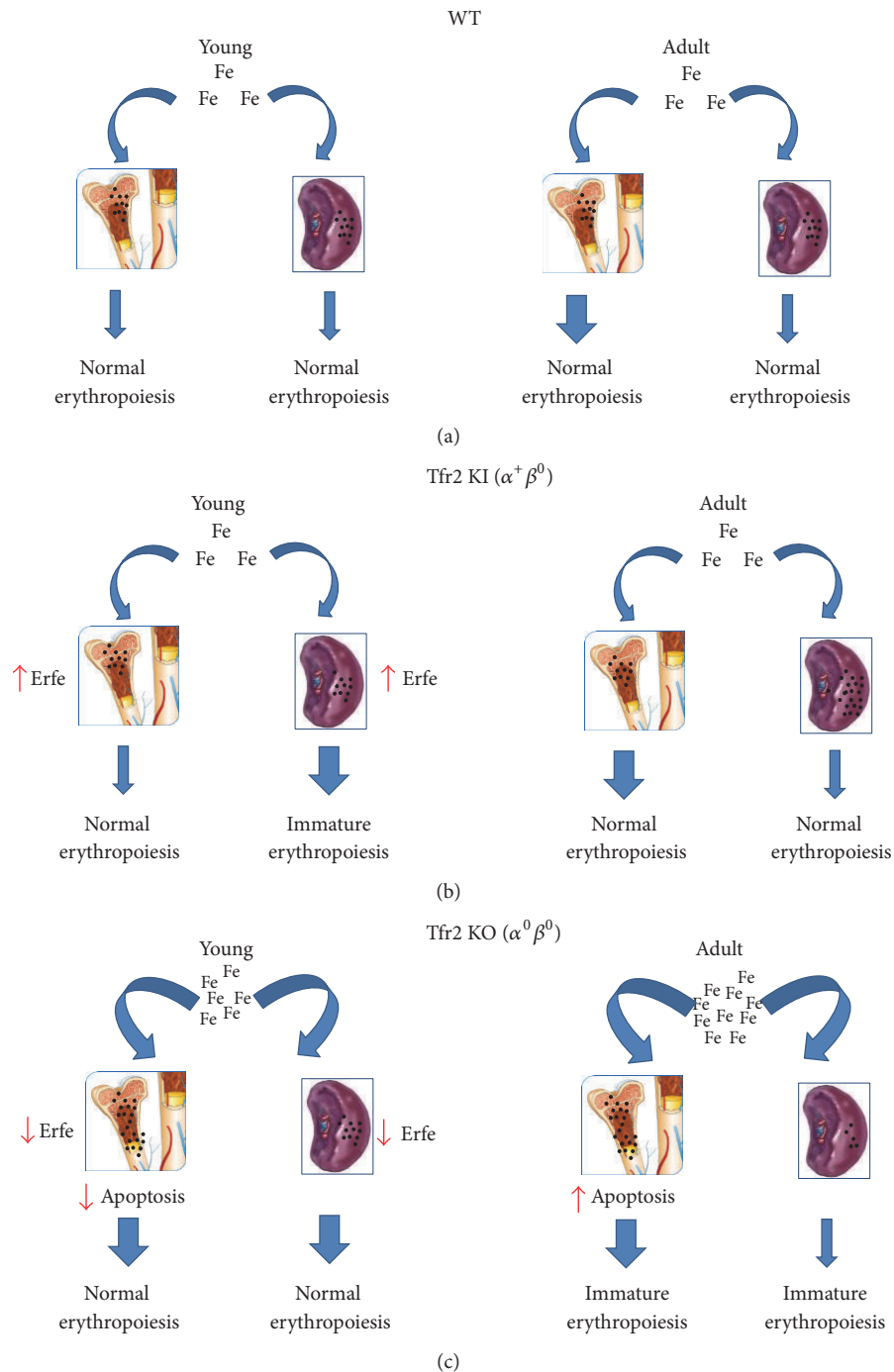


FIGURE 6: Model depicting the involvement of iron and Tfr2 isoforms in erythropoiesis. (a) In young (14 d) WT mice, erythropoiesis takes place in both bone marrow (BM) and spleen while in adult animals, BM erythropoiesis is predominant as compared to splenic RBC production (blue arrows); (b) in the presence of normal circulating iron levels, lack of Tfr2 β provokes iron retention in macrophages that causes immature splenic erythropoiesis and Erythroferrone (Erfe) increase in young mice, that generally have a high iron requirement. This is normalized in adult animals, although an increased amount of iron is retained in the spleen; (c) the same should be observed in the spleen of Tfr2 KO animals, but they have sufficient circulating iron amount to normalize splenic erythropoiesis (Erfe is decreased). High iron availability also causes an increase of the early stage of BM erythropoiesis in adult mice, that does not result in reticulocytosis because of increased apoptosis.

previously demonstrated as well. Germinal lack of Tfr2 α (Tfr2 KO) causes an anticipation of adult erythropoiesis in young mice in both BM and the spleen. On the other hand, lack of Trf2 β is responsible for an increased but immature splenic erythropoiesis that is normalized during animal growth. This effect due to Trf2 β absence in Tfr2 KO mice is compensated by the increased amount of circulating iron available for erythrocyte production.

Conflicts of Interest

The authors declare that they have no conflicts of interest.

Authors' Contributions

Authors R. M. Pellegrino and F. Riondato contributed equally to this work as the first authors.

Acknowledgments

This work was supported by grants from University of Turin, Progetti di Ateneo/CSP 2012 (12-CSP-C03-065) and AIRC (IG2011 cod 12141), to G. Saglio; University of Turin, RILO 2015 (RICerca LOcale 2015) project acronym MeCCaSARiC_3 to A. Roetto. The authors wish to thank Professor Marco De Gobbi for the helpful discussion and Dr. Ishira Nanavaty for the final manuscript editing.

References

- [1] C. Camaschella and A. Roetto, "TFR2-related hereditary hemochromatosis," in *GeneReviews*[®], R. A. Pagon, M. P. Adam, H. H. Ardinger et al., Eds., University of Washington, Seattle, WA, USA, 2014.
- [2] C. Camaschella, A. Roetto, A. Cali et al., "The gene TFR2 is mutated in a new type of haemochromatosis mapping to 7q22," *Nature Genetics*, vol. 25, no. 1, pp. 14–15, 2000.
- [3] H. Kawabata, R. Yang, T. Hiramata et al., "Molecular cloning of transferrin receptor 2. A new member of the transferrin receptor-like family," *Journal of Biological Chemistry*, vol. 274, no. 30, pp. 20826–20832, 1999.
- [4] R. E. Fleming, M. C. Migas, C. C. Holden et al., "Transferrin receptor 2: continued expression in mouse liver in the face of iron overload and in hereditary hemochromatosis," *Proceedings of the National Academy of Sciences of the United States of America*, vol. 97, no. 5, pp. 2214–2219, 2000.
- [5] M. U. Muckenthaler, B. Galy, and M. W. Hentze, "Systemic iron homeostasis and the iron-responsive element/iron-regulatory protein (IRE/IRP) regulatory network," *Annual Review of Nutrition*, vol. 28, pp. 197–213, 2008.
- [6] J. Chen, J. Wang, K. R. Meyers, and C. A. Enns, "Transferrin-directed internalization and cycling of transferrin receptor 2," *Traffic*, vol. 10, no. 10, pp. 1488–1501, 2009.
- [7] M. W. Hentze, M. U. Muckenthaler, B. Galy, and C. Camaschella, "Two to tango: regulation of mammalian iron metabolism," *Cell*, vol. 142, no. 1, pp. 24–38, 2010.
- [8] A. Roetto, F. Di Cunto, R. M. Pellegrino et al., "Comparison of 3 Tfr2-deficient murine models suggests distinct functions for Tfr2- α and Tfr2- β isoforms in different tissues," *Blood*, vol. 115, no. 16, pp. 3382–3389, 2010.
- [9] A. Roetto, A. Totaro, A. Piperno et al., "New mutations inactivating transferrin receptor 2 in hemochromatosis type 3," *Blood*, vol. 97, no. 9, pp. 2555–2560, 2001.
- [10] S. Majore, F. Milano, F. Binni et al., "Homozygous p.M172K mutation of the TFR2 gene in an Italian family with type 3 hereditary hemochromatosis and early onset iron overload," *Haematologica*, vol. 91, 8, Article ID ECR33, 2006.
- [11] H. Forejtníková, M. Vieillevoys, Y. Zermati et al., "Transferrin receptor 2 is a component of the erythropoietin receptor complex and is required for efficient erythropoiesis," *Blood*, vol. 116, no. 24, pp. 5357–5367, 2010.
- [12] A. Nai, R. M. Pellegrino, M. Rausa et al., "The erythroid function of transferrin receptor 2 revealed by Tmprss6 inactivation in different models of transferrin receptor 2 knockout mice," *Haematologica*, vol. 99, no. 6, pp. 1016–1021, 2014.
- [13] D. F. Wallace, E. S. Secondes, G. Rishi et al., "A critical role for murine transferrin receptor 2 in erythropoiesis during iron restriction," *British Journal of Haematology*, vol. 168, no. 6, pp. 891–901, 2015.
- [14] X. Troussard, S. Vol, E. Cornet et al., "Full blood count normal reference values for adults in France," *Journal of Clinical Pathology*, vol. 67, no. 4, pp. 341–344, 2014.
- [15] L. Kautz, G. Jung, E. V. Valore, S. Rivella, E. Nemeth, and T. Ganz, "Identification of erythroferrone as an erythroid regulator of iron metabolism," *Nature Genetics*, vol. 46, no. 7, pp. 678–684, 2014.
- [16] L. Kautz, G. Jung, E. Nemeth, and T. Ganz, "Erythroferrone contributes to recovery from anemia of inflammation," *Blood*, vol. 124, no. 16, pp. 2569–2574, 2014.
- [17] Y. Liu, R. Pop, C. Sadegh, C. Brugnara, V. H. Haase, and M. Socolovsky, "Suppression of Fas-FasL coexpression by erythropoietin mediates erythroblast expansion during the erythropoietic stress response in vivo," *Blood*, vol. 108, no. 1, pp. 123–133, 2006.
- [18] H.-C. Chu, H.-Y. Lee, Y.-S. Huang et al., "Erythroid differentiation is augmented in Reelin-deficient K562 cells and homozygous reeler mice," *FEBS Letters*, vol. 588, no. 1, pp. 58–64, 2014.
- [19] M. L. Chen, T. D. Logan, M. L. Hochberg et al., "Erythroid dysplasia, megaloblastic anemia, and impaired lymphopoiesis arising from mitochondrial dysfunction," *Blood*, vol. 114, no. 19, pp. 4045–4053, 2009.
- [20] K. J. Livak and T. D. Schmittgen, "Analysis of relative gene expression data using real-time quantitative PCR and the 2^{- $\Delta\Delta C_T$} method," *Methods*, vol. 25, no. 4, pp. 402–408, 2001.
- [21] U. Testa, "Apoptotic mechanisms in the control of erythropoiesis," *Leukemia*, vol. 18, no. 7, pp. 1176–1199, 2004.
- [22] M. Silva, A. Benito, C. Sanz et al., "Erythropoietin can induce the expression of Bcl-x(L) through Stat5 in erythropoietin-dependent progenitor cell lines," *Journal of Biological Chemistry*, vol. 274, no. 32, pp. 22165–22169, 1999.
- [23] J. L. Beard, "Iron requirements in adolescent females," *The Journal of Nutrition*, vol. 130, pp. 440S–442S, 2000.
- [24] J. M. Guralnik, R. S. Eisenstaedt, L. Ferrucci, H. G. Klein, and R. C. Woodman, "Prevalence of anemia in persons 65 years and older in the United States: evidence for a high rate of unexplained anemia," *Blood*, vol. 104, no. 8, pp. 2263–2268, 2004.
- [25] H. Nilsson-Ehle, R. Jagenburg, S. Landahl, and A. Svanborg, "Blood haemoglobin declines in the elderly: implications for reference intervals from age 70 to 88," *European Journal of Haematology*, vol. 65, no. 5, pp. 297–305, 2000.

- [26] L. Silvestri, A. Nai, A. Pagani, and C. Camaschella, "The extrahepatic role of TFR2 in iron homeostasis," *Frontiers in Pharmacology*, vol. 5, p. 93, 2014.
- [27] M. B. Johnson, J. Chen, N. Murchison, F. A. Green, and C. A. Enns, "Transferrin receptor 2: evidence for ligand-induced stabilization and redirection to a recycling pathway," *Molecular Biology of the Cell*, vol. 18, no. 3, pp. 743–754, 2007.
- [28] A. Nai, M. R. Lidonnici, M. Rausa et al., "The second transferrin receptor regulates red blood cell production in mice," *Blood*, vol. 125, no. 7, pp. 1170–1179, 2015.
- [29] S. D. Nimer, "Myelodysplastic syndromes," *Blood*, vol. 111, no. 10, pp. 4841–4851, 2008.
- [30] E. Messa, D. Cilloni, F. Messa, F. Arruga, A. Roetto, and G. Saglio, "Deferasirox treatment improved the hemoglobin level and decreased transfusion requirements in four patients with the myelodysplastic syndrome and primary myelofibrosis," *Acta Haematologica*, vol. 120, no. 2, pp. 70–74, 2008.

5.3 Tfr2 in the brain

Iron enters the brain primarily through the blood-brain barrier (BBB) and the ventricular system (Knutson et al, 2004; McCarthy et al, 2012).

Tfr2 gene expression has been shown in total brain extracts (Kawabata et al, 1999; Moos et al, 2007), in defined cerebral compartments and brain tumor cell lines (Hänninen et al, 2009), and in specific neuronal subtypes, since a novel Tf/Tfr2-mediated iron transport pathway in the mitochondria of dopaminergic neurons in the nervous system has been reported (Mastroberardino et al, 2009). Disruptions of Tf/Tfr2-dependent system have been associated with PD, this finding highlighting the role for iron accumulation in this movement disorder (Mastroberardino et al, 2009). Also, a protective association between PD and a haplotype in Tf and Tfr2 genes was reported, suggesting that Tf or a Tf-Tfr2 complex may play a role in the etiology of PD (Rhodes et al, 2014). Furthermore, a transcriptome study on Tfr2 null mice revealed that several genes involved in the control of neuronal functions are abnormally transcribed (Ackyol et al, 2013).

These premises induced our group to further investigate CNS iron metabolism alteration in our Tfr2 mouse model in which both Tfr2 isoforms are germinally inactivated (Tfr2-KO) (Roetto et al, 2010) and I contributed to this study analyzing in particular iron and iron proteins localization in cerebral compartments.


To distinguish the effects of Tfr2 abrogation from those due to Tfr2-independent iron load modifications, WT sib pairs were submitted to an iron enriched (IED) or an iron deficient diet (IDD) and utilized for the same experiments. Results showed that Tfr2 silencing caused a blunting of brain Hepc response to the systemic increase of circulating iron levels, with altered iron mobilization and/or cellular distribution in the nervous tissue.

In particular, Tfr2-KO brains sections compared to WT ones showed increased iron deposits in selective parenchymal regions (hippocampal CA1 and CA3 regions, the paraventricular nucleus PVN) as well as in small microglial cells and choroid plexi. No significant brain iron content (BIC) increase was evidenced in WT IED organs. These results show that iron accumulates in the nervous tissue when Tfr2 is abrogated.

Moreover, Tfr2-KO mice presented a selective over-activation of neurons in the limbic circuit and the emergence of an anxious-like behavior. These anxiety signs were not present in WT iron overloaded mice (WT IED), so Tfr2 resulted to be a key regulator of brain iron homeostasis and Tfr2 alpha could have a role in the regulation of anxiety circuits

(Pellegrino et al, 2016 see attached paper).

SCIENTIFIC REPORTS



OPEN

Transferrin Receptor 2 Dependent Alterations of Brain Iron Metabolism Affect Anxiety Circuits in the Mouse

Received: 05 January 2016

Accepted: 06 July 2016

Published: 01 August 2016

Rosa Maria Pellegrino^{1,2,*}, Enrica Boda^{3,4,*}, Francesca Montarolo⁴, Martina Boero^{1,2}, Mariarosa Mezzanotte^{1,2}, Giuseppe Saglio^{1,2}, Annalisa Buffo^{3,4,†} & Antonella Roetto^{1,2,†}

The Transferrin Receptor 2 (Tfr2) modulates systemic iron metabolism through the regulation of iron regulator Hepcidin (Hepc) and *Tfr2* inactivation causes systemic iron overload. Based on data demonstrating *Tfr2* expression in brain, we analysed *Tfr2*-KO mice in order to examine the molecular, histological and behavioural consequences of *Tfr2* silencing in this tissue. *Tfr2* abrogation caused an accumulation of iron in specific districts in the nervous tissue that was not accompanied by a brain Hepc response. Moreover, *Tfr2*-KO mice presented a selective overactivation of neurons in the limbic circuit and the emergence of an anxious-like behaviour. Furthermore, microglial cells showed a particular sensitivity to iron perturbation. We conclude that Tfr2 is a key regulator of brain iron homeostasis and propose a role for Tfr2 alpha in the regulation of anxiety circuits.

Body iron amount and availability is finely regulated by Hepcidin (Hepc), a peptide produced mainly by the liver, that acts on the cellular iron exporter Ferroportin 1 (Fpn1), causing its degradation and decreasing *de facto* the amount of serum iron¹. A complex protein network is involved in hepatic Hepc regulation according to the body iron needs, causing Hepc decrease in iron demand conditions (anaemia, hypoxia, ineffective erythropoiesis) and, on the contrary, a Hepc increase when a sufficient iron amount is present in the body or during inflammatory processes². Dysfunction of most Hepc regulatory proteins is responsible of hereditary disorders of iron metabolism^{3,4}. Among these regulators, Transferrin receptor 2 (Tfr2) is codified by a gene whose mutations are responsible for a rare form of hereditary haemochromatosis named HFE3^{5,6}. The *TFR2* gene is transcribed in two main isoforms, Tfr2 alpha and Tfr2 beta. Tfr2 alpha is highly produced in the liver and works as an iron sensor that regulates serum Hepc level. Accordingly, *Tfr2* targeted animals show iron overload due to an inappropriately low level of Hepc^{7–9}. The Tfr2 beta isoform, instead, appears to play a specific role in the regulation of iron export from reticulo-endothelial cells⁹.

In the central nervous system (CNS), iron levels need to be tightly controlled to appropriately regulate key functions such as neurotransmission and myelination as well as neural cell division¹⁰. Iron overload in defined CNS areas associates with neurodegeneration in Parkinson's and Alzheimer's diseases^{11–13}, suggesting a role for iron overload in circuit malfunctioning and damage. Furthermore, studies in animal models in which iron amount was experimentally increased show an alteration of the main iron-related proteins Ferritin (Ft) and Transferrin Receptor 1 (Tfr1) in the brain^{14–16}, revealing perturbation of iron brain homeostasis.

It is generally accepted that iron enters neurons¹⁰, microglial^{17,18} and choroid plexi cells¹⁹ bound to Tfr1 and it has been shown that the iron hormone Hepc is expressed in the brain^{20–23}, similar to other Hepc regulatory proteins¹⁰. Yet, it is still unclear how iron levels and localization are regulated in cerebral compartments. Similarly, it remains to be fully understood whether the iron protein regulatory network in the CNS is the same operating in the rest of the body and how systemic and cerebral iron regulation are interconnected.

¹Department of Clinical and Biological Sciences, University of Torino, Turin, Italy. ²AOU San Luigi Regione Gonzole 10043 Orbassano Turin, Italy. ³Department of Neuroscience Rita Levi-Montalcini, University of Torino, Turin, Italy. ⁴Neuroscience Institute Cavalieri Ottolenghi Regione Gonzole 10043 Orbassano Turin, Italy. *These authors contributed equally to this work. †These authors jointly supervised this work. Correspondence and requests for materials should be addressed to A.R. (email: antonella.roetto@unito.it)

Similar to other Hcpc regulatory proteins, *Tfr2* gene expression has been shown in total brain extracts²³, in defined cellular compartments of specific neuronal subtypes²⁴ and in brain tumor cell lines^{23,25}. Furthermore, a transcriptome study on *Tfr2* null mice revealed that several genes involved in the control of neuronal functions are abnormally transcribed¹⁶.

In this study we aimed to clarify *Tfr2* functions in the brain by examining a mouse model in which both *Tfr2* isoforms are inactivated (*Tfr2*-KO)⁹. To distinguish the effects of *Tfr2* abrogation from those due to *Tfr2*-independent iron load modifications, we also examined WT sib pairs subjected to an iron enriched diet (IED) and WT or *Tfr2*-KO mice upon an iron deficient diet (IDD).

Results show that *Tfr2* silencing determines an increased brain iron availability that associates with anxious-like behaviours.

Materials and Methods

Animals. Ten weeks old *Tfr2*-KO male mice⁹ maintained on 129 X 1/svJ strain were analyzed and compared to wild type (WT) sex and age matched sib pairs. Animal housing and all the experimental procedures were performed in accordance with European (Official Journal of the European Union L276 del 20/10/2010, Vol. 53, p. 33–80) and National Legislation (Gazzetta Ufficiale n° 61 del 14/03/2014, p. 2–68) for the protection of animals used for scientific purposes. Groups of 4–5 mice were housed in transparent conventional polycarbonate cages (Tecnoplast, Buggirate, Italy) provided with sawdust bedding, boxes/tunnels hideout as environmental enrichment and striped paper as nesting material. Food and water were provided ad libitum; environmental conditions were 12 h/12 h light/dark cycle, room temperature 21 °C ± 1 °C and room humidity 55% ± 5%. Experimental procedure was preventively approved by the Ethical Committee of the University of Turin.

Experimental conditions. *Tfr2*-KO mice were fed with a standard diet (SD) (GLOBAL DIET 2018, Mucedola SrL, Italy, 0, 2 g iron/Kg food). Age and sex matched animals in SD were used as WT controls. Subgroups of mice were further kept on:

a) *iron deficient diet (IDD)* to induce anaemia in WT mice and to decrease iron amount in *Tfr2*-KO mice, by feeding mice with a purified diet without added iron (Mucedola SrL, Italy) starting from weaning until sacrifice (8 weeks of treatment);

b) *iron enriched diet (IED)* to trigger secondary iron overload in WT animals by feeding them with a 2% iron enriched standard diet from weaning until sacrifice (8 weeks of treatment).

IED was preferred to parenteral iron injection because it resembles iron overload occurring in chronic haemochromatosis. Furthermore, since it has been demonstrated that an iron enriched diet for a short period of time does not cause changes in iron regulating proteins²⁶, we decided to submit animals to 8 weeks of IED. On the other hand, IDD treatment was chosen to avoid the side-effects of acute iron deprivation obtained by extensive phlebotomies that, by causing inflammation, influence the Hcpc pathway^{27,28}.

At the end of the experiments, mice were given an anaesthetic overdose (see below) and sacrificed. Blood, brain and liver were collected for subsequent analysis.

For behavioural analyses, 8 WT and 9 *Tfr2*-KO naïve mice in SD were tested in the *Morris water maze* and elevated plus maze (*EPM*) tests. Subsequently, 19 WT and 13 *Tfr2*-KO naïve mice in SD, 12 WT and 17 *Tfr2*-KO naïve mice in IDD and 5 WT naïve mice in IED were tested in EPM.

A subset of *Tfr2*-KO and WT mice was transcardially perfused with 0.12 M phosphate buffer (PB) pH 7.2–7.4 (50 ml, 15 min) to remove blood from brain tissue before Western Blot analysis and the measurement of brain iron content (see below). Perfusions were carried out under deep general anaesthesia (ketamine, 100 mg/kg; Ketavet, Bayern, Leverkusen, Germany; xylazine, 5 mg/kg; Rompun; Bayer, Milan, Italy).

Molecular biology analyses. Frozen dissected regions or total brains from WT mice were utilized for quantitative PCR while only total brain of *Tfr2*-KO and WT animals was used for Western Blot analysis.

Real time quantitative PCR analysis. For reverse transcription, 1 µg of total RNA, 25 µM random hexamers, and 100 U of reverse transcriptase (Applied Biosystems) were used. Gene expression levels were measured by real-time quantitative PCR in a CFX96 Real-Time System (BIO-RAD). For *Tfr2* alpha, *Tfr2* beta and BDNF, SYBR Green PCR technology (EVAGreen, BIO-RAD, Italy) was used utilising specific primers whose sequences are reported in Supplemental Informations. *Gus* (β-glucuronidase) gene was utilized as housekeeping control^{9,29}. The results were analysed using the $\Delta\Delta C_t$ method³⁰. All analyses were carried out in triplicate; results showing a discrepancy greater than one cycle threshold in one of the wells were excluded.

Western Blot analysis. WB experiments were done with at least 6 animals for each experimental group. Fifty µg of total brain lysates were separated on an 8–15% SDS polyacrylamide gel and immunoblotted according to standard protocols. Antibodies against the following proteins were used: Transferrin (Tf) (F-8), Tfr1 (CD71 H-300), Divalent Metal Transporter 1 (DMT1) (H-108), Fpn1 (G-16) and β-Actin (C-4) (*Santa Cruz Biotechnology*); *Tfr2* alpha and Hcpc (Alpha Diagnostic International). Antibodies against the two Ferritins (Ft-H and Ft-L) were kindly provided by Sonia Levi, University of Vita Salute, Milan, Italy. Data from WB quantification (Image Lab Software, BIO-RAD, Italy) were normalized on levels of β-Actin bands and expressed as fold increase relative to the mean value obtained from WT mice.

Liver and brain iron content. Iron concentration on livers (Liver Iron Content, LIC) and brains (Brain Iron Content, BIC) freshly dissected was assessed according to standard procedures⁹ using at least 20 mg of dried total tissue. For histological assessment of non-heme iron deposition, brain slices of perfused animals were stained with DAB-enhanced Prussian blue Perls' staining³¹.

Histological and immunofluorescence procedures. For histological analyses experimental animals were perfused with 4% paraformaldehyde in PB. Brains were removed and post-fixed for 24 h at 4 °C, cryoprotected in 30% sucrose in 0.12 M phosphate buffer and processed according to standard protocols³². Brains were cut in 30 µm thick coronal sections collected in PBS and then stained to detect the expression of different antigens: Glial fibrillary acidic protein (GFAP) (1:1000, Dakopatts); Iba1 (1:1000, Wako); cFos (1:1000, Santa Cruz Biotechnology); Zif-268 (1:1000, Santa Cruz Biotechnology); vGlut1 (1:1500, Synaptic System); vGlut2 (1:1500, Synaptic System); Tfr2 alpha (1:500, Alpha Diagnostics); hepcidin/pro-hepcidin (1:1000 with amplification with tyramide kit, see below, Alpha Diagnostics). Incubation with primary antibodies was made overnight at 4 °C in PBS with 0.5% Triton-X 100. The sections were then exposed for 2 h at room temperature (RT) to secondary Cy3- (Jackson ImmunoResearch Laboratories, West Grove, PA) and Alexafluor- (Molecular Probes Inc, Eugene Oregon) conjugated antibodies³³. 4,6-diamidino-2-phenylindole (DAPI, Fluka, Milan, Italy) was used to counterstain cell nuclei. After processing, sections were mounted on microscope slides with Tris-glycerol supplemented with 10% Mowiol (Calbiochem, LaJolla, CA). For colabelling of primary antibodies developed in the same species, the high sensitivity tyramide signal amplification kit (Perkin Elmer, Monza, Italy) was utilized according to the manufacturer's instruction³³. Myelin Gallyas staining was performed as documented³⁴.

Image Processing and Data Analysis. Histological specimens were examined using an E-800 Nikon microscope (Nikon, Melville, NY) connected to a colour CCD Camera and a Leica TCS SP5 (Leica Microsystems, Wetzlar, Germany) confocal microscope. Adobe Photoshop 6.0 (Adobe Systems, San Jose, CA) was used to adjust image contrast and assemble the final plates. Quantitative evaluations (densitometry of staining intensities, cell densities) were performed on confocal images followed by NeuroLucida- (MicroBrightfield, Colchester, VT) and ImageJ- (Research Service Branch, National Institutes of Health, Bethesda, MD; available at: <http://rsb.info.nih.gov/ij/>) based analyses. For the analysis of microglia in the cerebral cortex, we routinely scanned the entire cortical grey matter included in slices from Bregma 1.10 mm to Bregma-2.00 mm. Analyses were performed on slices from Bregma-1.50 mm to Bregma-2.00 mm for the dorsal hippocampus; from Bregma-2.50 mm to Bregma-3.00 mm for the ventral hippocampus; from Bregma 1.50 mm to Bregma 2.20 mm for the medial prefrontal cortex (mPFC); from Bregma-1.20 mm to Bregma-1.60 mm for the basolateral and central amygdala (BLA and CeA); from Bregma-0.70 mm to Bregma-1.00 mm for the hypothalamic periventricular nucleus (PVN). When the high density of cFos/Zif-268-positive cells impaired the easy recognition of individual nuclei (i.e., in *Cornu Ammonis* 1, CA1 and medial prefrontal Cortex, mPFC), the mean cFos/Zif-268 staining intensity (with background subtraction) over the whole area of the region of interest was evaluated. Measurements derived from at least 3 sections per animal. At least three animals were analysed for each experimental condition.

Behavioural tests. The *Morris water maze*³⁵ and EPM³⁶ tests were performed to evaluate learning and anxious-like behaviours, respectively. Data were recorded automatically from the digitized image by using a computerized video tracking software. Details about the procedures can be found in Supplemental Information.

Serum Collection and Analysis. Blood samples were collected, centrifuged, and serum was frozen at -20 °C until analysis. Serum was assayed for corticosterone levels by using commercially available kits (Corticosterone 3H RIA, MP Biomedicals, Italy). All the blood samples were collected at the same time in the morning to minimize the physiological variations.

Statistical analysis. Statistical analyses were carried out by GraphPad Prism (San Diego California, USA) or SPSS software packages (Bangalore, India, www.spss.co.in). In most cases we used Unpaired t-test or one-way ANOVA followed by Bonferroni's post hoc analysis. As regards behavioural data, repeated-measures two-way ANOVA followed by Bonferroni's post hoc analysis was performed to evaluate *Morris water maze* performances during days. Mann-Whitney U test was assessed to evaluate the statistical significance for Accuracy Ratio (AR) and path length in *Morris water maze* test. One-way ANOVA followed by Bonferroni's post hoc analysis was used to evaluate the EPM performances. In all instances, $P < 0.05$ was considered as statistically significant. Data were expressed as averages \pm standard error of the mean. Only statistically significant results vs WT and vs *Tfr2*-KO were shown in the figures while all statistically significant P and F values as well as outputs of post hoc analyses were included in Table 1S. Statistically not-significant results were omitted.

Results

Tfr2 alpha expression in anxiety and stress-related circuits. A transcriptional analysis on WT mice major brain compartments revealed that Tfr2 alpha mRNA is expressed, although less than in the liver, in all analysed areas, and reaches the highest level in the hippocampus (Fig. 1A).

Conversely, real time analysis, performed with primers of similar efficiency, showed a low and homogeneous level of Tfr2 beta mRNA expression in the same brain areas that, also in this case, was lower compared to the liver (Fig. 1A). Based on these data, we concluded that Tfr2 alpha is the main Tfr2 isoform in the brain and consequently we focused on Tfr2 alpha for the next experiments.

Tfr2 alpha protein in total brain extracts showed a trend to decrease in WT IDD mice compared to WT mice, while it did not vary in WT IED animals (Fig. 1B). These data are in line with the role of Tfr2 as an iron sensor contributing to iron homeostasis and with previous data demonstrating that Tfr2 protein is stabilized on plasma membranes by iron loaded Transferrin (Fe-Tf)³⁷.

Immunofluorescence labelling with an anti-Tfr2 alpha specific antibody showed elongated thin structures occurring either as tightly associated fascicles or isolated fibers (Fig. 1C,G). In grey matter nuclei, a dense punctate staining was occasionally seen (Fig. 1E,F,H). Both patterns are consistent with labelling of neurites or fiber tracts. Interestingly, anti-Tfr2 alpha labelling was prominent in brain circuits controlling anxiety and stress^{38,39} including the hippocampus (where Mossy fibers, Mf; were strongly stained, Fig. 1C,D), the amygdala (namely

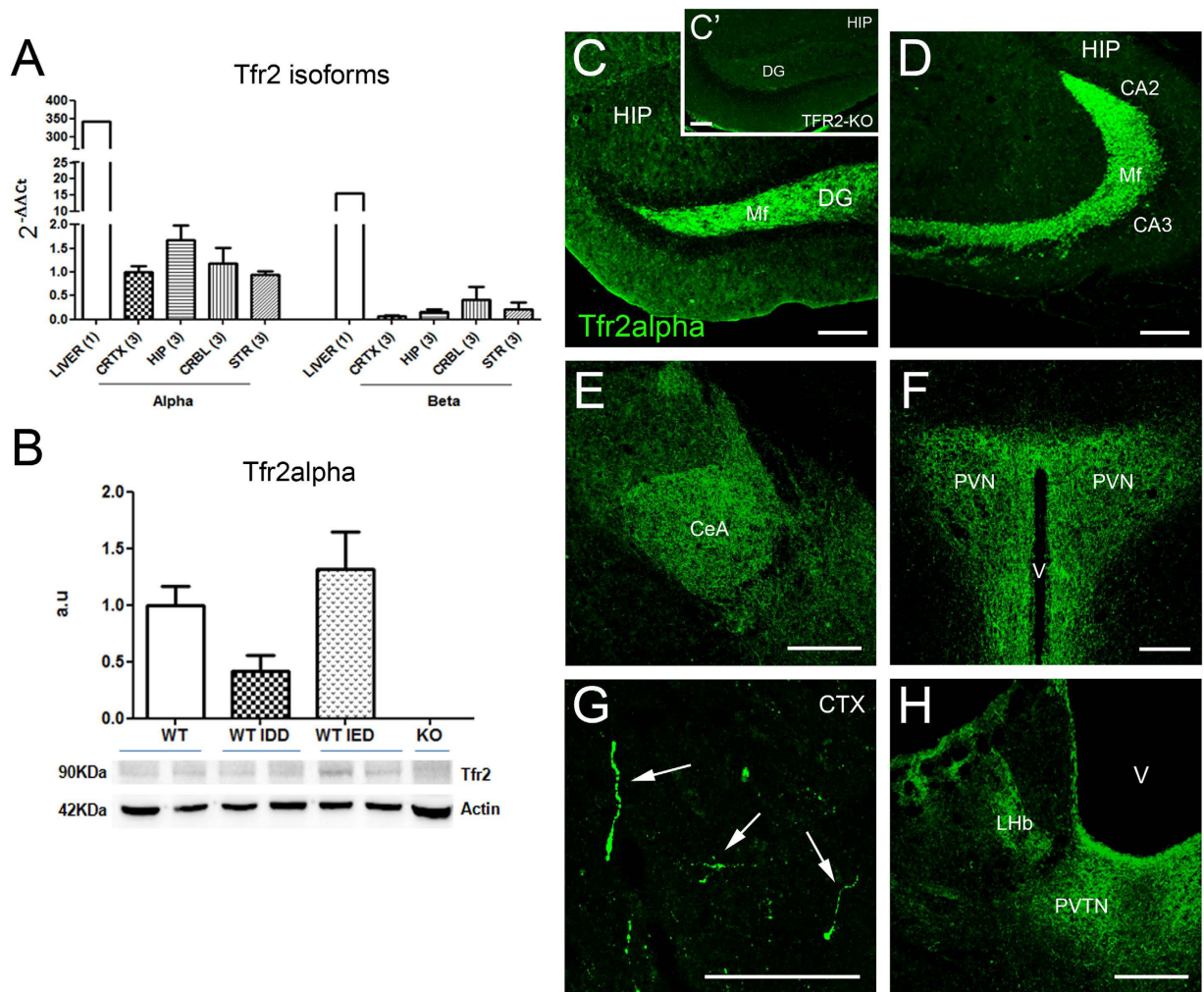


Figure 1. Tfr2 alpha expression in the adult telencephalon. (A) Tfr2 alpha and beta isoforms transcription pattern in major brain compartments of WT SD mice. CRTX, cortex; HIP, hippocampus; CRBL, cerebellum; STR, striatum; transcription amount of both Tfr2 isoforms in the liver was used as comparison. Number in parenthesis under each column indicates the number of animals compartments analysed. The expression level of the two Tfr2 isoforms was normalized to levels of GUS housekeeping gene as described in the MM section. In order to perform a double comparison of the same genes in different brain compartments and of the two Tfr2 isoforms in the same compartment we normalized all data on the value of Tfr2 alpha in the cerebral cortex (CRTX). (B) Western blot analysis and quantification of brain Tfr2 alpha protein. Results are shown as averages \pm standard error of the mean of 3 independent experiments. All the statistically significant results are reported in Table 1S. a.u. arbitrary unit; SD standard diet, IDD iron deficient diet; IED iron enriched diet. (C–H) Immunofluorescence localization of Tfr2 alpha in brain. In WT brains Tfr2 alpha positivity is found in fibers of the dentate gyrus of the hippocampus and their terminal region in the CA3/CA2 areas (D). A dense dotted staining is also detected in the CeA (E), PVN (F), LHb (H) and PVN (H) grey matter nuclei. Sparse axon fibers are labelled for Tfr2 alpha in the cerebral cortex (G). Absence of staining in *Tfr2*-KO mice confirms the antibody specificity (C). Scale bars: 100 μ m. DG, dentate gyrus; CA, Cornus Ammonis; CeA, central nucleus of the amygdala; PVN, paraventricular nucleus of hypothalamus; CTX, neocortex (primary M1 motor cortex); LHb, lateral habenula; PVTN, paraventricular nucleus of thalamus; Mf, mossy fibers; V, ventricle.

the central nucleus, CeA; Fig. 1E) and the hypothalamic paraventricular nucleus (PVN; Fig. 1F). Scattered Tfr2 alpha-positive (+) fiber-like structures were also found in the in the cerebral cortex (Fig. 1G) and in thalamic paraventricular and habenular nuclei (Fig. 1H). Absence of labelling in *Tfr2*-KO mouse brain testified the specificity of anti-Tfr2 alpha staining (Fig. 1C').

Increased iron amount in Tfr2-KO brain. All mice were examined at 10 weeks of age, when tissue alterations have been observed in other mouse models of iron loading^{40,41}. *Tfr2*-KO showed a significant increase in total brain iron amount compared to WT mice (Table 1). However, this increase was attributable to circulating iron, since brains of *Tfr2*-KO mice in which blood was removed through tissue perfusion, have a BIC (Brain Iron Content) similar to WT (Table 1). Interestingly, aged-matched WT IED mice, despite being iron overloaded in

| Genotype Diet | WT SD | WT IDD | WT IED | <i>Tfr2</i> -KO SD | <i>Tfr2</i> -KO IDD |
|---|-----------------------------|----------------------------------|-------------------------------------|-----------------------------------|-----------------------------------|
| BIC ($\mu\text{g/g dry tissue}$) | 237.3 \pm 30.8 | 189.8 \pm 17.4 ^{ooo} | 240.2 \pm 30.5 ^o | 317.8 \pm 81.9 ^{**} | 175.7 \pm 25.3 ^{*,ooo} |
| BIC [^] ($\mu\text{g/g dry tissue}$) | 154.5 \pm 18.3 | ND | ND | 178.1 \pm 21.7 | ND |
| LIC ($\mu\text{g/g dry tissue}$) | 480.2 \pm 116.7 | 246.1 \pm 34.5 ^{ooo} | 1099.2 \pm 87.2 ^o | 1839.3 \pm 448.9 ^{***} | 326.2 \pm 105.4 ^{ooo} |
| hepatic Hepc ($\Delta\Delta\text{Ct mean}$) | 1 \pm 0.152 ^{oo} | 0.003 \pm 0.001 ^{***} | 2.78 \pm 0.360 ^{***,ooo} | 0.424 \pm 0.174 ^{**} | 0.002 \pm 0.003 ^{***} |

Table 1. Brain and liver iron amount and hepatic Hepc transcription. WT, wild type; SD, standard diet; IDD, iron deficient diet; IED, iron enriched diet; ND, not determined; ^, perfused brain. * significance vs WT; ^o significance vs *Tfr2*-KO. Only statistically significant results vs WT and *Tfr2* KO are shown. All the other statistically significant results are reported in Table 1S.

the liver (Table 1) and in the serum (Transferrin saturation: 49,8 \pm 4.45% vs 26 \pm 4.95% P < 0,05), did not display evidence of global iron increase in the brain. In both *Tfr2*-KO and WT mice in IDD, BIC decreased below controls levels (Table 1).

To assess possible localised changes in iron levels or distribution, we performed histochemical analysis in PFA perfused brains by DAB-enhanced Prussian blue Perls' staining. *Tfr2*-KO brains sections showed an increased number of brown positive precipitates compared to control mice (Fig. 2) in defined parenchymal regions such as the hippocampal CA1 and CA3 regions (Fig. 2C–F), the PVN (Fig. 2I–J) and the striatal white matter (Fig. 2G,H). We also observed DAB-positive small cells, mostly resembling microglia (insets in 2G and H), that were more frequently detected in *Tfr2*-KO brains (Fig. 2A,B,I–J). Increased iron was also highlighted by intense staining of both choroid plexi and ependyma in mutant mice (Fig. 2A,B,I,J). These results show that iron accumulates in the nervous tissue when *Tfr2* is abrogated.

Brain Hepc levels in iron overloaded *Tfr2*-KO mice. Since *Tfr2* is a regulator of Hepc production² in the liver, we asked whether its deletion also affected Hepc amount in the brain. In agreement with its role of negative regulator of iron availability, in liver and brain of WT mice Hepc production changed according to the different systemic iron amount: it decreased in animals on IDD and increased in animals on IED (Table 1, Fig. 3A). On the contrary, in *Tfr2*-KO mice, despite increased systemic and circulating iron, cerebral Hepc was significantly lower than in WT mice (Fig. 3A). Furthermore, while liver Hepc transcription significantly decreased in *Tfr2*-KO IDD mice (Table 1) brain Hepc transcription increased in consequence of IDD, reaching WT IDD levels (Fig. 3A) and suggesting a deregulated expression of Hepc in the KO brain. In order to distinguish the contribution of the circulating protein to the Hepc level found in *Tfr2*-KO brain, Hepc quantification was repeated in brains of perfused animals. Despite iron accumulation in KO brains, there is no obvious dysregulation of brain-derived Hepc. These data are consistent with lack of overexpression of Hepc in perfused *Tfr2*-KO brain (Fig. 1S).

To further corroborate these data with an independent approach, we examined anti-Hepc immunostaining on brain slices. Consistently with previous data⁴², Hepc positive cells in the cerebral cortex and hippocampus mainly displayed neuronal morphologies (Fig. 3B,C,F,G). In these areas no relevant differences were observed in the Hepc expression pattern or in the densities of positive cells of WT and *Tfr2*-KO mice, although the latter seems to have a slight decrease in overall staining. Conversely, and in line with systemic Hepc regulation², WT IED mice had a marked increase in the number of Hepc + cells in the cortex and in the hippocampal dentate gyrus (DG) (Fig. 3E–I). Surprisingly, and on the contrary to what occurs in the liver, where Hepc transcription significantly decreases (Table 1), the pattern and the density of brain Hepc + cells in *Tfr2*-KO IDD mice remains comparable to WT (Fig. 3B–D,F–H), confirming the result of WB analysis.

Brain iron regulatory proteins are altered in *Tfr2*-KO mice. Transcriptional analysis of main Hepc regulatory genes, *Hfe* and *Hju*² did not reveal significant variations in the brain of *Tfr2*-KO mice compared to WT animals (not shown). Total brain production of the Hepc target protein Fpn1⁴³, resulted to be modulated in the different WT experimental groups with an opposite trend compared to cerebral Hepc amount, even if results did not reach statistical significance (Fig. 3L). Inverse relationship between the two proteins in WT animals is further evidenced by a very good fitting in regression analysis, while an apparent opposite trend, despite not statistically different from the WT pattern, could be observed in *Tfr2*-KO mice (Fig. 2S).

To molecularly analyse the increased amount of intracellular iron in the brain parenchyma, we evaluated the three main iron proteins responsible of cellular iron storage (Ft subunits H and L) and transport (Tf). They all resulted modulated. While in *Tfr2*-KO mice brain both Ft-H and Ft-L were higher, in WT IED mice only Ft-L was significantly increased (Fig. 3M,N). Iron transport protein Tf was incremented in IDD mice, as expected on the basis of its capability to supply with iron tissues in which iron amount is decreased^{44,45} (Table 1). Surprisingly, also *Tfr2*-KO mice presented an overall higher Tf amount, while this was not true for WT IED mice (Fig. 3O).

Again to verify that these proteins amount was not due to blood presence in non-perfused brains, Fts and Tf were analysed in brain of perfused animals. Blood removal in *Tfr2*-KO brains seems to cause a decrease of the three proteins amount. While an overall increase for Fts was confirmed, Tf displayed levels similar to WT brains, indicating a major role of circulating Tf in measurements in non-perfused brains (Fig. 1S).

As regards the main proteins responsible of cellular iron import, no significant variations were found for *Tfr1* levels in all the experimental groups (Fig. 3P). A lower amount of DMT1 protein was instead observed in *Tfr2*-KO brains compared to WT controls (Fig. 3Q). This result supports the hypothesis that the higher iron amount in *Tfr2*-KO mouse brains triggers a decrease in DMT1 protein according to the IRE/IRP pathway⁴⁵. The same

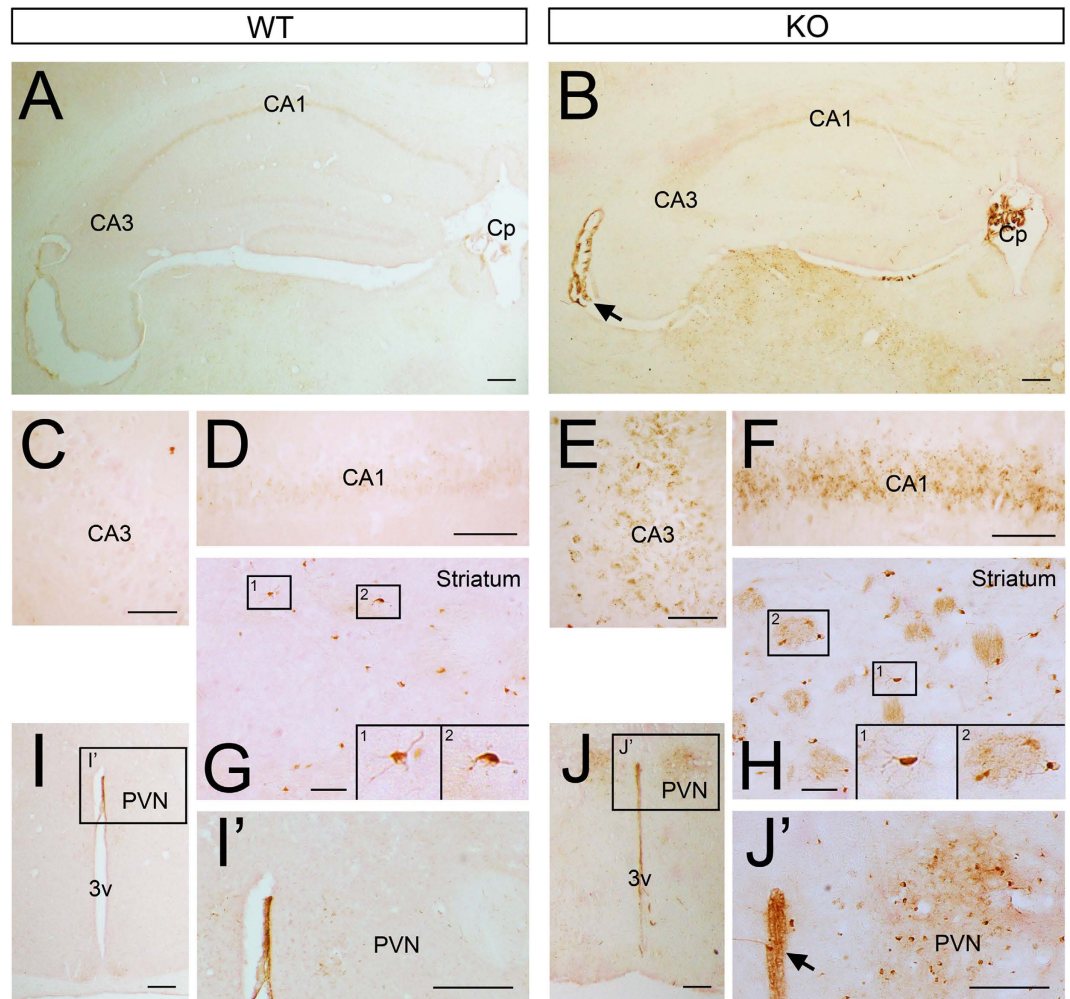
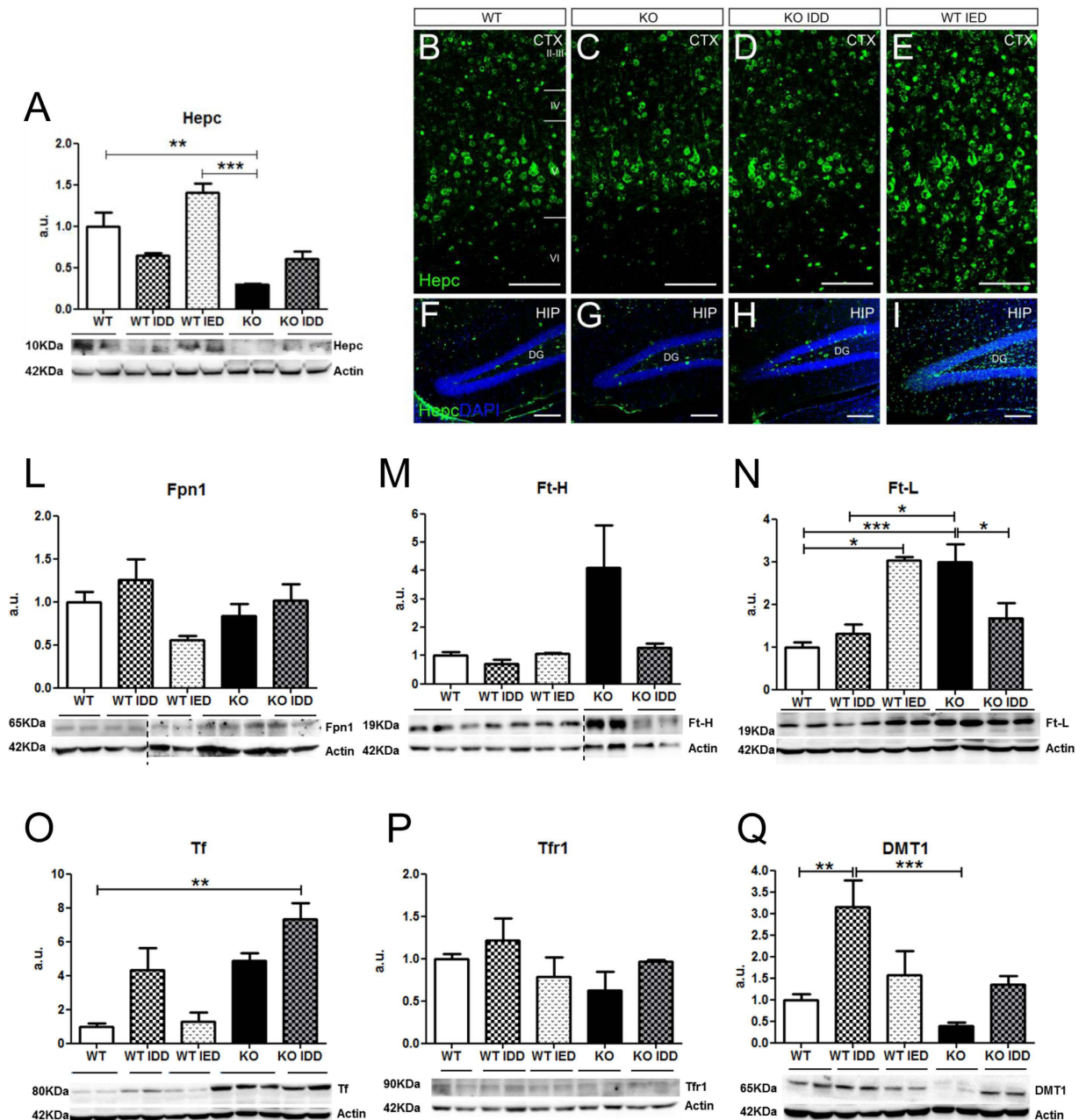


Figure 2. Iron accumulation in *Tfr2*-KO mouse brain. Iron in sections of the brain of WT and *Tfr2*-KO mice (**A,B**) DAB-enhanced Prussian Blue staining revealed iron accumulation in the choroid plexi (Cp) and ependyma (arrows) of *Tfr2*-KO mice (**B,I'**) compared to WT controls (**A,I'**). Higher magnification analysis also showed increased density of brown precipitates in the CA1 and CA3 of the mutant hippocampus (**E,F**), striatum (**H**) and paraventricular nucleus (**J,J'**) compared to WT tissues (**C-I'**). (**G,H,I,I'**). Iron labelling also decorates small glial cells that appeared more frequent in *Tfr2*-KO mice. This pattern was confirmed on 3 *Tfr2*-KO and WT mice. Scale bars: (**A,B,I-I'**): 100 μ m; (**B-G**): 50 μ m. CA1, Cornus Ammonis 1, CA3, Cornus Ammonis 3, Cp, choroid plexus, PVN, paraventricular nucleus, 3v, third ventricle.

regulatory mechanism accounts for DMT1 increase in WT IDD mice compared to WT, as well as in *Tfr2*-KO IDD animals compared to *Tfr2*-KO (Fig. 3Q).

In conclusion, *Tfr2* silencing associates with changes in both CNS iron import and storage proteins, in line with an altered cellular distribution and availability of the metal in the brain of these mice.

***Tfr2*-KO mice exhibit increased anxiety.** Based on high expression of *Tfr2* in the hippocampus and limbic circuits, we examined learning abilities and anxiety in the *Tfr2*-KO mice by behavioural tests. In the Morris water maze test no differences were found between WT and *Tfr2*-KO mice in the initial performance (day 1) (Fig. 4A). Furthermore, both WT and *Tfr2*-KO mice were able to improve their performance across days without differences (Fig. 4A). In the probe trial, the mean accuracy ratio (AR) did not show any significant difference between WT and *Tfr2*-KO mice, although *Tfr2*-KO mice spent about 2 fold more time in the target quadrant compared to wild type mice (Fig. 4B). Also in swim velocity and distance there were no differences between WT and *Tfr2*-KO mice (mean velocity \pm SE, WT = 23.1 ± 1.4 cm/s, *Tfr2*-KO = 26.4 ± 0.8 cm/s; mean travelled distance \pm SE, WT = 1380 ± 83.9 cm, *Tfr2*-KO = 1582 ± 48.4 cm; Mann-Whitney U; $P > 0.05$). Thus, *Tfr2*-KO mice do not show impairments of hippocampal-related spatial memory tasks. However, the trend for a stronger preference for the probe quadrant in *Tfr2*-KO mice (Fig. 4B) led us to measure the path length after mice reached the target zone. An increased path length outside the target zone, after reaching the original location of the platform, would suggest increased flexibility in an attempt to look for a new location of the platform. On the contrary, longer path length in the target zone would suggest persistency possibly related to increased anxiety³⁵. *Tfr2*-KO



mice displayed a significantly longer path length in the target zone after reaching the original position occupied by the platform compared with their WT sib pairs (Fig. 4C,D).

Furthermore, to avoid confounding effects due to changes in mutants of innate preference for swimming in defined areas of the maze⁴⁶, we calculated the distance travelled and the time spent in the centre zone of the pool versus the periphery region on the first trial of the first day, when the spatial location of the platform was completely unknown to the mice. WT and *Tfr2*-KO mice did not show significant differences in the percentages of travelled distances and time spent in the centre of the pool (mean percentage of distance travelled in centre \pm SE,

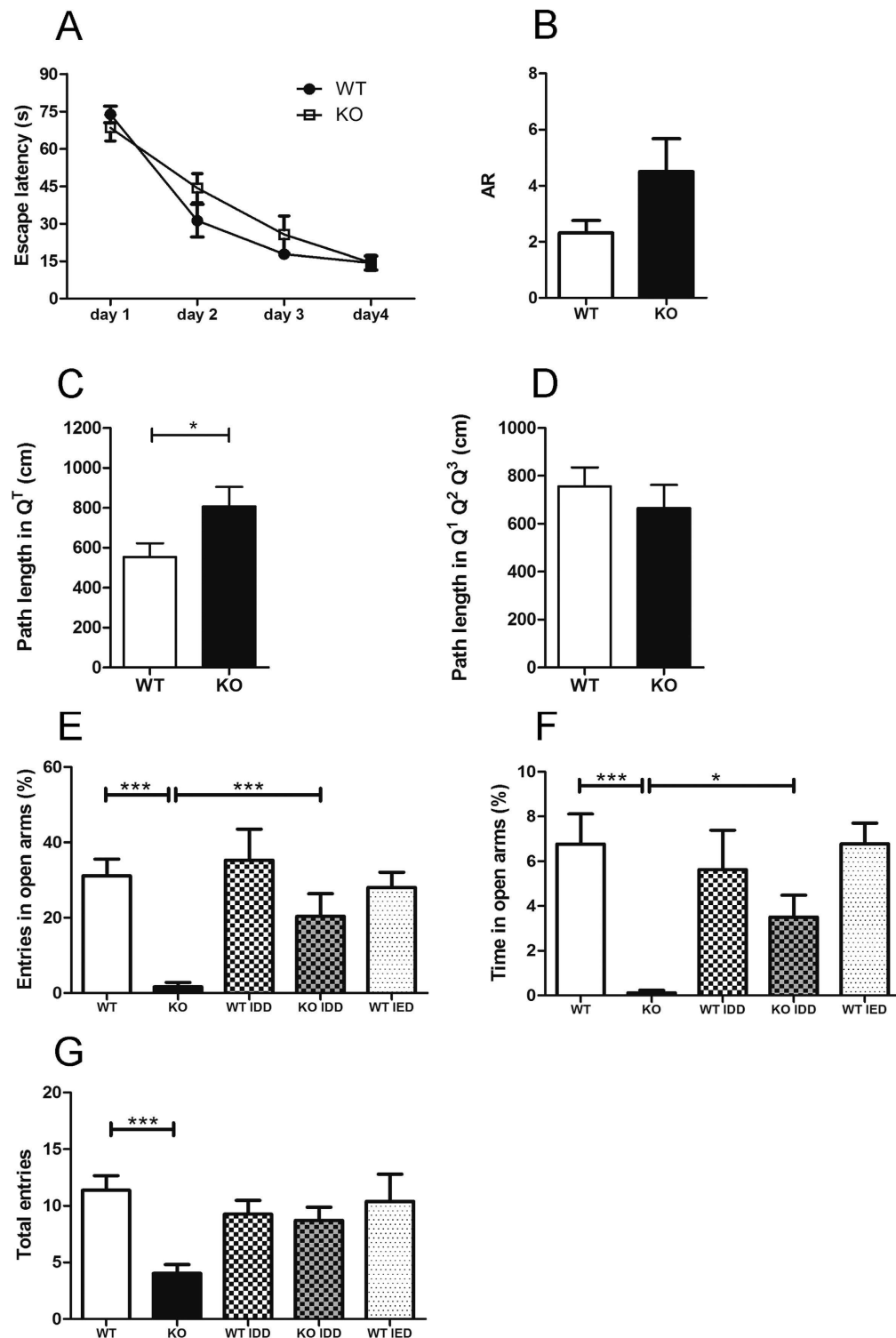


Figure 4. Overt anxiety-like behaviour in *Tfr2*-KO mice. (A,B) Performance in Morris water maze test. Both WT ($n = 8$) and *Tfr2*-KO ($n = 9$) mice improve their performance across days and during the probe trial without differences between genotypes. (C,D) Path length in Morris water maze test. Measures of the total distance (cm) covered by WT mice and *Tfr2*-KO mice after they reached the target zone in the probe trial. (C) *Tfr2*-KO mice showed longer path length in the target quadrant (Q_T) compared to WT mice. No differences are found in quadrants outside the target zone (Q^1 , Q^2 , Q^3). (E–G) Performance in EPM test. *Tfr2*-KO ($n = 22$) mice reveal anxiety levels higher than WT SD mice ($n = 27$). In IDD, *Tfr2*-KO mice ($n = 17$) show a rescue in anxious behaviors and perform similarly to WT mice ($n = 12$). AR, accuracy ratio; EPM, elevated plus maze; SD, standard diet, IDD, iron deficient diet, IED, iron enriched diet; Q_T target quadrant; error bars, standard error of the mean. Asterisks refer to statistically significant differences: * $P < 0.05$, ** $P < 0.01$, *** $P < 0.001$. Statistically significant results are reported in Table 1S.

WT = 7.1 ± 3.4 , *Tfr2*-KO = 7.1 ± 2.2 ; mean percentage of time spent in centre \pm SE, WT = 5.4 ± 2.5 cm, *Tfr2*-KO = 5.8 ± 2.0 Mann-Whitney U; $P > 0.05$) thus showing that both WT and *Tfr2*-KO mice have the same innate preference for swimming in distinct areas of the maze.

Finally, we further assessed anxiety in the EPM. Notably, *Tfr2*-KO mice showed increased anxiety as expressed by a dramatically low frequency of entries in the open arms of the EPM (Fig. 4E). Consistently, they spent a little time in the open arms of the EPM (Fig. 4F) compared with WT siblings. Also, the total number of entries was reduced in *Tfr2*-KO mice (Fig. 4G). Then, we asked whether such anxious-like behaviour depends on iron levels by examining mice subjected to IDD and IED. Reductions in the frequency and time spent in open arms and in total entries were reverted to control values by IDD in *Tfr2*-KO mice (Fig. 4E,F,G). Notably, neither IDD nor IED affected the anxious behaviour of WT mice (Fig. 4E,F). Altogether, these data show that loss of *Tfr2* associated with iron overload promotes the occurrence of anxious behaviours.

Higher levels of activation of the anxiety circuitry in *Tfr2*-KO mice. The marked anxious behaviour in *Tfr2*-KO mice suggests that *Tfr2* deletion in combination with iron overload might cause an abnormal activation of the anxiety system. We therefore investigated the expression pattern of cFos and Zif-268, the immediate early genes frequently used as markers for neuronal activity⁴⁷, in brain nuclei belonging to the anxiety circuitry, including the hippocampus, the medial prefrontal cortex (mPFC), the basolateral (BLA), and central (CeA) amygdala and the hypothalamic paraventricular nuclei (PVN). Interestingly, in the hippocampus of *Tfr2*-KO mice the two activity markers were highly upregulated in CA3 (Fig. 5A,B,L,P) and CA1 neurons (Fig. 5A,B,F,G,I,J,M,Q), while their expression in the dentate gyrus (DG) did not differ from that of WT mice (Fig. 3SB and not shown). Of note, in *Tfr2*-KO mice fed with IDD anti-cFos and Zif-268 staining decreased to the levels of the WT mice in both CA3 and CA1 subregions (Fig. 5C,H,K,L,M,P,Q). The medial prefrontal cortex (mPFC) is one of the main targets of the hippocampal neurons and contributes to the anxiety control and stress responses by projecting to the BLA and, indirectly, to the PVN³⁹. The levels of both cFos and Zif-268 increased significantly in this area of *Tfr2*-KO mice compared to WT or *Tfr2*-KO IDD mice (Fig. 5N,R). Consistently, both transcription factors appeared significantly upregulated in the BLA of the *Tfr2*-KO mice (Fig. 5O,S). Furthermore, anti-cFos/Zif-268 immunostainings did not reveal differences in activity levels of neurons included either in the PVN (Fig. 5D,E) and CeA (or in other areas unrelated to anxiety control) (not shown). In line with the maintenance of WT activation levels in the CeA and PVN, the corticotropin-releasing factor (CRF) immunostaining in the PVN of *Tfr2*-KO mice did not differ from that of WT mice (Fig. 4SA,B), showing that, despite being associated with a pronounced anxious behaviour, *Tfr2* deletion does not alter CRF release into the hypothalamo-hypophyseal portal system³⁸. Accordingly, we did not find differences in corticosterone levels in *Tfr2*-KO serum compared to WT (Fig. 4SC). We further tested whether the altered activity pattern of *Tfr2*-KO was associated with changes in levels of BDNF, a key-regulator of synaptic plasticity and hippocampal activity, whose alterations were associated with iron changes and anxiety⁴⁸. However, we did not find changes of BDNF mRNA levels in hippocampus of *Tfr2*-KO mice compared to WT animals (Fig. 4SD). Of note, IED in WT animals also triggered a response that promoted a diffuse and aspecific upregulation of cFos throughout most brain areas (Fig. 3S). Thus, iron alterations due to *Tfr2* deficiency positively and specifically modulate neuronal activation in the CA3-CA1-mPFC-BLA circuitry, while they do not alter the neuroendocrine compartment implicated in anxiety regulation.

Given the high levels of expression of *Tfr2* alpha in the Mossy fiber pathway, we further hypothesized that the activation of the anxiety circuitry were triggered by altered signals conveyed by Mf to CA3 neurons. Therefore, we investigated possible changes in the density of glutamatergic vGlut1/2+ terminals in CA3. While no difference was observed in the number of vGlut1+ puncta, the density of anti-vGlut2 positivity significantly increased at this site, suggesting incremented excitation and terminal remodelling (Fig. 5T,U,V). Collectively, these data are consistent with a role of *Tfr2* alpha in the regulation of both the Mf output and the activity of the anxiety system.

Increased microglia reactivity, dystrophic changes and death in *Tfr2*-KO mice. Recent findings indicate that microglia alterations are frequently associated with increased stress and anxiety⁴⁹. Although immunohistological analyses did not reveal alterations of the gross anatomy of the *Tfr2*-KO mouse brain (Fig. 5S), in *Tfr2*-KO we found a decrease in the density of microglial cells identified by labelling for the ionized calcium-binding adaptor molecule 1 (Iba1), (Fig. 6A,B). This decrease occurred throughout the brain and was quantified in *Tfr2*-KO mouse cerebral cortex (Fig. 6A,B,F) and hippocampus (Fig. 6G,H).

Here, the density of both reactive (i.e. showing hypertrophy and very thick short processes Fig. 6C) or degenerating (i.e. bearing fragmented or dystrophic processes and a pyknotic nucleus; Fig. 6D–E') Iba1+ cells appeared significantly increased compared to WT mice (Fig. 6G,H), suggesting that reactive and degenerative events occur in parallel and that the latter changes dominate, thereby resulting in the reduction of the microglial pool in the *Tfr2*-KO mice.

In order to understand the correlation of the *Tfr2*-KO microglial phenotype with iron overload and/or anxiety, we looked at microglia in *Tfr2*-KO IDD and WT IED mice. Despite recovering a physiological density of Iba1+ cells in the cerebral cortex, (Fig. 6F), KO IDD mice still displayed some microglia activation and degeneration in the examined areas (Fig. 6G,H). Low iron levels in these mice (Table 1) indicated that such microglial alterations might not be due to iron overload *per se*. Yet, the decrease in microglial density could be a factor participating in the behavioural abnormalities found in *Tfr2*-KO mice. However, in WT IED animals microglia are also diminished in the absence of anxiety signs (Fig. 6F). Moreover, microglial reactivity and degeneration occurred in both *Tfr2*-KO IDD (Fig. 5) and WT IED mice (Fig. 6S) in the absence of an anxious phenotype, indicating that these features are also not directly linked to anxiety. Interestingly, we found signs of ongoing inflammation (as monitored by levels of the Serum Amyloid A1 (SAA1) acute phase protein⁵⁰; Fig. 7S) in the brain of WT IED mice but not in those of *Tfr2*-KO animals, suggesting that *Tfr2* may be implicated in the regulation of the inflammatory

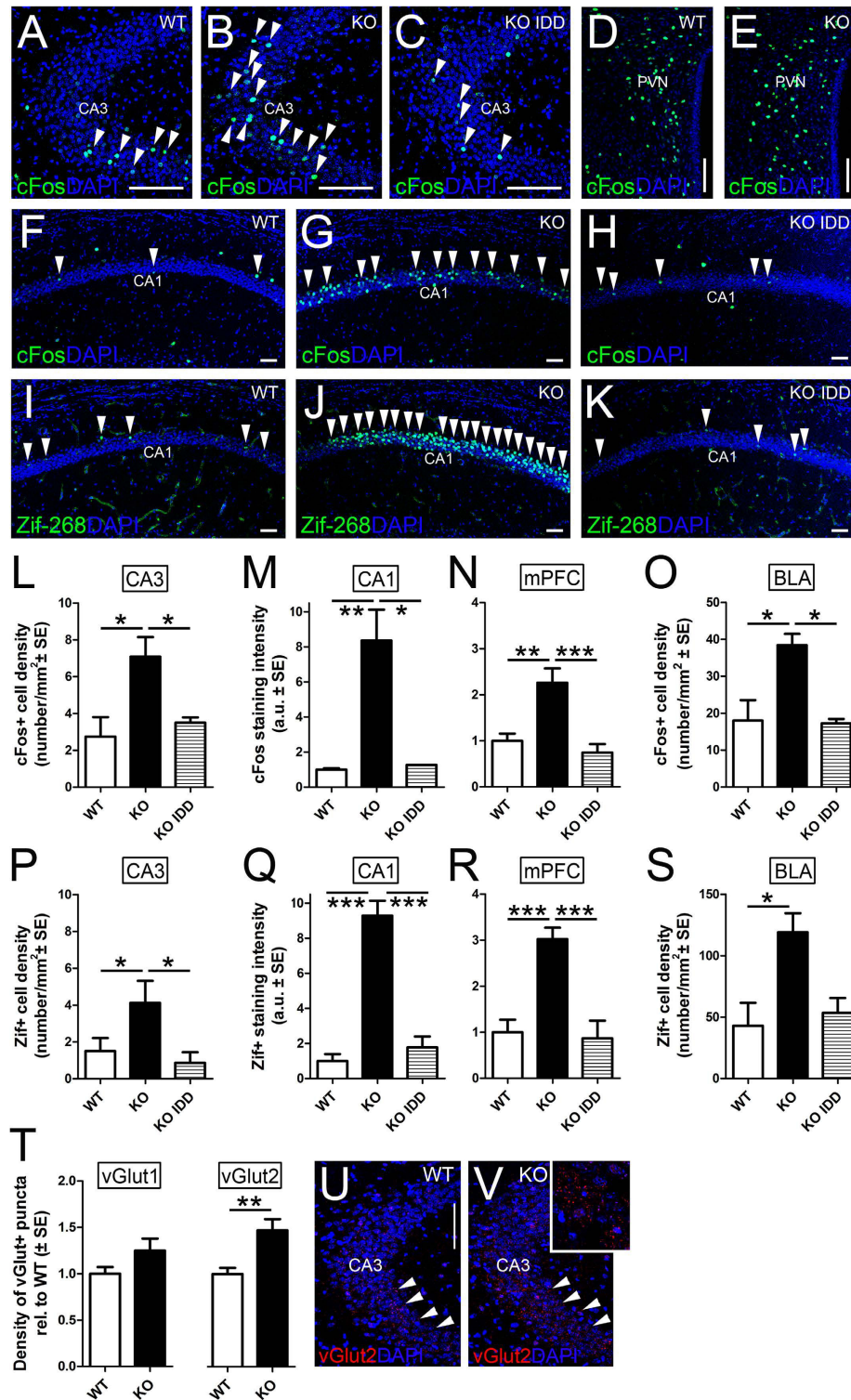


Figure 5. Activity-related immediate early genes in anxiety circuits. The immediate early genes cFos (A–H) and Zif-268 (I–K) are upregulated in neurons of the CA1 (F,G) and CA3 (A,B) areas of *Tfr2*-KO mice compared to WT brains, while no increase in positive cells occurs in the PVN (D,E). Quantifications of the number of positive nuclei over the area of the corresponding layers show that cFos+ or Zif-268+ cells significantly increased in mutant mice in standard conditions while they return to control levels in mutant fed with IDD diet (H,K,L,M,P,Q). This very same trend is found in the mPFC and BLA (N,O,R,S). (T–V) Quantifications of glutamatergic terminals in CA3 (red in (U,V)) show that vGlut2+ puncta are higher in number in *Tfr2*-KO mice, while vGlut1+ ones do not differ from WT. Asterisks refer to statistically significant differences: * $P < 0.05$, ** $P < 0.01$, *** $P < 0.001$. Scale bars: 100 μ m, IDD, iron deficient diet; IED, iron enriched diet; PVN, periventricular hypothalamic nucleus; mPFC, medial prefrontal cortex; BLA, basolateral amygdala; error bars, standard error of the mean. Statistically significant results are reported in Table 1S.

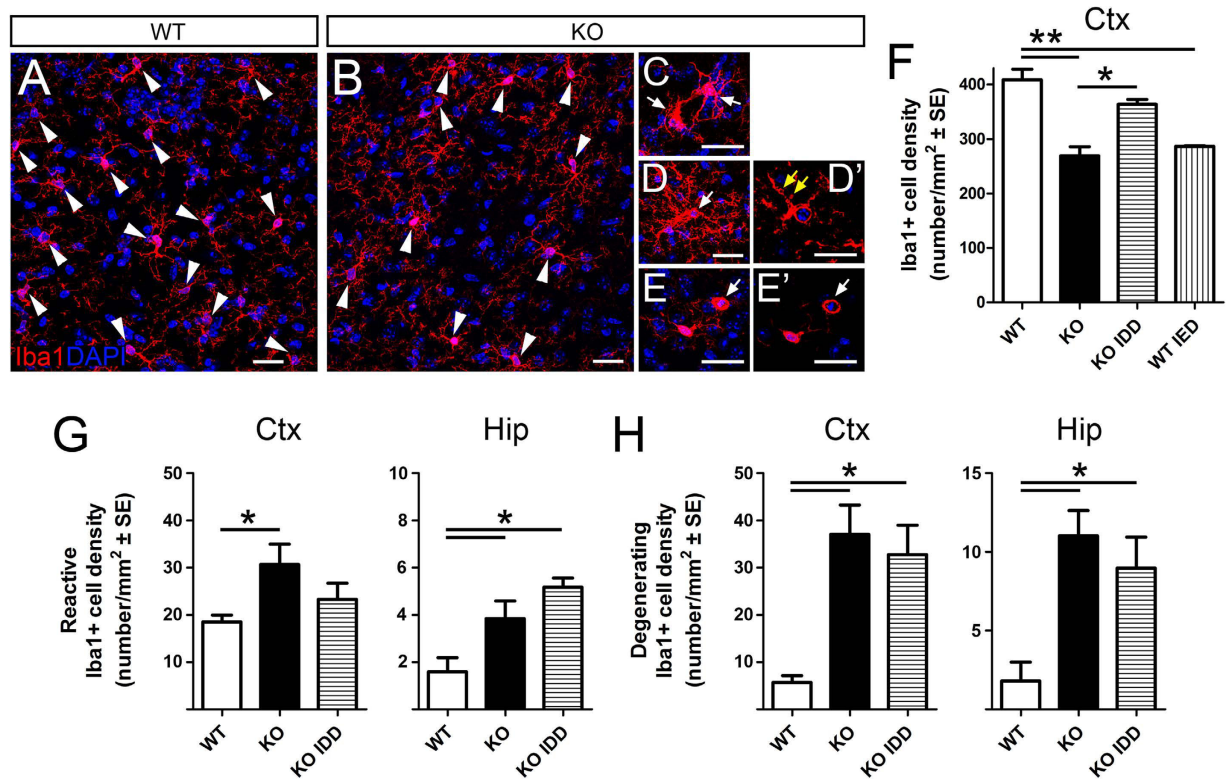


Figure 6. Microglial phenotypes in *Tfr2*-KO and WT mice. Immunofluorescence (A–E') and quantification (F) of microglial cells using Iba1 marker in total brain. Quantification of reactive (G) and degenerating (H) cells in cortex (Ctx) and hippocampus (Hip). Arrowheads indicate Iba1+ microglia density (A,B). Arrows indicate reactive morphologies (C), signs of degeneration (yellow arrows, D') and pyknosis (arrows in (E), E'). Asterisks refer to statistically significant differences: * $P < 0.05$, ** $P < 0.01$. Statistically significant results are reported in Table 1S. CTX, neocortex (primary M1 motor cortex); HIP, hippocampus; IDD, iron deficient diet; IED, iron enriched diet; error bars, standard error of the mean. D', E', single optical slices. Scale bars: 20 μ m.

profile of these cells. Thus, microglia appear to strongly respond to alteration of iron metabolism but they do not play a specific role in the behavioural alterations of *Tfr2*-KO.

Discussion

In this work we show that *Tfr2* germinal silencing affects brain iron homeostasis. Furthermore, we reveal that *Tfr2* alpha is highly expressed in neurites of brain circuits of anxiety and stress disorders. This pattern, together with the prominent anxious behaviour of *Tfr2*-KO mice, strongly suggests a role for *Tfr2* alpha in the regulation of anxiety circuits. Finally, our results further highlight a particular sensitivity of microglia to perturbations of iron metabolism, even when peripheral iron accumulation is moderate and does not associate with behavioural alterations.

Tfr2 alpha is the mainly transcribed isoform of the *TFR2* gene, whose mutations are responsible of a form of hereditary hemochromatosis named HFE3⁶. Hereditary haemochromatosis is a genetically heterogeneous disease due to functional impairment of the iron hormone Hpc and of several Hpc regulating proteins³.

Tfr2 alpha is a key iron sensor that, in liver, triggers a signal transduction cascade that activates the expression of Hpc, a small protein that reduces iron efflux from cells and leads to its intracellular accumulation². *Tfr2* beta isoform is instead known to exert a role in iron efflux in spleen reticuloendothelial cells⁹. So far, several papers reported a *Tfr2* alpha expression in the nervous tissue^{23–25} that was proposed to be restricted to specific brain regions^{23,24}. Our transcriptional and immunohistological analyses validated in *Tfr2*-KO mice, showed relevant *Tfr2* alpha expression in the nervous tissue and revealed *Tfr2* alpha protein distribution in the neurite compartment of limbic areas implicated in anxiety and stress response. This expression pattern is not fully consistent with those previously reported in human tissues²³, that described *Tfr2* expression only in the cerebellum. While this discrepancy may be due to species-specific factors, open access transcriptome data published on GEO Profiles indicate that in both humans and rodents *Tfr2* is not exclusively expressed in the cerebellum and is detected in hippocampus, cerebral cortex, basal ganglia and amygdala (Profile: GDS2678/40311_at/, Brain regions of humans and chimpanzees; Profile: GDS1406/160674_at/*Tfr2*, Brain regions of various inbred strains). Further, a low and ubiquitous *Tfr2* alpha expression in mouse neural cells and brain endothelium below the sensitivity of the detection approach applied in this study may occur. Indeed, the diffuse upregulation of Hpc in WT IED brains supports the presence of a more widespread *Tfr2* alpha expression.

Based on the key role of Tfr2 in regulating liver iron load, one obvious expectation was to find an increased iron amount in the parenchymal nervous tissue upon Tfr2 deletion. Indeed, in total brain extracts of *Tfr2*-KO including circulating blood, BIC was significantly higher than that of both WT and WT IED, underscoring that in these animals brain parenchyma is exposed to a higher iron amount. Moreover, Perls' staining on brains from *Tfr2*-KO perfused mice revealed that iron accumulates in some of the brain regions where we found relevant Tfr2 expression (hippocampal CA1 and CA3, PVN) as well as in compartments, such as the choroid plexi, which are sites of iron trafficking between systemic circulation and the brain environment⁵¹.

Yet, despite iron deposition, no changes in Hepc protein levels were observed in the nervous tissue, as detected by WB and immunofluorescence. Thus, the strong Hepc reduction in samples containing circulating blood reflects essentially peripheral/systemic Hepc blunting in the absence of Tfr2.

In line with an increased iron amount in *Tfr2*-KO brain, levels of the iron storage protein ferritin globally increase. Ferritin H subunit in particular, is specifically increased in *Tfr2*-KO mice. This induction may reflect the need to counteract the deleterious effects of an enhanced iron-based Fenton reaction, which produces damaging hydroxyl radicals⁵². Tf protein is overexpressed in both WT IDD and *Tfr2*-KO IDD brain, as expected in condition of iron deprivation^{44,45}. Unexpectedly Tf displays an increase, although not statistically significant, also in *Tfr2*-KO brains from non-perfused mice, while it is comparable to WT levels in brains from perfused animals. These results are consistent with the additional presence of blood Tf in non-perfused brains.

There is a tendency to decrease for the iron importer DMT1 in *Tfr2*-KO brains, in agreement with a higher iron content, at least in defined cell type(s) of the brain tissue. Moreover, its increase both in *Tfr2*-KO IDD and in WT IDD mice brain is a correct response to iron deprivation based on the activation of the intracellular iron regulatory IRE/IRP response system⁴⁵. Overall these alterations are consistent with a Tfr2 alpha-dependent dysfunctional iron handling in the brain, even though we cannot exclude that over time an exacerbation of the iron burden in WT IED animals could eventually lead to a phenotype overlapping that of *Tfr2*-KO mice.

From the behavioural point of view, iron increase in *Tfr2*-KO mice was accompanied by anxious-like behaviour as assessed by the EPM, where *Tfr2*-KO SD mice spent proportionally less time in the anxiogenic arm compared to other genotypes and conditions. Anxiety-like behaviours were dependent on iron increase, because they were reverted by IDD in *Tfr2*-KO mice. Despite in this study we cannot definitively dissect the contribution of systemic vs. parenchymal iron overload to the anxious phenotype, lack of anxiety signs in WT IED mice that are systemically overloaded but with normal brain iron content - as notably detected without perfusion to wash away the contaminating blood-, suggests that increased parenchymal iron deposits play a prominent role in promoting behavioural alterations. However, the lower systemic iron load in WT IED mice compared to *Tfr2*-KO mice may take part in the absence of the phenotype. In former studies both iron deficiency and iron overload during critical developmental windows or at adult ages have been shown to affect emotional behaviour in rodents⁵³. However, the biological mechanisms mediating the effect of iron level alterations at early or mature stages are likely to be distinct. While precocious actions are plausible to rely on abnormal circuit formation, here we find changes of circuit activity, possibly accompanied by some degree of remodelling (see below). In line with our findings, a former study on the effects of experimental brain iron overload (i.p. injections of 3 mg/kg of ferrous sulphate for 5 consecutive days) also reported anxiety in rats, though in association with defects in spatial learning⁵⁴. Moreover, iron-deficiency was also shown to lead to anxiety in mutant mice, likely due to the iron requirement in the synthesis of serotonin and noradrenaline⁴⁸. Since WT IDD mice in this study did not show a brain-specific iron decrease, they are not expected to show behavioural alterations associated with brain iron deficiency. Finally, no data are known about brain iron metabolism in the few HFE3 iron overloaded patients available and no sign of neurological alterations has been evidenced so far. Nevertheless, it must be taken into account that these patients nowadays undergo early diagnosis and efficient phlebotomy until serum iron parameters normalization.

Consistent with behavioural data, in *Tfr2*-KO mice we found a specific and selective overactivation of the limbic circuits controlling anxiety and stress responses, as demonstrated by increased expression of cFos and Zif-268 (Fig. 8S). Surprisingly, also IED in WT mice promoted cFos/Zif-268 upregulation in the brain, but that was far more broad and intense compared to *Tfr2*-KO animals, suggesting that distinct mechanisms account for the induction in the two experimental models. These data provide in-depth explanation to former hints indicating that alterations of iron homeostasis affect expression of neurotransmitters and trophic factors^{15,16,26,48,53}. Importantly, in *Tfr2*-KO cFos/Zif-268 upregulation declined in IDD, thereby showing dependence on iron levels. Notably, in *Tfr2*-KO mice all the limbic stations displayed enhanced activity, with the exception of areas belonging to the neuroendocrine stress axis, whose functioning appears unaffected as shown by absence of alterations in PVN CRF and blood corticosterone (Fig. 4S). Moreover, we report an increased V-Glut2 positivity compared to control levels in the CA3 Mf terminal field suggesting that Tfr2 deletion may affect the final output of the Mf pathway by inducing terminal remodeling or promoting immature traits in these fibers, in line with restriction of V-Glut2 during immature developmental stages⁵⁵. Several studies have shown a positive correlation between Mf sprouting and increased anxiety-like behaviour in rodents⁵⁶⁻⁵⁹, suggesting that the Mf system may contribute to modulation of anxiety-like responses. Thus, collectively data are consistent with a model where Tfr2-dependent alterations in iron homeostasis affect the activity of the main brain areas responsible for the neural control of emotional behaviour, and promote anxiety. Further, high Tfr2 alpha expression along Mf and in nuclei of the limbic circuit suggests a specific role for this isoform in the regulation of the anxiety circuits.

It is interesting to note that activity alterations and behavioural abnormalities in *Tfr2*-KO mice are not due to degenerative events in neurons or astrocytes. We found degeneration only in microglia, that also display increased iron storage in KO mice, as detected by Perls' staining. This suggests that iron-mediated challenge may be compensated in other neural cells. Yet, microglial loss and alterations were also found in WT IED brains that did not show behavioural alterations, ruling out their role in the detected anxious-like traits. Nevertheless, microglial cells were clearly affected in the *Tfr2*-KO mice and displayed reactivity, dystrophic changes and death. These findings are in line with their known action as buffering elements that counteract disturbances in iron regulation⁶⁰.

However, in our study, microglial alterations are detected not only in *Tfr2*-KO SD but also in WT IED mice, thereby excluding their specific dependence on *Tfr2* abrogation and supporting the hypothesis that either the altered or increased iron processing is responsible for the observed dystrophic modifications and degeneration in microglia.

Taken together, these data add to the growing body of evidence that alterations of systemic iron loading affect brain homeostasis and functioning, and reveal a specific role for *Tfr2*-dependent iron overload in the control of iron regulatory network in the brain tissue as well as in the control of anxious behaviours.

References

- Ganz, T. Systemic iron homeostasis. *Physiol Rev.* **93**, 1721–1741 (2013).
- Hentze, M. W., Muckenthaler, M. U., Galy, B. & Camaschella, C. Two to tango: regulation of Mammalian iron metabolism. *Cell.* **142**, 24–38 (2010).
- Roetto, A. & Camaschella, C. New insights into iron homeostasis through the study of non-HFE hereditary haemochromatosis. *Best Pract Res Clin Haematol.* **18**, 235–250 (2005).
- Finberg, K. E. Iron-refractory iron deficiency anemia. *Semin Hematol.* **46**, 378–386 (2009).
- Kawabata, H. *et al.* Molecular cloning of transferrin receptor 2. A new member of the transferrin receptor-like family. *J Biol Chem.* **274**, 20826–20832 (1999).
- Camaschella, C. *et al.* The gene TFR2 is mutated in a new type of haemochromatosis mapping to 7q22. *Nat Genet.* **25**, 14–15 (2000).
- Fleming, R. E. *et al.* Targeted mutagenesis of the murine transferrin receptor-2 gene produces hemochromatosis. *Proc Natl Acad Sci USA* **99**, 10653–10658 (2002).
- Wallace, D. F., Summerville, L., Lusby, P. E. & Subramaniam, V. N. First phenotypic description of transferrin receptor 2 knockout mouse, and the role of hepcidin. *Gut.* **54**, 980–986 (2005).
- Roetto, A. *et al.* Comparison of 3 *Tfr2*-deficient murine models suggests distinct functions for *Tfr2*-alpha and *Tfr2*-beta isoforms in different tissues. *Blood.* **115**, 3382–3389 (2010).
- Moos, T., Rosengren Nielsen, T., Skjørringe, T. & Morgan, E. H. Iron trafficking inside the brain. *J Neurochem* **103**, 1730–1740 (2007).
- Rouault, T. A. Iron metabolism in the CNS: implications for neurodegenerative diseases. *Nat Rev Neurosci.* **14**, 551–564 (2013).
- Crespo, Á. C. *et al.* Genetic and biochemical markers in patients with Alzheimer's disease support a concerted systemic iron homeostasis dysregulation. *Neurobiol Aging.* **35**, 777–785 (2013).
- Ayton, S. & Lei, P. Nigral iron elevation is an invariable feature of Parkinson's disease and is a sufficient cause of neurodegeneration. *Biomed Res Int.* **581256** (2014) <http://dx.doi.org/10.1155/2014/581256>.
- Yu, S., Feng, Y., Shen, Z. & Li, M. Diet supplementation with iron augments brain oxidative stress status in a rat model of psychological stress. *Nutrition.* **27**, 1048–1052 (2011).
- Johnstone, D. *et al.* Brain transcriptome perturbations in the *Hfe*($-/-$) mouse model of genetic iron loading. *Brain Res.* 1448–1452 (2012).
- Acikyol, B. *et al.* Brain transcriptome perturbations in the transferrin receptor 2 mutant mouse support the case for brain changes in iron loading disorders, including effects relating to long-term depression and long-term potentiation. *Neuroscience.* **235**, 119–128 (2013).
- Kaur, C. & Ling, E. A. Transient expression of transferrin receptors and localisation of iron in amoeboid microglia in postnatal rats. *J Anat.* **186**, 165–173 (1995).
- Kaur, C. & Ling, E. A. Increased expression of transferrin receptors and iron in amoeboid microglial cells in postnatal rats following an exposure to hypoxia. *Neurosci Lett.* **262**, 183–186 (1999).
- Aldred, A. R., Dickson, P. W., Marley, P. D. & Schreiber G. Distribution of transferrin synthesis in brain and other tissues in the rat. *J Biol Chem.* **11**, 5293–5297 (1987).
- Zechel, S., Huber-Wittmer, K. & von Bohlen und Halbach, O. Distribution of the iron-regulating protein hepcidin in the murine central nervous system. *J Neurosci Res.* **84**, 790–800 (2006).
- Clardy, S. L. *et al.* Is ferroportin-hepcidin signaling altered in restless legs syndrome? *J Neurol Sci.* **247**, 173–179 (2006).
- Wang, Q. *et al.* Lipopolysaccharide induces a significant increase in expression of iron regulatory hormone hepcidin in the cortex and substantia nigra in rat brain. *Endocrinology.* **149**, 3920–3925 (2008).
- Hänninen, M. M. *et al.* Expression of iron-related genes in human brain and brain tumors. *BMC Neurosci.* **10**, 36 (2009).
- Mastroberardino, P. G. *et al.* A novel transferrin/TFR2-mediated mitochondrial iron transport system is disrupted in Parkinson's disease. *Neurobiol Dis.* **34**, 417–431 (2009).
- Calzolari, A. *et al.* Transferrin receptor 2 is frequently and highly expressed in glioblastomas. *Transl Oncol.* **3**, 123–134 (2010).
- Johnstone, D. & Milward, E. A. Genome-wide microarray analysis of brain gene expression in mice on a short-term high iron diet. *Neurochem Int.* **56**, 856–863 (2010).
- Bondi, A. *et al.* Hepatic expression of hemochromatosis genes in two mouse strains after phlebotomy and iron overload. *Haematologica.* **90**, 1161–1167 (2005).
- Nicolas, G. *et al.* The gene encoding the iron regulatory peptide hepcidin is regulated by anemia, hypoxia, and inflammation. *J Clin Invest.* **110**, 1037–1044 (2002).
- Boda, E., Pini, A., Hoxha, E., Parolisi, R. & Tempia, F. Selection of reference genes for quantitative real-time RT-PCR studies in mouse brain. *J Mol Neurosci.* **37**, 238–253 (2009).
- Livak, K. J. & Schmittgen, T. D. Analysis of relative gene expression data using real-time quantitative PCR and the 2^{(-Delta Delta C(T))} Method. *Methods.* **25**, 402–408 (2001).
- Meguro, R., Asano, Y., Odagiri, S., Li, C., Iwatsuki, H. & Shoumura, K. Nonheme-iron histochemistry for light and electron microscopy: a historical, theoretical and technical review. *Arch Histol Cytol.* **70**, 1–19 (2007).
- Buffo, A. *et al.* Expression pattern of the transcription factor *Olig2* in response to brain injuries: implications for neuronal repair. *Proc Natl Acad Sci USA* **102**, 18183–18188 (2005).
- Boda, E. *et al.* The GPR17 receptor in NG2 expressing cells: focus on *in vivo* cell maturation and participation in acute trauma and chronic damage. *Glia.* **59**, 1958–1973 (2011).
- Pistorio, A. L., Hendry, S. H. & Wang, X. A modified technique for high-resolution staining of myelin. *J Neurosci Methods.* **153**, 135–146 (2006).
- Vorhees, C. V. & Williams, M. T. Morris water maze: Procedures for assessing spatial and related forms of learning and memory. *Nat Protoc.* **1**, 848–858 (2006).
- Longo, A. *et al.* Conditional inactivation of neuropeptide Y Y1 receptors unravels the role of Y1 and Y5 receptors coexpressing neurons in anxiety. *Biol Psychiatry.* **76**, 840–849 (2014).
- Johnson, M. B., Chen, J., Murchison, N., Green, F. A. & Enns, C. A. Transferrin receptor 2: evidence for ligand-induced stabilization and redirection to a recycling pathway. *Mol Biol Cell.* **18**, 743–754 (2007).
- Ulrich-Lai, Y. M. & Herman, J. P. Neural regulation of endocrine and autonomic stress responses. *Nat Rev Neurosci.* **10**, 397–409 (2009).

39. Adhikari, A. Distributed circuits underlying anxiety. *Front Behav Neurosci.* **8**, 112 (2014).
40. Omara, F. O., Blakley, B. R. & Wanjala, L. S. Hepatotoxicity associated with dietary iron overload in mice. *Hum Exp Toxicol.* **12**, 463–467 (1993).
41. Boero, M. *et al.* A comparative study of myocardial molecular phenotypes of two *tfr2/3* null mice: Role in ischemia/reperfusion. *Biofactors.* **41**, 360–371 (2015).
42. Ding, H. *et al.* Hephcidin is involved in iron regulation in the ischemic brain. *PLoS One.* **6**, e25324 (2011).
43. Nemeth, E. *et al.* Hephcidin regulates cellular iron efflux by binding to ferroportin and inducing its internalization. *Science.* **306**, 2090–2093 (2004).
44. Zakin, M. M. Regulation of transferrin gene expression. *FASEB J.* **6**, 3253–3258 (1992).
45. Muckenthaler, M. U., Galy, B. & Hentze, M. W. Systemic iron homeostasis and the iron-responsive element/iron-regulatory protein (IRE/IRP) regulatory network. *Annu Rev Nutr.* **28**, 197–213 (2008).
46. Pritchett, D. *et al.* Searching for cognitive enhancement in the Morris water maze: Better and worse performance in D-amino acid oxidase knockout (Dao^{-/-}) mice. *Eur J Neurosci.*, doi: 10.1111/ejn.13192 (2016).
47. Sheng, M. & Greenberg, M. E. The regulation and function of *c-fos* and other immediate early genes in the nervous system. *Neuron.* **4**, 477–485 (1990).
48. Texel, S. J. *et al.* Ceruloplasmin deficiency results in an anxiety phenotype involving deficits in hippocampal iron, serotonin, and BDNF. *J Neurochem.* **120**, 125–134 (2012).
49. Kreisel, T. *et al.* Dynamic microglial alterations underlie stress-induced depressive-like behavior and suppressed neurogenesis. *Mol Psychiatry.* **19**, 699–709 (2014).
50. Uhlar, C. M. & Whitehead, A. S. Serum amyloid A, the major vertebrate acute-phase reactant. *Eur J Biochem.* **265**, 501–523 (1999).
51. Rouault, T. A., Zhang, D. L. & Jeong, S. Y. Brain iron homeostasis, the choroid plexus, and localization of iron transport proteins. *Metab Brain Dis.* **24**, 673–684 (2009).
52. Chelikani, P., Fita, I. & Loewen, P. C. Diversity of structures and properties among catalases. *Cell Mol Life Sci.* **6**, 192–208 (2004).
53. Kim, J. & Wessling-Resnick, M. Iron and mechanisms of emotional behavior. *J Nutr Biochem.* **25**, 1101–1107 (2014).
54. Maaroufi, K. *et al.* Impairment of emotional behavior and spatial learning in adult Wistar rats by ferrous sulfate. *Physiol Behav.* **96**, 343–349 (2009).
55. Herzog, E., Takamori, S., Jahn, R., Brose, N. & Wojcik, S. M. Synaptic and vesicular co-localization of the glutamate transporters VGLUT1 and VGLUT2 in the mouse hippocampus. *J Neurochem.* **99**, 1011–1018 (2006).
56. Prior, H., Schwegler, H. & Dücker, G. Dissociation of spatial reference memory, spatial working memory, and hippocampal mossy fiber distribution in two rat strains differing in emotionality. *Behav Brain Res.* **87**, 183–194 (1997).
57. de Oliveira, D. L. *et al.* Effects of early-life LiCl-pilocarpine-induced status epilepticus on memory and anxiety in adult rats are associated with mossy fiber sprouting and elevated CSF S100B protein. *Epilepsia.* **49**, 842–852 (2008).
58. Oztan, O., Aydin, C. & Isgor, C. Chronic variable physical stress during the peripubertal-juvenile period causes differential depressive and anxiogenic effects in the novelty-seeking phenotype: functional implications for hippocampal and amygdalar brain-derived neurotrophic factor and the mossy fibre plasticity. *Neuroscience.* **192**, 334–344 (2011).
59. Aydin, C., Oztan, O. & Isgor, C. Hippocampal Y2 receptor-mediated mossy fiber plasticity is implicated in nicotine abstinence-related social anxiety-like behavior in an outbred rat model of the novelty-seeking phenotype. *Pharmacol Biochem Behav.* **125**, 48–54 (2014).
60. Simmons, D. A., Casale, M., Alcon, B., Pham, N., Narayan, N. & Lynch, G. Ferritin accumulation in dystrophic microglia is an early event in the development of Huntington's disease. *Glia.* **55**, 1074–1084 (2007).

Acknowledgements

We are indebted to our colleague Sonia Levi for providing us anti Ferritin antibodies and for critical discussion of the results. We thank Angela Longo and Paolo Mele for assistance with behavioural tests and data interpretation and Filippo Tempia, Carola Eva, Sonia Levi for manuscript critical reading. We are particularly grateful to Marco De Gobbi for his contribution in improving manuscript clarity and language. This work was supported by grants from University of Turin, Progetti di Ateneo/CSP 2012 (12-CSP-C03-065) and AIRC (IG2011 cod 12141) to GS; Ministero dell'Istruzione, dell'Università e della Ricerca (PRIN 2010 20107MSMA4) to AB; University of Turin, RILO 2015 (Ricerca LOcale 2015) project acronym MeCCaSARiC_3. to AR. EB was supported by postdoctoral fellowships granted by the Umberto Veronesi Foundation (2014–2015).

Author Contributions

R.M.P. and E.B. performed molecular biology and immunohistochemical experiments, respectively, analysed and discussed data and wrote the manuscript; M.B. and M.M. performed iron dosage experiments and analysis; F.M. performed behavioural experiments and analysed results; G.S. contributed to data interpretation. A.B. and A.R. conceived experiments, interpreted the data and wrote the manuscript. All authors reviewed and approved the final manuscript.

Additional Information

Supplementary information accompanies this paper at <http://www.nature.com/srep>

Competing financial interests: The authors declare no competing financial interests.

How to cite this article: Pellegrino, R. M. *et al.* Transferrin Receptor 2 Dependent Alterations of Brain Iron Metabolism Affect Anxiety Circuits in the Mouse. *Sci. Rep.* **6**, 30725; doi: 10.1038/srep30725 (2016).



This work is licensed under a Creative Commons Attribution 4.0 International License. The images or other third party material in this article are included in the article's Creative Commons license, unless indicated otherwise in the credit line; if the material is not included under the Creative Commons license, users will need to obtain permission from the license holder to reproduce the material. To view a copy of this license, visit <http://creativecommons.org/licenses/by/4.0/>

© The Author(s) 2016

6. CONCLUSION

The process of iron homeostasis is complex, and since there is no apparent significant excretory pathway for iron, the amount of iron absorbed from mature duodenal enterocytes and that is recycled by macrophages needs to be tightly regulated. This equilibrium, in fact, is compromised in several genetic diseases (hereditary hemochromatosis) and this leads to excessive iron deposition in the liver and, subsequently, other parenchymal cells compromising organ functionality and, if not treated, patient's life expectancies. The identification of many key proteins of iron metabolism, especially hepcidin, has led to advances in the field of its regulation, but the elucidation of their functions is far from complete. At the end of my studies about the role of one of these proteins, Tfr2, in extrahepatic organ I can say that: 1) The hearts of the two Tfr2 β null mice (Tfr2 KO and tfr2 LCKO-KI) have a different cardiac status and enzymatic setting. It is likely that Tfr2 β silencing causes a modification of iron handling in cardiac cells, which may induce a selective activation of different proteins involved in cell survival. In fact, the myocardium of these two targeted murine lines results to have different levels of basal pro-apoptotic factors, which seems correlated with systemic iron overload, and to be enriched of specific iron protein tool kit, antioxidant enzymes and kinases involved in cardioprotective pathways ready to be activated after stressful stimuli. In fact, Tfr2 β null mice's hearts develop a greater resistance against acute I/R challenge, irrespective of systemic iron content (Boero et al, 2015). 2) Tfr2 is a modulator of erythropoiesis in keeping with its function as an EpoR partner. It is possible that Tfr2, as an iron sensor, modulates the erythropoietin sensitivity of the erythroid precursors. The increased red cell numbers in iron-deficient Tmprss6/Tfr2 double KO animals might be the result of this function. More specifically, since iron-loaded Tfr2KO mice are not characterized by increased red blood cell counts, we propose that Tfr2 is a limiting factor for erythropoiesis, which controls red cell numbers to avoid excessive production in conditions of iron-restriction (Nai et al, 2014). An analysis of erythropoiesis in mice with inactivation of one or both Tfr2 isoforms confirms that there is a specific function of Tfr2 α in erythropoiesis, which has been previously demonstrated as well. Germinal lack of Tfr2 α (Tfr2 KO) causes an anticipation of adult erythropoiesis in young mice both in BM and in the spleen. On the other hand, lack of Tfr2 β is responsible for an increased but immature splenic erythropoiesis that is normalized during animal growth. This result demonstrates that Tfr2 β also has an indirect effect on erythropoiesis, regulating iron availability from reticular endothelial cells. (Pellegrino et al, 2017). 3) The alteration of systemic iron availability affects brain homeostasis and functioning and Tfr2 silencing

determines an impairment of the brain Hepcidin response with consequent increased brain iron availability that associates with anxious-like behaviors (Pellegrino et al, 2016).

7. REFERENCES

- Abboud S, Haile DJ. A novel mammalian iron-regulated protein involved in intracellular iron metabolism. *J Biol Chem* 2000; **275**: 19906–19912.
- Acikyoğlu B, Graham RM, Trinder D, House MJ, Olynyk JK, Scott RJ, Milward EA, Johnstone DM. Brain transcriptome perturbations in the transferrin receptor 2 mutant mouse support the case for brain changes in iron loading disorders, including effects relating to long-term depression and long-term potentiation. *Neuroscience*. 2013 Apr 3;235:119-28.
- Anderson S. A., Nizzi C. P., Chang Y. I., Deck K. M., Schmidt P. J., Galy B., et al. (2013). The IRP1-HIF-2 α axis coordinates iron and oxygen sensing with erythropoiesis and iron absorption. *Cell Metab.*17, 282–290
- Andrews NC. Disorders of iron metabolism. *N Engl J Med* 1999;341: 1986-95.
- Andrews NC. Iron homeostasis: insights from genetics and animal models. *Nature Reviews Genetics.*2000; 1:208–217
- Arndt S, Maegdefrau U, Dorn C, Schardt K, Hellerbrand C, Bosserhoff AK. 2010. Iron-induced expression of bone morphogenetic protein 6 in intestinal cells is the main regulator of hepatic hepcidin expression in vivo. *Gastroenterology* 138:372–82
- Arosio P, Levi S. Cytosolic and mitochondrial ferritins in the regulation of cellular iron homeostasis and oxidative damage. *Biochim Biophys Acta*. 2010 ;Aug;1800(8):783-92.
- Auer PL, et al. Rare and low-frequency coding variants in CXCR2 and other genes are associated with hematological traits. *Nat Genet*. 2014 Jun;46(6):629-34
- Babitt JL, Huang FW, Xia Y, Sidis Y, Andrews NC, Lin HY. Modulation of bone morphogenetic protein signaling in vivo regulates systemic iron balance. *J Clin Invest*. 2007 Jul;117(7):1933-9.
- Babitt, J. L., Huang, F. W., Wrighting, D. M., Xia, Y., Sidis, Y., et al. (2006) Bone morphogenetic protein signaling by hemojuvelin regulates hepcidin expression. *Nat. Genet.* 38, 531–539. May
- Barton JC, Edwards CQ, Acton RT. HFE gene: Structure, function, mutations, and associated iron abnormalities. *Gene*. 2015 Dec 15;574(2):179-92.
- Bautista, L., Castro, M.J., López-Barneo, J., and Castellano, A. (2009) Hypoxia inducible factor-2 α stabilization and maxi-K⁺ channel β 1-subunit gene repression by hypoxia in cardiac myocytes: role in preconditioning. *Circ. Res.* 104, 1364-1372.
- Besson-Fournier, C., Latour, C., Kautz, L., Bertrand, J., Ganz, T., et al. (2012) Induction of activin B by inflammatory stimuli up-regulates expression of the iron-regulatory peptide hepcidin through Smad1/5/8 signaling. *Blood* 12;120, 431–439.
- Boero M, Pagliaro P, Tullio F, Pellegrino RM, Palmieri A, Ferbo L, Saglio G, De Gobbi M, Penna C, Roetto A. A comparative study of myocardial molecular

phenotypes of two TFR2 β null mice: role in ischemia/reperfusion. *Biofactors*. 2015 Sep-Oct;41(5):360-71. doi: 10.1002/biof.1237

- Bolli, R., Dawn, B., Tang, X.L., Qiu, Y., Ping, P., et al. (1998) The nitric oxide hypothesis of late preconditioning. *Basic Res. Cardiol.* 93, 325-338.
- Brune M, Magnusson B, Persson H, Hallberg L. Iron losses in sweat. *Am J Clin Nutr* 1986; 43: 438–443.
- Bulvik, B.E., Berenshtein, E., Meyron-Holtz, E.G., Konijn, A.M., and Chevion, M. (2012) Cardiac protection by preconditioning is generated via an iron-signal created by proteasomal degradation of iron proteins. *PLoS One* 7, e48947.
- Calzolari A, Raggi C, Deaglio S, Sposi NM, Stafsnes M, Fecchi K, Parolini I, Malavasi F, Peschle C, Sargiacomo M, Testa U. TfR2 localizes in lipid raft domains and is released in exosomes to activate signal transduction along the MAPK pathway. *J Cell Sci.* 2006 1;119(Pt 21):4486-98.
- Camaschella C, Roetto A, Cali A, De Gobbi M, Garozzo G, Carella M, Majorano N, Totaro A, Gasparini P. The gene TFR2 is mutated in a new type of haemochromatosis mapping to 7q22. *Nat Genet.* 2000;25(1):14-5.
- Camaschella C, Pagani A, Nai A, Silvestri L. The mutual control of iron and erythropoiesis. *Int J Lab Hematol.* 2016.
- Canali, S., Core, A. B., Zumbrennen-Bullough, K. B., Merkulova, M., Wang, C. Y., et al. (2016) Activin B induces noncanonical SMAD1/5/8 signaling via BMP type I receptors in hepatocytes: evidence for a role in hepcidin induction by inflammation in male mice. *Endocrinology* 157, 1146–1162.
- Casanovas, G., Swinkels, D. W., Altamura, S., Schwarz, K., Laarakkers, C. M., et al. (2011) Growth differentiation factor 15 in patients with congenital dyserythropoietic anaemia (CDA) type II. *J. Mol. Med. (Berl.)* 89, 811–816
- C. J. Murphy and G. Y. Oudit, “Iron-overload cardiomyopathy: pathophysiology, diagnosis, and treatment,” *Journal of Cardiac Failure*, vol. 16, no. 11, pp. 888–900, 2010.
- Chen J, Wang J, Meyers KR, Enns CA. Transferrin-directed internalization and cycling of transferrin receptor 2. *Traffic.* 2009 Oct;10(10):1488-501.
- Chevion, M., Leibowitz, S., Aye, N.N., Novogrodsky, O., Singer, A., et al. (2008) Heart protection by ischemic preconditioning: a novel pathway initiated by iron and mediated by ferritin. *J. Mol. Cell. Cardiol.* 45, 839-845.
- Chiabrando D1, Vinchi F1, Fiorito V1, Mercurio S1, Tolosano E. Heme in pathophysiology: a matter of scavenging, metabolism and trafficking across cell membrane.1 *Front Pharmacol.* 2014 Apr 8;5:61.
- Cooperman S. S., Meyron-Holtz E. G., Olivierre-Wilson H., Ghosh M. C., McConnell J. P., Rouault T. A. (2005). Microcytic anemia, erythropoietic protoporphyria and neurodegeneration in mice with targeted deletion of iron regulatory protein 2. *Blood* 106, 1084–1091

- Cozzi, A., Corsi, B., Levi, S., Santambrogio, P., Albertini, A., and Arosio, P. (2000) Overexpression of wild type and mutated human ferritin H-chain in HeLa cells: in vivo role of ferritin ferroxidase activity. *J. Biol. Chem.* 275, 25122-25129.
- Darshan, D., Vanoaica, L., Richman, L., Beermann, F., and Kühn, L.C. (2009) Conditional deletion of ferritin H in mice induces loss of iron storage and liver damage. *Hepatology* 50, 852-860.
- D.Q. Lou, J.C. Lesbordes, G. Nicolas, L. Viatte, M. Bennoun, R.N. Van, A. Kahn, L. Renia, S. Vaulont. Iron- and inflammation-induced hepcidin gene expression in mice is not mediated by Kupffer cells in vivo *Hepatology*, 41 (2005), pp. 1056-1064
- D'Alessio F, Hentze MW, Muckenthaler MU. The hemochromatosis proteins HFE, TfR2, and HJV form a membrane-associated protein complex for hepcidin regulation. *J Hepatol.* 2012 Nov;57(5):1052-60.
- Daher R, Kannengiesser C, Houamel D, et al. Heterozygous mutations in BMP6 propeptide lead to inappropriate hepcidin synthesis and moderate iron overload in humans. *Gastroenterology.* 2016;150:672–683. e674
- Donovan A, Lima CA, Pinkus JL, Pinkus GS, Zon LI, Robine S, Andrews NC. The iron exporter ferroportin/Slc40a1 is essential for iron homeostasis. *Cell Metab* 2005; 1: 191–200. during mitosis. *EMBO J* 1984; 3: 2217–2225.
- Du X, She E, Gelbart T, Truksa J, Lee P, Xia Y, Khovananth K, Mudd S, Mann N, Moresco EM, Beutler E, Beutler B. The serine protease TMPRSS6 is required to sense iron deficiency. *Science.* 2008 23;320(5879):1088-92
- Elena Gammella, Stefania Recalcati, Ilona Rybinska, Paolo Buratti, and Gaetano Cairo. Iron-Induced Damage in Cardiomyopathy: Oxidative-Dependent and Independent Mechanisms. Hindawi Publishing Corporation *Oxidative Medicine and Cellular Longevity* Volume 2015
- Elena Gammella, Paolo Buratti, Gaetano Cairo and Stefania Recalcati. The transferrin receptor: the cellular iron gate. *Metallomics*, 2017, 9, 1367
- Enns CA, Ahmed R, Wang J, Ueno A, Worthen C, et al. 2013. Increased iron loading induces Bmp6 expression in the non-parenchymal cells of the liver independent of the BMP signaling pathway. *PloS ONE* 8:e60534
- Enns CA, Shindelman JE, Tonik SE, Sussman HH. Radioimmunochemical measurement of the transferrin receptor in human trophoblast and reticulocyte membranes with a specific antireceptor *Proc Natl AcadSci U S A.* 1981 78(7): 4222–4225
- Epsztejn, S., Glickstein, H., Picard, V., Slotki, I.N., Breuer, W., et al. (1999) H-ferritin subunit overexpression in erythroid cells reduces the oxidative stress response and induces multidrug resistance properties. *Blood* 94, 3593-3603.
- Fahmy M, Young SP. Modulation of iron metabolism in monocyte cell line U937 by inflammatory cytokines: changes in transferrin uptake, iron handling and ferritin mRNA. *Biochem J* 1993; 296: 175–181.

- Ferdinandy, P., Schulz, R., and Baxter, G.F. (2007) Interaction of cardiovascular risk factors with myocardial ischemia/reperfusion injury, preconditioning, and postconditioning. *Pharmacol, Rev.* 59, 418-458
- Finberg KE, Heeney MM, Campagna DR, Aydinok Y, Pearson HA, Hartman KR, Mayo MM, Samuel SM, Strouse JJ, Markianos K, Andrews NC, Fleming MD Mutations in Tmprss6 cause iron-refractory iron deficiency anemia (IRIDA) *Nat Genet.* 2008;40(5):569-71.
- Fleming RE, Migas MC, Holden CC, Waheed A, Britton RS, Tomatsu S, Bacon BR, Sly WS. Transferrin receptor 2: continued expression in mouse liver in the face of iron overload and in hereditary hemochromatosis. *Proc Natl Acad Sci USA* 2000; **97**: 2214–2219.
- Fleming RE, Ahmann JR, Migas MC, Waheed A, Koeffler HP, Kawabata H, Britton RS, Bacon BR, Sly WS. Targeted mutagenesis of the murine transferrin receptor-2 gene produces hemochromatosis *Proc Natl Acad Sci U S A.* 2002 Aug 6;99(16):10653-8
- Folgueras AR, de Lara FM, Pendás AM, Garabaya C, Rodríguez F, Astudillo A, Bernal T, Cabanillas R, López-Otín C, Velasco G. Membrane-bound serine protease matriptase-2 (Tmprss6) is an essential regulator of iron homeostasis. *Blood.* 2008 Sep 15;112(6):2539-45.
- Forejtníková H, Vieillevoje M, Zermati Y, et al. Forejtníková H, Vieillevoje M, Zermati Y, Lambert M, Pellegrino RM, Guihard S, Gaudry M, Camaschella C, Lacombe C, Roetto A, Mayeux P, Verdier F (2010) Transferrin receptor 2 is a component of the erythropoietin receptor complex and is required for efficient erythropoiesis. *Blood*, 2010; 116(24):5357-5367.
- Frazer DM, Wilkins SJ, Becker EM, Vulpe CD, McKie AT, Trinder D, Anderson GJ. Hcpidin expression inversely correlates with the expression of duodenal iron transporters and iron absorption in rats. *Gastroenterology* 2002; 123: 835–844.
- Frazer DM, Wilkins SJ, Millard KN, McKie AT, Vulpe CD, Anderson GJ. Increased hcpidin expression and hypoferraemia associated with an acute phase response are not affected by inactivation of HFE. *Br J Haematol* 2004; 126: 434–436.
- Fuqua BK, Vulpe CD, Anderson GJ. Intestinal iron absorption. *J Trace Elem Med Biol.* 2012; Jun;26(2-3):115-9.
- G. Montosi, E. Corradini, C. Garuti, S. Barelli, S. Recalcati, G. Cairo, L. Valli, E. Pignatti, C. Vecchi, F. Ferrara, A. Pietrangelo. Kupffer cells and macrophages are not required for hepatic hcpidin activation during iron overload. *Hepatology*, 41 (2005), pp. 545-552
- Galy B., Ferring D., Minana B., Bell O., Janser H. G., Muckenthaler M., et al. (2005b). Altered body iron distribution and microcytosis in mice deficient for iron regulatory protein 2 (IRP2). *Blood* 106, 2580–2589
- Gao J, Chen J, Kramer M, Tsukamoto H, Zhang AS, Enns CA. Interaction of the hereditary hemochromatosis protein HFE with transferrin receptor 2 is required for transferrin-induced hcpidin expression. *Cell Metab.* 2009; (3):217-27.

- Girelli D, Trombini P, Busti F, Campostrini N, Sandri M, Pelucchi S, Westerman M, Ganz T, Nemeth E, Piperno A, Camaschella C. A time course of hepcidin response to iron challenge in patients with HFE and TFR2 hemochromatosis. *Haematologica*. 2011;96(4):500-6.
- Ghosh M. C., Ollivierre-Wilson H., Cooperman S., Rouault T. A. (2006). Reply to “Iron homeostasis in the brain: complete iron regulatory protein 2 deficiency without symptomatic neurodegeneration in the mouse”. *Nat. Genet.*38, 969–970
- Ghosh M. C., Tong W. H., Zhang D., Ollivierre-Wilson H., Singh A., Krishna M. C., et al. (2008). Tempol-mediated activation of latent iron regulatory protein activity prevents symptoms of neurodegenerative disease in IRP2 knockout mice. *Proc. Natl. Acad. Sci. U.S.A.*105, 12028–12033
- Goswami T, Andrews NC. Hereditary hemochromatosis protein, HFE, interaction with transferrin receptor 2 suggests a molecular mechanism for mammalian iron sensing. *J Biol Chem* 2006; **281**: 28494–28498.
- Ghosh M. C., Zhang D. L., Jeong S. Y., Kovtunovych G., Ollivierre-Wilson H., Noguchi A., et al. (2013). Deletion of iron regulatory protein 1 causes polycythemia and pulmonary hypertension in mice through translational derepression of HIF2alpha. *Cell Metab.*17, 271–281
- Gruenheid S, Canonne-Hergaux F, Gauthier S, Hackam DJ, Grinstein S, Gros P. The iron transport protein NRAMP2 is an integral membrane glycoprotein that colocalizes with transferrin in recycling endosomes. *J Exp Med* 1999; 189: 831–841.
- Hänninen MM1, Haapasalo J, Haapasalo H, Fleming RE, Britton RS, Bacon BR, Parkkila S. Expression of iron-related genes in human brain and brain tumors. *BMC Neurosci.* 2009 Apr 22;10:36.
- Hentze MW, Muckenthaler MU, Andrews NC. Balancing acts: molecular control of mammalian iron metabolism. *Cell* 2004;117:285e7.
- Hentze MW, Muckenthaler MU, Galy B, Camaschella C. Two to tango: regulation of Mammalian iron metabolism. *Cell.*2010 Jul 9;142(1):24-38.
- Heusch, G., and Schulz, R. (2009) Neglect of the coronary circulation: some critical remarks on problems in the translation of cardioprotection. *Cardiovasc. Res.* 84, 111-114.
- Hubert N, Hentze MW. Previously uncharacterized isoforms of divalent metal transporter (DMT)-1: implications for regulation and cellular function. *Proc Natl Acad Sci U S A.* 2002
- Hunter HN, Fulton DB, Ganz T, Vogel HJ. The solution structure of human hepcidin, a peptide hormone with antimicrobial activity that is involved in iron uptake and hereditary hemochromatosis. *J Biol Chem* 2002; 277: 37597–37603.
- Kanamori, Y., Sugiyama, M., Hashimoto, O., Murakami, M., Matsui, T., and Funaba, M. (2016) Regulation of hepcidin expression by inflammation-induced activin B. *Sci. Rep.* 6, 38702–38706.

- Kattamis, A., Papassotiriou, I., Palaiologou, D., Apostolakou, F., Galani, A., et al. (2006) The effects of erythropoietic activity and iron burden on hepcidin expression in patients with thalassemia major. *Haematologica* 91, 809–812.
- Kautz, L., Jung, G., Valore, E. V., Rivella, S., Nemeth, E., and Ganz, T.(2014) Identification of erythroferrone as an erythroid regulator of iron metabolism. *Nat. Genet.* 46, 678–684.
- Kawabata H, Germain RS, Vuong PT, Nakamaki T, Said JW, Koeffler HP. Transferrin receptor 2-alpha supports cell growth both in iron-chelated cultured cells and in vivo. *J Biol Chem* 2000; **275**: 16618–16625.
- Kawabata H, Yang R, Hiramata T, Vuong PT, Kawano S, Gombart AF, Koeffler HP. Molecular cloning of transferrin receptor 2. A new member of the transferrin receptor-like family. *J Biol Chem* 1999; **274**: 20826–20832.
- Kawabata H, Fleming RE, Gui D, Moon SY, Saitoh T, O’Kelly J, Umehara Y, Wano Y, Said JW, Koeffler HP. Expression of hepcidin is down-regulated in TfR2 mutant mice manifesting a phenotype of hereditary hemochromatosis. *Blood* 2005; 105: 376–381.
- Koorts AM, Viljoen M Ferritin and ferritin isoforms II: protection against uncontrolled cellular proliferation, oxidative damage and inflammatory processes. *Arch Physiol Biochem.* 2007 Apr;113(2):55-64
- Kuninger D, Kuns-Hashimoto R, Nili M, Rotwein P. Pro-protein convertases control the maturation and processing of the iron-regulatory protein, RGMc/hemojuvelin. *BMC Biochem.* 2008 Apr 2;9:9.
- Knutson M, Menzies S, Connor J, Wessling-Resnick M (2004) Developmental, regional, and cellular expression of SFT/UbcH5A and DMT1 mRNA in brain. *J Neurosci Res* 76(5):633–641.
- Lacerda, L., Somers, S., Opie, L.H., and Lecour, S. (2009) Ischaemic postconditioning protects against reperfusion injury via the SAFE pathway. *Cardiovasc. Res.* 84, 201-208.
- Lakhali-Littleton S, Wolna M, Carr CA, Miller JJ, Christian HC, Ball V, Santos A, Diaz R, Biggs D, Stillion R, Holdship P, Larner F, Tyler DJ, Clarke K, Davies B, Robbins PA. Cardiac ferroportin regulates cellular iron homeostasis and is important for cardiac function. *Proc Natl Acad Sci USA* 112: 3164–3169, 2015.
- Lakhali-Littleton S, Wolna M, Chung YJ, Christian HC, Heather LC, Brescia M, Ball V, Diaz R, Santos A, Biggs D, Clarke K, Davies B, Robbins PA. An essential cell-autonomous role for hepcidin in cardiac iron homeostasis. *eLife* 5: 5, 2016. doi:10.7554/eLife.19804.
- Latour C, Besson-Fournier C, Meynard D, Silvestri L, Gourbeyre O, Aguilar-Martinez P, Schmidt PJ, Fleming MD, Roth MP, Coppin H. Differing impact of the deletion of hemochromatosis-associated molecules HFE and transferrin receptor-2 on the iron phenotype of mice lacking bone morphogenetic protein 6 or hemojuvelin. *Hepatology.* 2016 ;63(1):126-37.

- LaVaute T., Smith S., Cooperman S., Iwai K., Land W., Meyron-Holtz E., et al. (2001). Targeted deletion of the gene encoding iron regulatory protein-2 causes misregulation of iron metabolism and neurodegenerative disease in mice. *Nat. Genet.* 27, 209–214
- Liu XB, Hill P, Haile DJ. Role of the ferroportin iron-responsive element in iron and nitric oxide dependent gene regulation. *Blood Cells Mol Dis* 2002; **29**: 315–326.
- Lymboussaki A, Pignatti E, Montosi G, Garuti C, Haile DJ, Pietrangelo A. The role of the iron responsive element in the control of ferroportin1/IREG1/MTP1 gene expression. *J Hepatol* 2003;**39**: 710–715.
- Massague J, Gomis RR. 2006. The logic of TGF β signaling. *FEBS Lett.* 580:2811–20
- Mastroberardino PG, Hoffman EK, Horowitz MP, Betarbet R, Taylor G, Cheng D, Na HM, Gutekunst CA, Gearing M, Trojanowski JQ, Anderson M, Chu CT, Peng J, Greenamyre JT. A novel transferrin/TfR2-mediated mitochondrial iron transport system is disrupted in Parkinson's disease. *Neurobiol Dis.* 2009 Jun;**34**(3):417-31
- McCarthy RC, Kosman DJ (2012) Mechanistic analysis of iron accumulation by endothelial cells of the BBB. *Biometals* 25(4):665–675
- McKie AT, Marciani P, Rolfs A, Brennan K, Wehr K, Barrow D, Miret S, Bomford A, Peters TJ, Farzaneh F, Hediger MA, Hentze MW, Simpson RJ. A novel duodenal iron-regulated transporter, IREG1, implicated in the basolateral transfer of iron to the circulation. *Mol Cell* 2000; **5**: 299–309 .
- Merle U, Theilig F, Fein E, Gehrke S, Kallinowski B, Riedel HD, Bachmann S, Stremmel W, Localization of the iron-regulatory proteins hemojuvelin and transferrin receptor 2 to the basolateral membrane domain of hepatocytes. *Histochem Cell Biol* 2007; **127**: 221–226.
- Merle, U., Fein, E., Gehrke, S.G., Stremmel, W., and Kulaksiz, H. (2007) The iron regulatory peptide hepcidin is expressed in the heart and regulated by hypoxia and inflammation. *Endocrinology* **148**, 2663-2668.
- Meynard, D., Kautz, L., Darnaud, V., Canonne-Hergaux, F., Coppin, H., and Roth, M. P. (2009) Lack of the bone morphogenetic protein BMP6 induces massive iron overload. *Nat. Genet.* 1, 478–481.
- Miret S, Simpson RJ, McKie AT. Physiology and molecular biology of dietary iron absorption. *Annu Rev Nutr* 2003; **23**: 283–301.
- Moos, T., Rosengren Nielsen, T., Skjørringe, T., Morgan, E.H. Iron trafficking inside the brain. *J Neurochem.* 2007. 103, 1730-1740 (2007).
- Muckenthaler, M.U., Galy, B., and Hentze, M.W. (2008). Systemic iron homeostasis and the iron-responsive element/iron-regulatory protein (IRE/IRP) regulatory network. *Annu. Rev. Nutr.* 28, 197–213.
- Nai A, Pellegrino RM, Rausa M, et al. (2014) The erythroid function of transferrin receptor 2 revealed by Tmprss6 inactivation in different models of transferrin receptor 2 knockout mice. *Haematologica*, 2014; **99**(6): 1016-1021.

- Nai A, Lidonnici MR, Rausa M, et al. (2015) The second transferrin receptor regulates red blood cell production in mice. *Blood*. 2005, 125(7):1170-1179.
- Nai, A., Rubio, A., Campanella, A., Goubeyre, O., Artuso, I., et al. (2016) Limiting hepatic Bmp-Smad signaling by matriptase-2 is required for erythropoietin-mediated hepcidin suppression in mice. *Blood* 127, 2327–2336
- Nemeth E, Tuttle MS, Powelson J, Vaughn MB, Donovan A, Ward DM, Ganz T, Kaplan J. Hepcidin regulates cellular iron efflux by binding to ferroportin and inducing its internalization. *Science* 2004;
- Nemeth E, Roetto A, Garozzo G, Ganz T, Camaschella C. Hepcidin is decreased in TFR2 hemochromatosis. *Blood* 2005; 105: 1803–1806.
- Nicolas, G., Chauvet, C., Viatte, L., Danan, J. L., Bigard, X., et al. (2002) The gene encoding the iron regulatory peptide hepcidin is regulated by anemia, hypoxia, and inflammation. *J. Clin. Invest.* 110, 1037–1044.
- Papanikolaou G. Pantopoulos K. Systemic Iron Homeostasis and Erythropoiesis. *International Union of Biochemistry and Molecular Biology Volume 69, Number 6, June 2017, Pages 399–413*
- Papanikolaou G, et al. Mutations in HFE2 cause iron overload in chromosome 1q-linked juvenile *Nat Genet* 2004; **36**: 77–82.
- Papanikolaou, G., Tzilianos, M., Christakis, J. I., Bogdanos, D., Tsimirika, K., et al. (2005) Hepcidin in iron overload disorders. *Blood* 105, 4103–4105.
- Pellegrino RM, Boda E, Montarolo F, Boero M, Mezzanotte M, Saglio G, Buffo A, Roetto A. Transferrin Receptor 2 Dependent Alterations of Brain Iron Metabolism Affect Anxiety Circuits in the Mouse. *Sci Rep*. 2016 Aug 1;6:30725. doi: 10.1038/srep30725
- Pellegrino RM, F. Riondato, L. Ferbo, M. Boero, A. Palmieri, L. Osella, P. Pollicino, B. Miniscalco, G. Saglio, and A. Roetto. Altered Erythropoiesis in Mouse Models of Type 3 Hemochromatosis. *BioMed Research International Volume 2017 (2017), Article ID 2408941, 12 pages doi: 10.1155/2017/2408941*
- Picard V, Govoni G, Jabado N, Gros P. Nramp 2 (DCT1/DMT1) expressed at the plasma membrane transports iron and other divalent cations into a calcein-accessible cytoplasmic pool. *J Biol Chem* 2000; 275: 35738–35745.
- Pietrangelo, A., Dierssen, U., Valli, L., Garuti, C., Rump, A., et al. (2007) STAT3 is required for IL-6-gp130-dependent activation of hepcidin in vivo. *Gastroenterology* 132, 294–300. Jan
- Pigeon, C., Ilyin, G., Courselaud, B., Leroyer, P., Turlin, B., et al. (2001) A new mouse liver-specific gene, encoding a protein homologous to human antimicrobial peptide hepcidin, is overexpressed during iron overload. *J. Biol. Chem.* 276, 7811–7819.
- Poli M, Lusciati S, Gandini V, Maccarinelli F, Finazzi D, Silvestri L, Roetto A, Arosio P. Transferrin receptor 2 and HFE regulate furin expression via mitogen-activated protein kinase/extracellular signal-regulated kinase (MAPK/Erk) signaling.

Implications for transferrin-dependent hepcidin regulation. *Haematologica*. 2010 Nov;95(11):1832-40

- Pollack S, Campana T. Low molecular weight non heme iron and a highly labeled heme pool in the reticulocyte. *Blood* 1980; 56: 564–566.
- Pollack S. Intracellular iron. *AdvExp Med Biol* 1994; 356: 165–171.
- Qian, Z.M., Chang, Y.Z., Leung, G., Du, J.R., Zhu, L., et al. (2007) Expression of ferroportin1, hephaestin and ceruloplasmin in rat heart. *Biochim. Biophys. Acta* **1772**, 527– 532
- Ramey, G., Deschemin, J. C., and Vaulont, S. (2009) Cross-talk between the mitogen activated protein kinase and bone morphogenetic protein/hemojuvelin pathways is required for the induction of hepcidin by holotransferrin in primary mouse hepatocytes. *Haematologica* 94, 765–772.
- Ramsay AJ1, Reid JC, Velasco G, Quigley JP, Hooper JD. The type II transmembrane serine protease matriptase-2--identification, structural features, enzymology, expression pattern and potential roles. *Front Biosci*. 2008 Jan 1;13:569-79.
- Recalcatti, S., Minotti, G., and Cairo, G. (2010). Iron regulatory proteins:from molecular mechanisms to drug development. *Antioxid. Redox Signal*.Published online May 22, 2010. 10.1089/ars.2009.2983.
- Rhodes SL, Buchanan DD, Ahmed I, Taylor KD, Lorient MA, Sinsheimer JS, Bronstein JM, Elbaz A, Mellick GD, Rotter JI, Ritz B (2014) Pooled analysis of iron-related genes in Parkinson's disease: association with transferrin. *Neurobiol Dis* (2014) 62:172–178.
- Rudeck M, Volk T, Sitte N, Grune T. Ferritin oxidation in vitro: implication of iron release and degradation by the 20S proteasome. *IUBMB Life* 2000; 49: 451–456.
- Roetto A, Di Cunto F, Pellegrino RM, Hirsch E, Azzolino O, Bondi A, Defilippi I, Carturan S, Miniscalco B, Riondato F, Cilloni D, Silengo L, Altruda F, Camaschella C, Saglio G. Comparison of 3 Tfr2-deficient murine models suggests distinct functions for Tfr2-alpha and Tfr2-beta isoforms in different tissues. *Blood*. 2010 Apr 22;115(16):3382-9.
- Roetto A, Totaro A, Cazzola M, Cicilano M, Bosio S, D'Ascola G, Carella M, Zelante L, Kelly AL, Cox TM, Gasparini P, Camaschella C. Juvenile hemochromatosis locus maps to chromosome 1q. *Am J Hum Genet*. 1999;64(5):1388-93.
- Samad TA, Srinivasan A, Karchewski LA, Jeong SJ, Campagna JA, Ji RR, Fabrizio DA, Zhang Y, Lin HY, Bell E, Woolf CJ. DRAGON: a member of the repulsive guidance molecule-related family of neuronal- and muscle-expressed membrane proteins is regulated by DRG11 and has neuronal adhesive properties. *J Neurosci*. 2004 Feb 25;24(8):2027-36.
- Smith SR, Ghosh MC, Ollivierre-Wilson H, Hang Tong W, Rouault TA Complete loss of iron regulatory proteins 1 and 2 prevents viability of murine zygotes beyond the blastocyst stage of embryonic development. *Blood Cells Mol Dis*. 2006 Mar-Apr; 36(2):283-7.

- Schmidt, P. J. (2015) Regulation of iron metabolism by hepcidin under conditions of inflammation. *J. Biol. Chem.* 290, 18975–18983.
- Schmidt PJ, Toran PT, Giannetti AM, Bjorkman PJ, Andrews NC. The transferrin receptor modulates Hfe-dependent regulation of hepcidin expression. *Cell Metab.* 2008;7(3):205-14.
- Sheth S, Brittenham GM. Genetic disorders affecting proteins of iron metabolism: clinical implications. *Annu Rev Med* 2000; **51**: 443–464.
- a) Silvestri L, Pagani A, Camaschella C. Furin-mediated release of soluble hemojuvelin: a new link between hypoxia and iron homeostasis. *Blood.* 2008 Jan 15;111(2):924-31.
- b) Silvestri L, Pagani A, Nai A, De Domenico I, Kaplan J, Camaschella C. The serine protease matriptase-2 (TMPRSS6) inhibits hepcidin activation by cleaving membrane hemojuvelin. *Cell Metab.* 2008 Dec;8(6):502-11.
- Simons K, Toomre D. Lipid rafts and signal transduction. *Nat Rev Mol Cell Biol.* 2000 Oct;1(1):31-9. Review. Erratum in: *Nat Rev Mol Cell Biol* 2001 Mar;2(3):216.
- Soranzo N, et al. A genome-wide meta-analysis identifies 22 loci associated with eight hematological parameters in the HaemGen consortium *Nat Genet.* 2009 Nov;41(11):118290.
- Sposi N.M., Interaction between Erythropoiesis and Iron Metabolism in Human β -thalassemia - Recent Advances and New Therapeutic Approaches, *Inherited Hemoglobin Disorders*, Chapter 4, InTech 2015.
- Subramaniam N, Cameron J. McDonald, Lesa Ostini, Patricia E. Lusby, Leesa F. Wockner Grant A. Ramm, and Daniel F. Wallace. Hepatic Iron Deposition Does Not Predict Extrahepatic Iron Loading in Mouse Models of Hereditary Hemochromatosis. *The American Journal of Pathology* 2012 Volume 181, Issue 4, Pages 1173–1179
- Tamary, H., Shalev, H., Perez-Avraham, G., Zoldan, M., Levi, I., et al. (2008) Elevated growth differentiation factor 15 expression in patients with congenital dyserythropoietic anemia type I. *Blood* 112, 5241–5244.
- Tanaka T, Roy CN, Yao W, Matteini A, Semba RD, Arking D, Walston JD, Fried LP, Singleton A, Guralnik J, Abecasis GR, Bandinelli S, Longo DL, Ferrucci L. A genome-wide association analysis of serum iron concentrations. *Blood.* 2010 Jan 7;115(1):94-6
- Tanno, T., Bhanu, N. V., Oneal, P. A., Goh, S. H., Staker, P., et al. (2007) High levels of GDF15 in thalassemia suppress expression of the iron regulatory protein hepcidin. *Nat. Med.* 13, 1096–1101. Sep
- Tanno, T., Porayette, P., Sripichai, O., Noh, S. J., Byrnes, C., et al. (2009) Identification of TWSG1 as a second novel erythroid regulator of hepcidin expression in murine and human cells. *Blood* 114, 181–186.
- Tran TN, Eubanks SK, Schaffer KJ, Zhou CY, Linder MC. Secretion of ferritin by rat hepatoma cells and its regulation by inflammatory cytokines and iron. *Blood* 1997; 90: 4979–4986.

- Tullio, F., Angotti, C., Perrelli, M.G., Penna, C., and Pagliaro, P. (2013) Redox balance and cardioprotection. *Basic Res Cardiol* 108, 392.
- Valore EV, Ganz T. Posttranslational processing of hepcidin in human hepatocytes is mediated by the prohormone convertase furin. *Blood Cells Mol Dis.* 2008 JanFeb;40(1):132-8.
- Velasco G1, Cal S, Quesada V, Sánchez LM, López-Otín C. Matriptase-2, a membranebound mosaic serine proteinase predominantly expressed in human liver and showing degrading activity against extracellular matrix proteins. *J Biol Chem.* 2002 Oct 4;277(40):37637-46.
- Verga Falzacappa, M. V., Vujic Spasic, M., Kessler, R., Stolte, J., Hentze, M. W., and Muckenthaler, M. U. (2007) STAT3 mediates hepatic hepcidin expression and its inflammatory stimulation. *Blood* 109, 353–358.
- Vujic Spasic M, Kiss J, Herrmann T, Kessler R, Stolte J, Galy B, Rathkolb B, Wolf E, Stremmel W, Hentze MW, Muckenthaler MU. Physiologic systemic iron metabolism in mice deficient for duodenal Hfe. *Blood.* 2007 May 15;109(10):4511-7.
- Vujic Spasic, M., Kiss, J., Herrmann, T., Galy, B., Martinache, S., et al. (2008) Hfe acts in hepatocytes to prevent hemochromatosis. *Cell Metab.* 7, 173–178.
- Wallace, D. F., Summerville, L., and Subramaniam, V. N. (2007) Targeted disruption of the hepatic transferrin receptor 2 gene in mice leads to iron overload. *Gastroenterology* 132, 301–310.
- West AP, Jr., Bennett MJ, Sellers VM, Andrews NC, Enns CA, Bjorkman PJ. Comparison of the interactions of transferrin receptor and transferrin receptor 2 with transferrin and the hereditary hemochromatosis protein HFE. *J Biol Chem* 2000; 275: 38135–38138.
- Wilkinson N., Pantopoulos K. (2013). IRP1 regulates erythropoiesis and systemic iron homeostasis by controlling HIF2alpha mRNA translation. *Blood* 122, 1658–1668 10.1182/blood-2013-03-492454
- Wrighting, D. M., and Andrews, N. C. (2006) Interleukin-6 induces hepcidin expression through STAT3. *Blood* 108, 3204–3209.
- Xu W, Barrientos T, Mao L, Rockman HA, Sauve AA, Andrews NC. Lethal cardiomyopathy in mice lacking transferrin receptor in the heart. *Cell Reports* 13: 533–545, 2015
- Yang F, Liu XB, Quinones M, Melby PC, Ghio A, Haile DJ. Regulation of reticuloendothelial iron transporter MTP1 (Slc11a3) by inflammation. *J Biol Chem* 2002; 277: 39786–39791.
- Young SP, Roberts S, Bomford A. Intracellular processing of transferrin and iron by isolated rat hepatocytes. *Biochem J* 1985; 232: 819–823.
- Y.-R. Chen and J. L. Zweier, “Cardiacmitochondria and reactive oxygen species generation,” *Circulation Research*, vol. 114, no. 3, pp. 524–537, 2014.

- Zhang AS1, Anderson SA, Meyers KR, Hernandez C, Eisenstein RS, Enns CA. Evidence that inhibition of hemojuvelin shedding in response to iron is mediated through neogenin. *J Biol Chem.* 2007 Apr 27;282(17):12547-56.
- Zimmer M., Ebert B. L., Neil C., Brenner K., Papaioannou I., Melas A., et al. (2008). Small-molecule inhibitors of HIF-2a translation link its 5'UTR iron-responsive element to oxygen sensing. *Mol. Cell* 32, 838–848
- Zimmermann MB, Hurrell RF, Nutritional iron deficiency. *Lancet.*2007 Aug 11;370(9586):511-20. Review.
- Zumerle S, Jacques R., R. Mathieu, S. Delga, M. Heinis, L. Viatte, S. Vaulont, C. Peyssonnaud Targeted disruption of hepcidin in the liver recapitulates the hemochromatotic phenotype *Blood* 2014 123:3646-3650